

THE GLIDER

Stelio Frati



Cover design: Jack Amos, Inc.

Dott. Ing. STELIO FRATI

Dal Centro studi ed Esperienze per il Volo a Vela del Politecnico di Milano

L'ALIANTE

ELEMENTI DI PROGETTO DEI MODERNI ALIANTI
VELEGGIATORI – AERODINAMICA – DISEGNO
CALCOLO STATICO – STRUTTURE

Con 256 illustrazioni, numerosi esempi
di calcolo e raccolta di 36 fra i
più noti alianti italiani e stranieri



EDITORE ULRICO HOEPLI MILANO

1946

Contents

Preface

Introduction

Chapter 1 Preliminary Considerations

1. Soaring	1-1
2. Gliders: Training and Soaring	1-1
3. Aerodynamic Characteristics	1-1
4. Practicality of Soaring	1-2
5. Launching Methods	1-2

Chapter 2 General Characteristics of Gliders

6. Introduction	2-1
7. Training Gliders	2-1
8. Sailplanes	2-1
9. The Structure of Sailplanes	2-1

Chapter 3 Elements of Aerodynamics

11. Aerodynamic Force	3-1
12. Airfoils	3-3
13. Charts	3-6
14. Moment of an Airfoil	3-7
15. Moment Equation and its Properties	3-10
16. Wing Aspect Ratio	3-18
17. Wings with Varying Airfoils	3-21
18. The Complete Airplane	3-24

Chapter 4 Flight Stability

19. Static and Dynamic Stability	4-1
20. Longitudinal Stability	4-1
21. Horizontal Tail Area	4-6
22. Lateral Stability	4-8
23. Lateral Control Surfaces	4-9
24. Directional Stability	4-11
25. Vertical Empennage	4-12

Chapter 5 Mechanics of Flight

26. Glide Angle and Glide Ratio	5-1
27. Horizontal and Vertical Speeds	5-2
28. Minimum Horizontal and Vertical Velocities	5-4
29. Top Speed in a Dive	5-5

Chapter 6 Applied Aerodynamics

30. Airfoils - Criteria for Choosing Them	6-1
---	-----

31. Airframe Components and Drag	6-2
32. Summary	6-5
Chapter 7 Design Plan	
33. General Considerations	7-1
34. Wing Span	7-1
35. Aspect Ratio and Wing Loading	7-2
36. Fuselage	7-3
37. Empennage	7-4
38. Basic Three-View Drawings	7-4
39. Centering	7-4
40. Side View	7-9
41. Frontal View	7-14
42. Top View	7-15
43. Control Surfaces	7-16
44. Landing Apparatus	7-16
45. Control of Maneuvering Surfaces	7-17
46. Options, Spoilers, Towing Hooks	7-21
Chapter 8 Aircraft Design	
47. Wing Design	8-1
48. Design of Wing Airfoil	8-2
49. Wing Twist and the Wing Reference Plane	8-4
50. Fuselage Design	8-7
51. Empennage Design	8-12
52. Design of Movements of Mechanical Controls	8-12
Chapter 9 Applied Loads and Structural Design	
53. Flight Loads	9-1
54. Static Tests	9-2
55. Flight Conditions	9-3
56. Wing Stress Analysis	9-5
57. Verification of the Bending Strength of the Wing Spar	9-27
58. Verification of the shear strength of the wing spar	9-44
59. Verification of the torsional strength of the wing structure	9-46
60. Determination of the fuselage structural loads	9-51
61. Verification of fuselage stability	9-60
62. Determination of the Tail Plane Loads	9-68
63. Calculation of Wing Attachments	9-70
64. Calculation of controls and related transmissions	9-81

Preface

At our Falco Builders Dinner at Oshkosh '89, Fernando Almeida mentioned “Mr. Frati’s book” in some context. This was the first I had heard of it, and Fernando explained that Mr. Frati had published a book years ago on aircraft design. Then and there, I decided I would have to get my hands on the book and get it translated into English.

Subsequently, Fernando mailed me his only copy of the book, *L’Aliante* (The Glider) which was a photocopy of the original. Since then, we have slowly worked our way through the book. The bulk of the work fell on Maurice Branzanti who translated the original text into English for the first eight chapters, then Giovanni and Francesca Nustrini do the translation for the last chapter. I then edited and polished the words into the copy you see here, at times with the help of Steve Wilkinson, Jim Petty and Dave Thurston and with the help of Mark Rhodes for one of the more difficult illustrations. Many thanks to Jack Amos for the cover design.

As you might imagine, the original 1946 book contained a lot of material that is hopelessly outdated now. The book contained many illustrative sketches of gliders circling clouds, launching by being towed by a car, and the like. There were many references to contemporary gliders and airfoils—indeed a large section of the book was simply a series of charts and tables of airfoil with the usual coordinate and aerodynamic data.

We have not included these outdated charts and decorative illustrations, and instead we have attempted to reproduce the original book in a form that covers the engineering and design principals in a way that doesn’t date the book in any obvious way. Thus we must apologize for a lack of strict fidelity to the original text, but we did this in the interest of producing a more immediate and interesting book.

Since Mr. Frati has no intention of reviving the book, we are happy to share it with everyone, first in installments of our Falco Builders Letter, and now in a book format that you can download from the Sequoia Aircraft web site at www.seqair.com. There are nine chapters in all.

This has been an enormous effort and after finishing the final page, I mentioned to Giovanni Nustrini “In my next lifetime, please remind me not to volunteer myself for a project like this. I’m not necessarily sorry I took it on, but what a pile of work! Any big project is like climbing a mountain, you never want to think of how high the mountain is, and just concentrate on the next few steps.”

However, now that all of this work is done, I intend to publish this book in an iBook to be available at the Apple iBookstore.

Alfred P. Scott

Introduction

Among the many types of flying machines that helped conquer our airways, from the most modest and delicate to the huge, rugged Flying Fortress with thousands of horsepower, there is one category of aircraft that does entirely without engines: the gliders.

The glider was developed in Germany after the first world war, and it found particular acceptance among younger pilots. Even though many used it as a new form of sport and excitement, others employed experimental gliders to advance their studies in aerodynamics and to develop new methods of construction.

Today, aviation owes a great tribute to these last individuals. In fact, the glider has taught a great deal to designers, builders and pilots. To realize how much, we need only look at how many ways our armed forces have used these vehicles in the recent conflict.

To build a glider, one needs no huge industrial facilities, complex technical equipment or large financial backing—just pure creativity, a clear understanding of aerodynamic phenomena, and a patient pursuit of perfection in design and construction. So even our country, thanks to the efforts and merits of the “Centro Studi ed Esperienze per il Volo a Vela” at the Milan Polytechnic, was able to compete vigorously in this field.

The author of this book is, in fact, a young graduate of our Polytechnic who has already tested his theories and practical notions by building several successful gliders.

In this volume, you will find in simple terminology all the necessary advice and information you’ll need to begin the project, complete the construction and fly your glider.

Don’t be frightened if this book seems rather large for such a simple subject. It also includes the specifications of a variety of gliders, so in addition to being a textbook, it is also a reference manual.

To the new student generation, may this book be the incentive to further cultivate the passion of flight.

Prof. Ing. Silvio Bassi
Milan, Italy
March 1946

Chapter 1

Preliminary Considerations

1. Soaring

Soaring is the complex of activities that results in the flight of a glider. To be exact: (a) to design and construct a glider, (b) to study a specialized aspect of meteorology, (c) to study the techniques of flying, and (d) to organize proper ground support.

In this book, we will discuss mainly the design of pure sailplanes, and only passing reference will be made to low-performance gliders used for dual instruction.

2. Gliders: Training and Soaring

Official Italian regulations define gliders as aircraft that are heavier than air and have no means of self-propulsion. The use of gliders varies: for dual instruction; for more specialized training in soaring; for aerobatic flight; and for distance, endurance, and altitude flights. A strict subdivision according to the particular use is difficult to make. In fact, from the training vehicle to the record-setting vehicle, there is a complete gamut of medium-performance but still important gliders.

As a convention, we will consider two major classes: gliders and sailplanes. Gliders are defined as those unpowered aircraft that due to their basic construction and flight characteristics are used only for free gliding. In this category, we'll find those gliders used for training. We consider sailplanes to be unpowered aircraft that due to their superior aerodynamics and construction have improved performance and can be used for true soaring.

To give an idea of the difference in performance, gliders generally have a minimum still-air sink rate of more than 2 m/sec, with a maximum glide ratio of approximately 10:1. Sailplanes, however, have a minimum sink rate less than 1 m/sec, and a glide ratio above 20:1. Under certain atmospheric conditions, admittedly, a glider can be made to soar, when the speed of the rising air is greater than the minimum sink rate of the glider. By the same token, even a high-performance sailplane can do no more than glide when rising air is absent.

In truth, even the most sophisticated sailplane is actually gliding—descending—in relation to the air mass within which it is operating. It will be soaring—gaining altitude—in reference to the earth's surface, but the altitude reached will depend on the relationship between glider and surrounding air, and the relationship between the air and the earth's surface.

Because of this anomaly, a glider “rises while descending.”

3. Aerodynamic Characteristics

The aerodynamic characteristics already mentioned are: efficiency, or glide ratio; and sink rate. Glide ratio is the ratio between the horizontal travel D and loss of altitude H in a given time. The value of this ratio,

$$E = D/H$$

is an indication of the quality of the glider, since at an equal altitude loss H , the distance D reached is proportional to the efficiency E , which can be expressed an efficiency value, say 20, or more commonly as a glide ratio, typically stated as 20:1.

The sink rate is the amount of altitude lost by the glider in the unit of time in relation to the surrounding air. This value is expressed in m/sec. Thus, from an altitude of 100 meters, a glider that has a minimum sink rate of 1 m/sec and a glide ratio of 20:1 will take 100 seconds to reach the ground after traveling a horizontal distance of 2000 meters. Modern competition sailplanes have achieved glide ratios of over 30:1, with minimum sink rates of .5 m/sec.

It is evident that the lower the sink rate, the longer the duration of any flight from a given altitude, and the higher the chance of being kept aloft by very light ascending air movements. At first glance, it would seem that obtaining the minimum possible sink rate would be of great importance for soaring. However there are two other factors of equal importance: the handling and the horizontal speed of the craft. To better understand this, let's briefly explain how soaring is achieved.

4. Practicality of Soaring

We can consider two types of soaring: thermal soaring; and ridge, or wave, soaring.

Thermal soaring takes advantage of the vertical movement of air masses caused by temperature differences. The rise of an air mass occurs when a so-called "thermal bubble" detaches from unevenly heated ground formations. These thermal currents are generally of small dimension. Larger masses of ascending air occur under cumulus clouds, and air movements caused by storm fronts are of particularly high intensity.

In ridge soaring, pilots take advantage of the vertical component that results from a horizontal air movement encountering a mountain, hill or slope.

In thermal soaring, either for endurance or distance, we try to gain altitude by flying tight spirals in a favorable site while the conditions are good. When conditions deteriorate and we cease to gain altitude, we move in search of a new area. It is obvious that when we are trying to gain altitude, the handling of sailplane is of great importance. The tighter the spiral flight, the greater the likelihood that we can stay within even the smallest thermals.

But during the straight-and-level flight from one rising mass to another, it is obviously important to do so as rapidly as possible to minimize the loss of altitude. In this case, it is important for the sailplane to be capable of the maximum possible horizontal speed and low vertical speed—i.e. high efficiency. Unfortunately, it is not possible to combine both pure speed and ultimate maneuverability, so a certain compromise between the two is necessary. Which preference is given to one over the other depends greatly on the intended use of the glider.

5. Launching Methods

Even though it is not directly related to a sailplane design project, it is important to know the launching methods used so we can study the airframe structure and the placement of the necessary hardware required for launching. Since the glider does not have an engine, it obviously needs some kind of external energy to get airborne. The launching methods most commonly used are: elastic cord, ground winch, automobile tow, and airplane tow.

Launch by Elastic Cord. This type of launching is the simplest and most economical, and it has been employed for several years by training schools in various countries.

An elastic cord is attached to the glider's nose while its tail is securely anchored to the ground. The cord is then stretched like a slingshot by two groups of people spread out at an angle of approximately 50-60°—so they won't be run over by the glider at the time of release. When the cord has reached the proper tension, the glider is freed. The slingshot action then catapults the glider into flight with an altitude gain proportional to the cord tensioning.

This system presents one major inconvenience: acceleration so high at the instant of launch that it can stun the pilot, with possible serious consequences. However, if the tension of the cord is reduced to diminish the acceleration effect, the glider will fail to gain sufficient altitude. For this reason, elastic-cord launching has been abandoned, except for launching from atop hills, where the acceleration can be reduced since only horizontal flight has to be sustained.

Launch by Ground Winch. This system has seen many modifications and improvements throughout the years. It is now the most practical and safest means of launching.

The system consists of a large rotating drum driven by a powerful motor. The glider is pulled by a steel cable, of approximately 1000 meters in length, that winds onto the drum. With this system, the speed of launching can be controlled, making a gradual and safe transition from ground to altitudes of 200-250 meters possible.

Launch by Automobile Tow. In the United States, it is common practice to tow a glider with an automobile. A cable of 1000 to 3000 meters in length is stretched between the automobile and the glider. This requires a paved runway or a well-maintained grass strip long enough so the automobile is able to reach the speed needed for the glider to fly.

Economically speaking, this system, is less efficient than a ground winch launch, which requires only enough power to pull the glider, while auto-tows need the extra power to run the automobile. As a bonus, however, altitude gain is far greater.

Launch by Airplane Tow. All the systems previously described are mainly used for launching of training gliders. For true sailplanes, it is essential to reach launch altitudes of between 500 and 1200 meters. The most practical way to accomplish this is a tow to altitude behind an airplane. A cable of 60 to 100 meters in length is stretched between the aircraft. When the desired altitude and conditions are reached, the cable is released by the sailplane.

This system has the advantage of not requiring a complex ground organization. The tow plane should be able to fly slowly, just over the cruising speed of the glider to avoid overstressing the glider and to allow it to maintain an altitude not too far above the towplane.

Chapter 2

General Characteristics of Gliders

6. Introduction

Because of their specialized use, gliders are quite different from powered airplanes. This is made obvious by several characteristics. One is the completely different arrangement of the landing gear, a result of the light weight of the aircraft and the absence of a propeller. Others are that the pilot's seat is located toward the front for center-of-gravity reasons, the wing span is always considerable, and the fuselage and other components are well streamlined to obtain the maximum aerodynamic efficiency.

Wood has been almost universally accepted as the prime building material. It is fairly inexpensive, practical to use, and easy to repair, even with simple tools. In some cases, a fuselage of welded steel tubing with fabric covering has been adopted. This provides a light and simple structure, but it will never beat the rigidity and aerodynamic finesse of wood construction.

A few examples of all-metal gliders are available, but this method of construction requires a well-equipped shop and specialized, skilled labor. The high cost involved limits such construction to high-volume, production-series aircraft, seldom the case with gliders.

Let's now consider the two major classes in which we categorize gliders and explain their characteristics in detail.

7. Training Gliders

This type of glider should be of simple construction, for low cost and easy maintenance. This is an important consideration, since a flight school often uses its own students to carry out small repairs, and the equipment at their disposal is usually not the best.

Gliders in this category should also be quite rugged, especially in the landing gear, since they often aren't flown with great skill.

A certain uniformity of design is characteristic of this class of glider. The wingspan is usually 10 meters, the wing area is 15-17 square meters, and the glider has a high, strut-braced wing of rectangular planform and a low aspect ratio.

The fuselage may be only an open framework of wood or tubing with the cockpit completely open, or it can be a closed, plywood-skinned box section. The wing loading of these aircraft is always very low, usually around 12-14 kg/square meters, and with an empty weight of 90-120 kg.

The wood wing is a double-spar structure, the spars braced together for torsion strength and the whole covered with fabric. The control surfaces are driven by steel cables and bushed pulleys, and the landing skid is incorporated in the fuselage and can be shock-absorbed.

In this glider there is absolutely no instrumentation, since due to their use it would be meaningless. The use of a parachute is also senseless; because of the low altitude of flight, a parachute would be useless in case of emergency. The common cruise speed is on the order of 50 km/h.

8. Sailplanes

Training Sailplanes. The uniformity of design that we have seen in training gliders does not exist in this category. In general, these designs have strut-braced wings, box-section fuselages, and open cockpits. The wing span is between the 12 and 14 meters, wing loading 15-17 kg/sq m, and they all have basic instrumentation.

Competition Sailplanes. As mentioned before, there are many variations of sailplanes. One may have a simple high wing and V tail, another a gull midwing. The wingspan may reach over 20 meters with variable flaps and up to 33 meters in some cases.

Particular care is given to the cockpit area, in terms of both instrumentation and pilot position. Reclining seats, adjustable pedals, cockpit ventilation, and anything else that might provide the pilot with the greatest possible comfort are important in these gliders, since endurance flights have lasted longer than 50 hours, and distance flights have reached the 700-km mark.

Almost all these gliders are single seat, but two-seat sailplanes are increasing in popularity, especially for endurance and distance flights. In these cases, the sailplanes have dual controls. The seats can either be side-by-side or tandem.

In the case of a tandem configuration, the second seat coincides with the aircraft's center of gravity, so the balance does not change whether flying with one or two persons. One advantage of the tandem configuration is to maintain the fuselage cross-section at a minimum, therefore increasing efficiency. While the aerodynamics of the side-by-side configuration aren't as good, the pilot's comfort and the copilot's visibility are improved.

9. The Structure of Sailplanes

While today's gliders may differ in design, they are all very similar in basic structure. Let's quickly describe the principal structures, keeping in mind that we will be referring to wood construction.

Wing Structure. The wing structure that has been in use for a number of years is based on a single spar with a D-tube torsion box. This design was developed in order to obtain the necessary strength in the long wingspan with minimum weight—an important concept in gliders. This is achieved by placing one single spar in the area of maximum wing thickness, of roughly 30-35% of the wing chord.

In these wings, there is always a second smaller aft spar, between 60-70% of wing chord. Its purpose is not to increase the wing strength, but merely to supply a mounting surface for the aileron hinges and to maintain the wing ribs in the proper position; otherwise they would be distorted by the tensioning of the covering fabric.

Notwithstanding the actual shape of the wing, the spar can be of three classical types: (a) double-T frame with center web, (b) C-frame with one side web, (c) box spar with two webs, one on each side. In sailplane construction, the most-used method is the third one—the box spar.

The spar is the element that withstands the forces of bending and drag. The wing is also affected, especially at high speeds, by great torsion forces. In the single-spar structure, this torsion is resisted in part by the box-like structure that exists between the leading edge and the spar (an area covered by thin plywood) and in part by the spar web itself.

The torsion is then transferred to the fuselage by the wing attachments. The usual solution is to transfer the torsion through a properly placed aft diagonal member that extends from the spar back toward the fuselage.

The area between the spar and the diagonal member is also covered with plywood to produce a closed and torsion-resistant structure.

A much simpler and more rational system is to transfer the torsion by means of a small forward spar. This will not only improve the flight characteristics of the assembly, but it offers a gain in weight due to the elimination of the cover between the spar and the diagonal.

The reason that this system is little used is due to the difficulty encountered in the connection of the forward part of the wing with the fuselage, which at this point usually coincides with the cockpit, and which does not offer sufficient strength for the connection.

The other structural elements of particular importance, since they contribute to the wing's shape, are the wing ribs. In most gliders, these ribs are of the truss style of design, and the members are glued in place and reinforced with gussets on each side. The truss may be made up of both vertical and diagonal members, or only diagonal members.

Sometimes, the ribs are completely covered with plywood on one surface, and in this case the diagonal members are omitted and only the vertical braces are used. This structure is much simpler than the truss, but it is slightly heavier and more costly.

The ribs are joined to the spar in two ways: full-chord ribs are slid over the spar, or partial ribs are glued to the spar faces and reinforced by gussets. The second method is more common because it allows for a thicker spar without any increase in weight.

Fuselage Structure. The fuselage is made up of wooden frames connected to each other by wooden stringers and finally covered with plywood. On tubular metal frames, a fabric covering is usually used. The fuselage frames are always of the truss type, with gusset connections like the ones we have seen in the rib construction. For the frames subjected to high stress, a full plywood face on one or both sides is used.

With a plywood skin covering, it is possible to obtain great torsional strength, while bending forces are resisted by the horizontal stringers and the portion of plywood covering glued to the same stringers.

The strongest frames should be the ones that attach to the wings, because they must support the plane's full weight. The frames that support the landing gear should also be particularly strong.

A fixed single wheel is attached to the fuselage with two wooden members between frames. There is no need for shock absorption, since the cushioning of the tire itself is sufficient. In the case of retractable gear, various retraction systems are used, but they always have considerable complications.

For the wing/fuselage connection, as in the most common case where each wing is a separate piece, the system currently adopted is one in which the wings are first connected with metal fittings and then the wing, now as one unit, is connected to the fuselage by

less complicated attachments. This way, the fuselage is not affected by the considerable forces of wing bending and needs to support only the wing weight and the forces applied to it.

Tail Section. The structure of the tail section is similar to that of the wing: a spar of box or C shape, truss-style ribs, plywood covering for the fixed surfaces (stabilizer and fin), and fabric covering for the control surfaces (elevator and rudder).

Sometimes the stabilizer is of a twin-spar structure with plywood covering from leading edge to forward spar and fabric covering for the remainder. This solution is of limited value, though, since the weight saving obtained the reduction of the plywood covering is balanced by the extra weight of the double spar, and obviously also by the extra construction complication encountered.

The elevators and the rudder, like the ailerons, are fabric-covered to reduce the weight, and this is also necessary to keep the inertia of the moving mass small. The required torsional strength is achieved by diagonal members between ribs, while more sophisticated gliders have a semi-circular plywood section on the leading edge of the control surfaces.

Chapter 3 Elements of Aerodynamics

11. Aerodynamic Force

A stationary body immersed in a flow of air is subjected to a force that is the total of all forces that act upon it. This resultant force is called the aerodynamic force and is designated by the letter F . Generally, the direction of this force is different from the air flow direction.

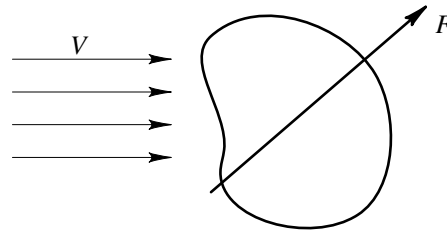


Figure 3-1

If the body has a symmetrical shape relative to the air flow, the aerodynamic force is also in the same direction.



Figure 3-2

However, if the same body is rotated in relation to the air flow at the angle α (“alpha”), called the angle of incidence, the direction of the force F is no longer in the direction of the air flow and is usually at a different angle than the angle of incidence.



Figure 3-3

The reason the force F is not in the same direction as the air flow is due to the difference in velocity of the air particles between the upper and lower surfaces of the body. This phenomenon was studied by Magnus and is demonstrated by Flettner’s rotating cylinder.

Rotating Cylinder. Let’s immerse a cylinder in a flow of air. This flow will produce a force F on the cylinder in the same direction, because the cylinder is symmetric with respect to the flow.

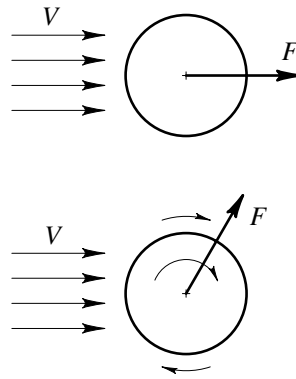


Figure 3-4

Now, if we rotate the cylinder around its axis in the direction shown, the fluid particles in direct contact with the surface will be carried by friction. Notice that while the velocity of the particles over the upper surface will be added to the stream velocity, in the lower portion the velocity will subtract. The result is a higher stream velocity in the upper surface and a lower velocity in the lower surface.

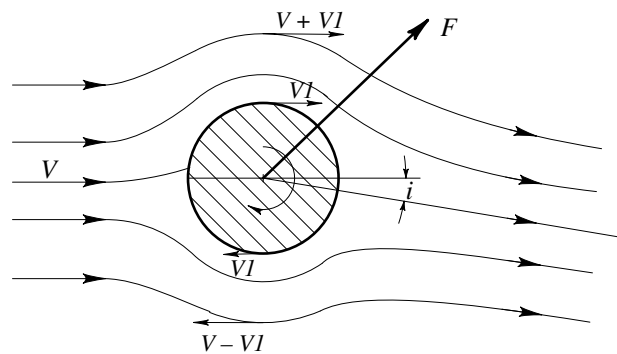


Figure 3-5

Thus, the motion of the fluid particles around the cylinder is a combination of the effects of the direction of the stream and the rotation of the cylinder. The direction of the air downstream of the cylinder is now at the angle i , called the induced air flow angle. The value of the aerodynamic force depends on various factors:

- air density ρ (“rho”—mass density of standard air)
- area of the body S
- relative velocity V (air flow velocity in relation to the body)
- shape and orientation of the body in relation of the direction of the stream, a factor we will call C .

Analytically, the dependence of F is expressed by the following equation:

$$F = C \cdot \rho \cdot S \cdot V^2 \quad [1]$$

where the units of measurement are:

- F = force in kg.
- V = velocity in m/sec.
- S = area in m^2
- ρ = density in $kg. sec^2/m^4$
- C = nondimensional coefficient

12. Airfoils

A solid section of particular importance is the airfoil. Its shape is such that the air flow around it generates a field of pressure that is a combination of fluid movements along and around it, as in the case of the rotating cylinder. In other words, a uniform air flow will undergo an increase in velocity over the upper surface of the airfoil and a decrease over the lower surface.

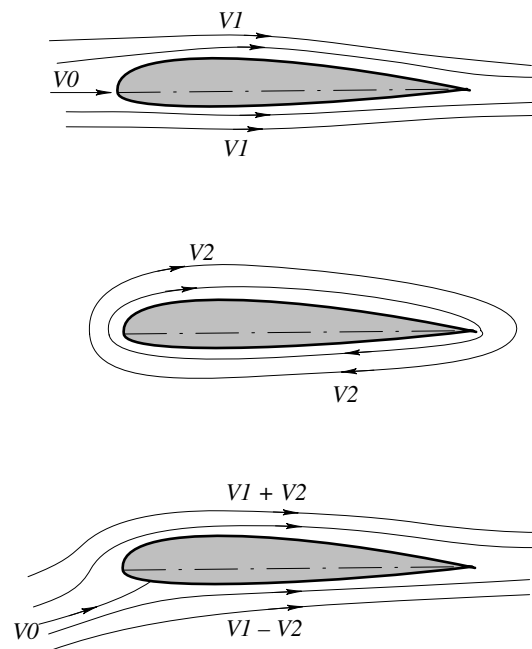


Figure 3-6

Due to the well-known Bernoulli theorem, we will have a decrease of pressure where the velocity increases and an increase of pressure where the velocity decreases. The aerodynamic force F therefore depends on positive pressure along the bottom and negative pressure—suction—on the top. The pressure and suction vary with the angle of incidence of the air flow.

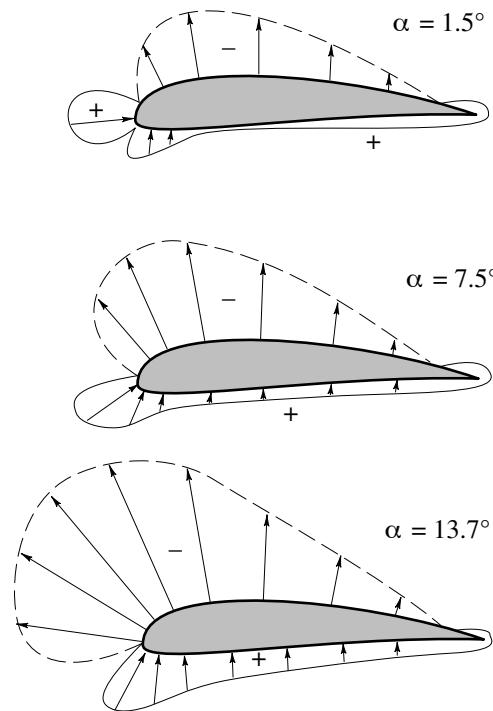


Figure 3-7

As you can see, the suction is much greater than the pressure at normal flight conditions. This means that the lift of the wing is due more to a suction effect than a pressure effect, contrary to what it may seem at first sight. In short, we may say that an airplane flies not because it is sustained by the air underneath, but because it is sucked by the air above it.

This experimental observation was of great importance in the understanding of many phenomena of flight. Moreover, this should be considered when designing the wing structure and skin covering, especially for very fast aircraft.

Lift and Drag. When we say “airfoil,” we are really talking about a section of a wing with its vertical plane parallel to the longitudinal axis of the aircraft. Let’s consider the force F in this plane, and let’s split it in two directions, one perpendicular to the direction of the relative velocity, and one parallel.

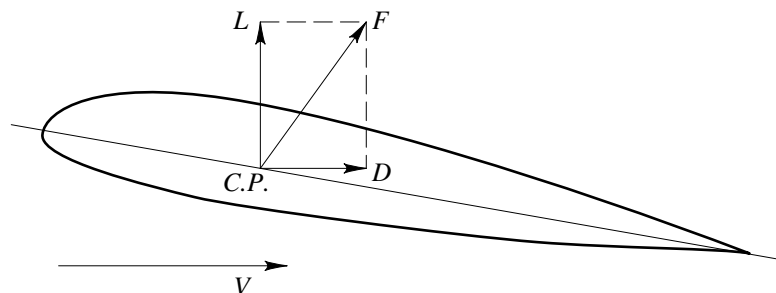


Figure 3-8

Let's call lift L and drag D . Flight is possible when the lift L is equal to the weight W . In the same manner as we have seen for the aerodynamic force F , lift and drag are expressed by the following equations:

$$L = C_L \cdot \left(\frac{\rho}{2}\right) \cdot S \cdot V^2 \quad [2]$$

$$D = C_d \cdot \left(\frac{\rho}{2}\right) \cdot S \cdot V^2 \quad [3]$$

where the non-dimensional coefficients C_L and C_d are called the coefficient of lift and coefficient of drag, respectively.

These coefficients are obtained in wind tunnels, which work on the principle of reciprocity. In other words, an air flow with velocity V will impose a force on a stationary body equal to the force derived from the body moving with velocity V in an atmosphere of stationary air.

The airfoil model under analysis is suspended from scales, which will register the forces that are caused by the wind. By changing the dimensions of the model and the velocity of the air, the forces on the airfoil will also change. The results are then reduced to standard units independent of the airfoil dimensions and the air velocity. The units measured are square meters for the surface area and meters per second for the velocity.

In reality, things are not as simple as this. The measurements given by the scales require a large number of corrections. These depend upon the characteristics of the wind tunnel and the Reynolds Number used in the experiment. However we will not elaborate on this, because the subject is too vast.

Center of Pressure. The intersection of the aerodynamic force F with the wing chord is called the center of pressure. It is shown with the letters $C.P.$ in Figure 3-8.

As we have seen so far, the aerodynamic force F is represented in magnitude and direction as a resultant of L and D . But as far as its point of origin (center of pressure) is concerned, things are not that simple. In fact, the force F for certain angles of incidence of lower lift will no longer cross the wing chord; therefore the $C.P.$ is no longer recognizable. We will see later how we can get around this.

Angle of Incidence. The pressure, suction, aerodynamic force, lift and drag will vary with the angle of the solid body form with the relative direction of the air flow. This angle of incidence is normally defined as the angle between the relative direction of the air flow and the chord line of the airfoil.

Efficiency. The ratio between lift and drag is very important in aerodynamics. This ratio is called efficiency, and it is indicated by the letter E .

$$E = \frac{L}{D} = \frac{C_L}{C_d} \quad [4]$$

Physically, efficiency represents the weight that can be lifted for a given amount of thrust. It is obvious, therefore, that is important to always obtain the maximum value of

E by reducing drag to a minimum. The efficiency $E = C_L/C_d$ improves gradually by increasing the wing span, as we will see later. The experimental values of C_L , C_d , and E of airfoils obtained in wind tunnels are generally for aspect ratios of 5 or 6.

13. Charts

To aid in the understanding of aerodynamics, it is helpful to show the characteristics of an airfoil in orthogonal or polar charts. Since the coefficients C_L and C_d are always less than one, their values are multiplied by 100 in these charts.

Orthogonal Charts. In this type of chart, the coefficients C_L , C_d and E are functions of the angle of incidence α . On the vertical axis, we have the C_L , C_d and E coefficients, and the angle of incidence α is on the horizontal axis. Thus we have three curves relative to C_L , C_d , and E . To obtain the value of a coefficient at a certain angle of incidence, for instance $\alpha = 6$ degrees, you draw a vertical line from the incidence angle axis equal to the given value. And for all the points of intersection of this line with the three curves, you draw corresponding horizontal lines to determine the values for C_L , C_d and E .

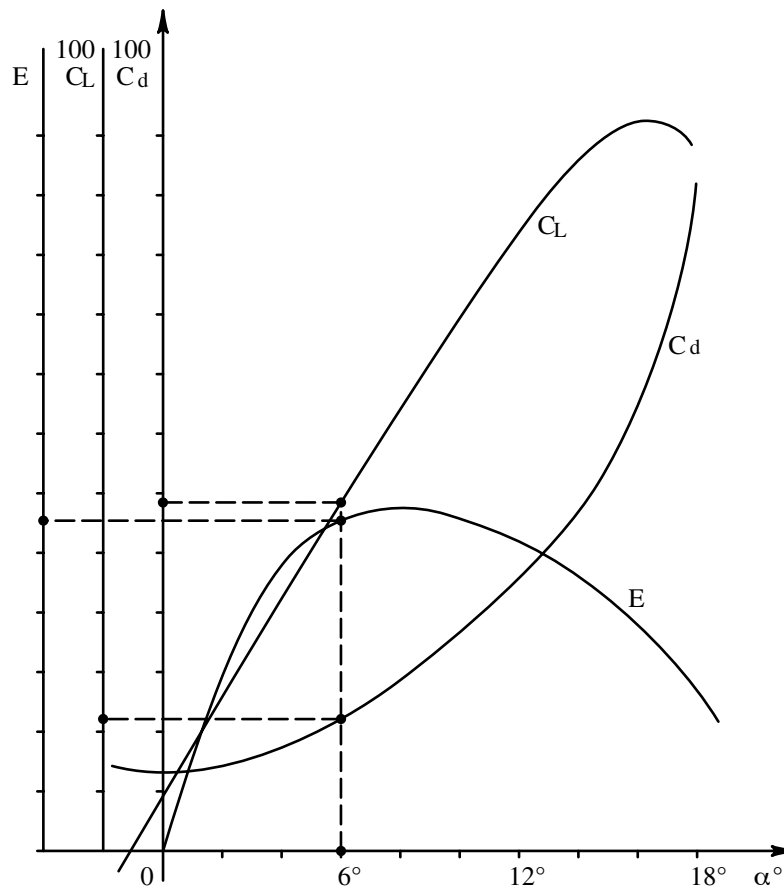


Figure 3-9

Polar Charts. In a polar chart, we have the value of C_d on the horizontal axis, and the value of C_L on the vertical axis. The values of C_L and C_d are given by a single curve called the polar profile, on which the angle of incidence alphas are marked.

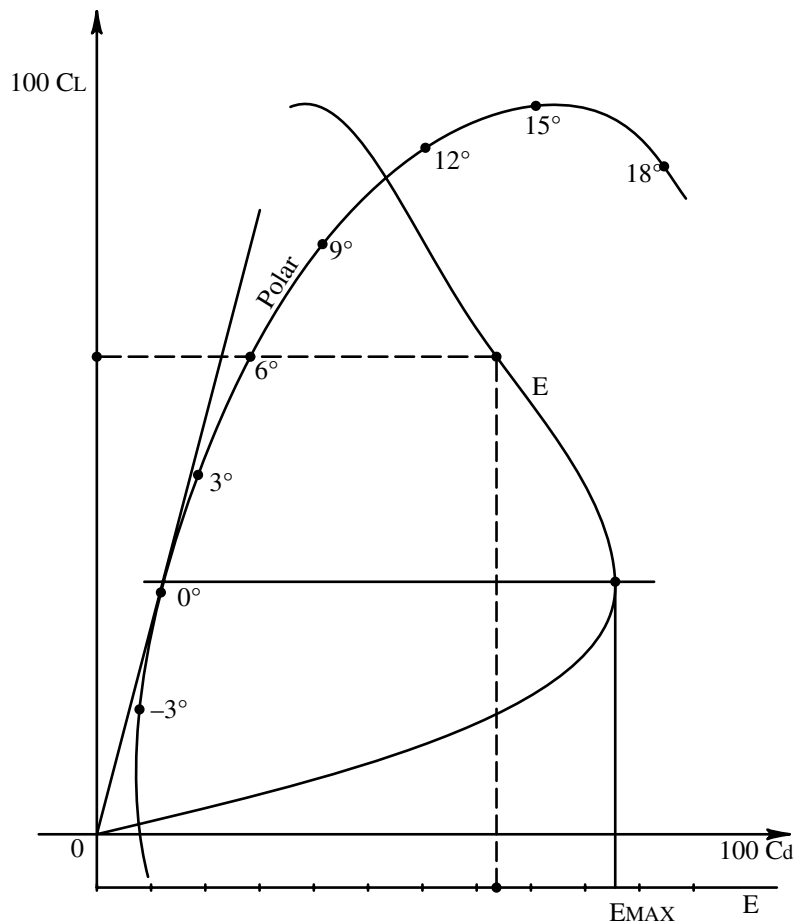


Figure 3-10

To determine these values for a certain incidence, for example $\alpha = 6$ degrees, on the point on the curve corresponding to that incidence you draw two lines, one vertical and one horizontal. The value of C_L and C_d are read on the proper corresponding axis.

A feature of the polar profile is that the point of tangency with a line drawn from the origin of the axes represents the angle of incidence of maximum efficiency.

The curve of the efficiency E relative to C_L is also shown in the polar chart. At a given angle of incidence, its value is obtained by drawing a horizontal line that will intersect the E curve. At this point of intersection a vertical line is drawn, and the value is read on the proper scale.

14. Moment of an Airfoil

To establish the position of the center of pressure, we first determine the moment of the aerodynamic force F with respect to a point on the airfoil. By convention, the leading edge is used. The moment and the coefficient of moment C_m are determined in a wind tunnel as was done for lift and drag.

The moment M is:

$$M = C_m \cdot \rho \cdot S \cdot V^2 \cdot c \quad [5]$$

where

c = chord of the airfoil
 C_m = coefficient to be determined

Having found the value for M by various measurements in the wind tunnel, the coefficient C_m will be:

$$C_m = \frac{M}{\rho \cdot S \cdot V^2 \cdot c} \quad [6]$$

where M is measured in kgm and c in meters.

Having found the moment, we now establish the position of $C.P.$

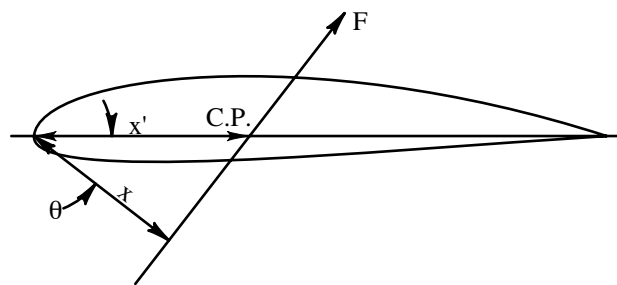


Figure 3-11

Let's consider the force F and its moment with respect to the leading edge. We can calculate the arm length x from F since

$$M = F \cdot x$$

then

$$x = \frac{M}{F}$$

The position of $C.P.$ is given by x' which is equal to

$$x' = \frac{x}{\cos \theta}$$

For normal angles of incidence, angle θ is very small so we can substitute L and F , giving

$$x' = \frac{M}{L}$$

and substituting M and L we will have

$$x' = \frac{\rho \cdot S \cdot V^2 \cdot C_m \cdot c}{\rho \cdot S \cdot V^2 \cdot C_L} = \frac{C_m \cdot c}{C_L}$$

If we would like to express the position of $C.P.$ in percent of the chord as it is usually expressed, then we have:

$$\frac{x'}{c} = \frac{C_m}{C_L} \quad [7]$$

In conclusion, we can say that the position of $C.P.$ in percent of the chord for an airfoil at a given angle of incidence is given by the ratio between the coefficient of the moment C_m and the coefficient of lift C_L at that angle of incidence.

15. Moment Equation and its Properties

The equation for the moment is represented by a polar chart as a function of the coefficient of lift. This curve is essentially a straight line until just before the maximum lift value is reached.

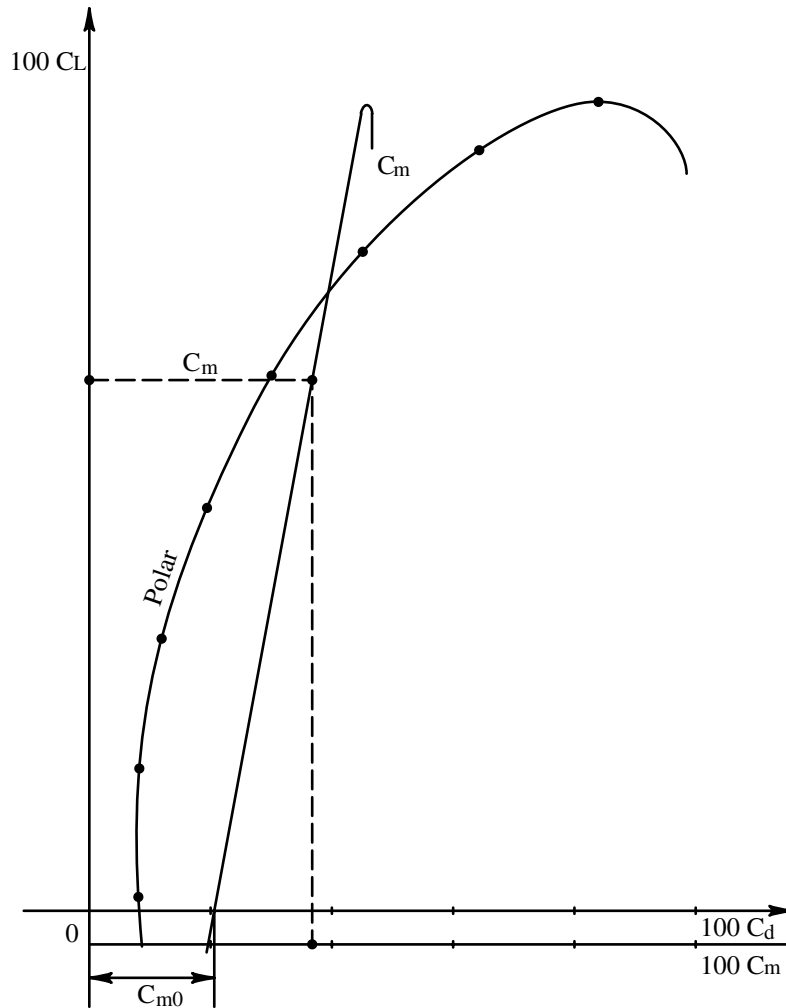


Figure 3-12

The value of the coefficient of moment in relation to zero lift, $C_L = 0$, is of particular importance in determining the airfoil's stability. This intersection on the horizontal axis is called C_{m0} . The position of the center of pressure may be determined graphically in the polar chart by looking at the moment curve.

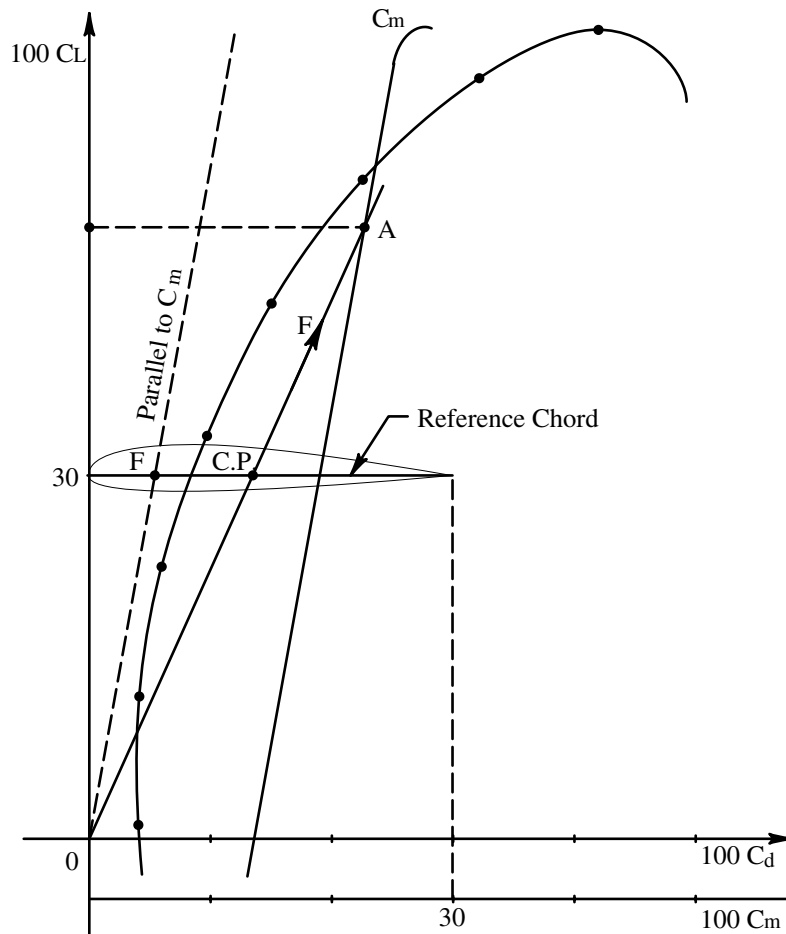


Figure 3-13

For a given value of C_L , a horizontal line is drawn with its origin on the vertical axis and its length equal to the value of C_m , i.e. $100 C_L = 30$, $100 C_m = 30$. This line is called the reference chord.

To determine the position of *C.P.* at a certain C_L value, a horizontal line is drawn through the C_L value in consideration, so that it will intersect the C_m curve at a point *A*. The line drawn from the axis origin *O* and the new-found point *A* or the extension of this line will intersect the reference chord at a point that represents the center of pressure.

Grade of Stability of an Airfoil. This graphic construction allows us to arrive at important conclusions about the stability of an airfoil. We can have three cases: (a) the moment curve intersects the horizontal axis to the right of the origin, (b) the curve coincides with the origin, or (c) the curve intersects the horizontal axis to the left of the origin.

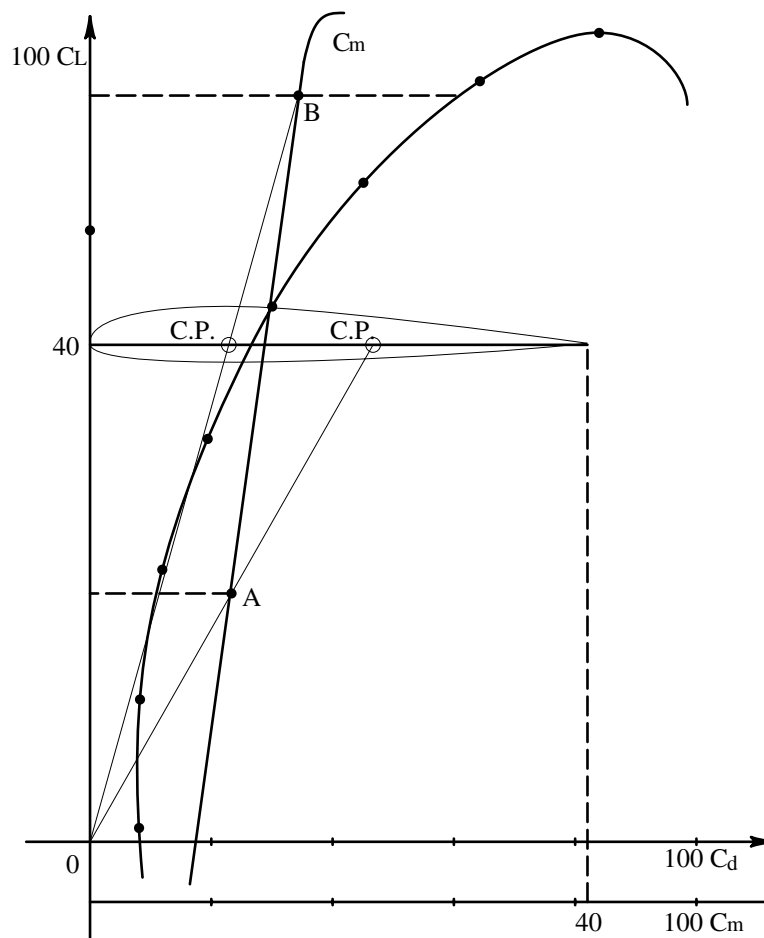


Figure 3-14

Case A. In this case, the curve intersects the horizontal axis at a positive value of C_{m0} . Let's determine, using the previous procedure, the position of the *C.P.* for a value of low lift, where *A* is the position of equilibrium. Let's suppose that now we increase the incidence angle, thus increasing lift (point *B* on the moment curve). We'll notice that the *C.P.* moves forward, toward the leading edge. On the other hand, if the incidence is reduced, the *C.P.* will move aft towards the trailing edge.

Therefore, in an airfoil where C_{m0} is positive, when a variation occurs, the center of pressure will move in a direction that helps to increase the variation. We then deduce that an airfoil with such characteristics is unstable because any variations will be accentuated and moved further away from the position of original equilibrium.

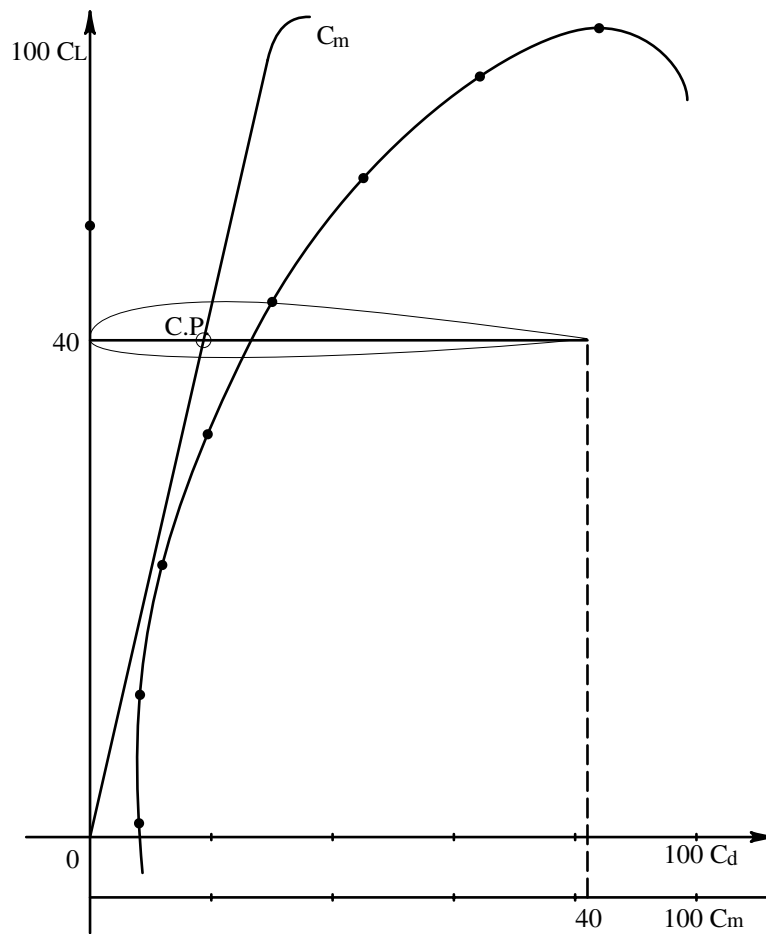


Figure 3-15

Case B. In this case, $C_L = 0$, $C_{m0} = 0$, and the curve goes through the origin. From the chart we note that for any variation the position of *C.P.* does not move, and it coincides with the focus of the airfoil. An airfoil with this characteristic is said to have neutral stability.

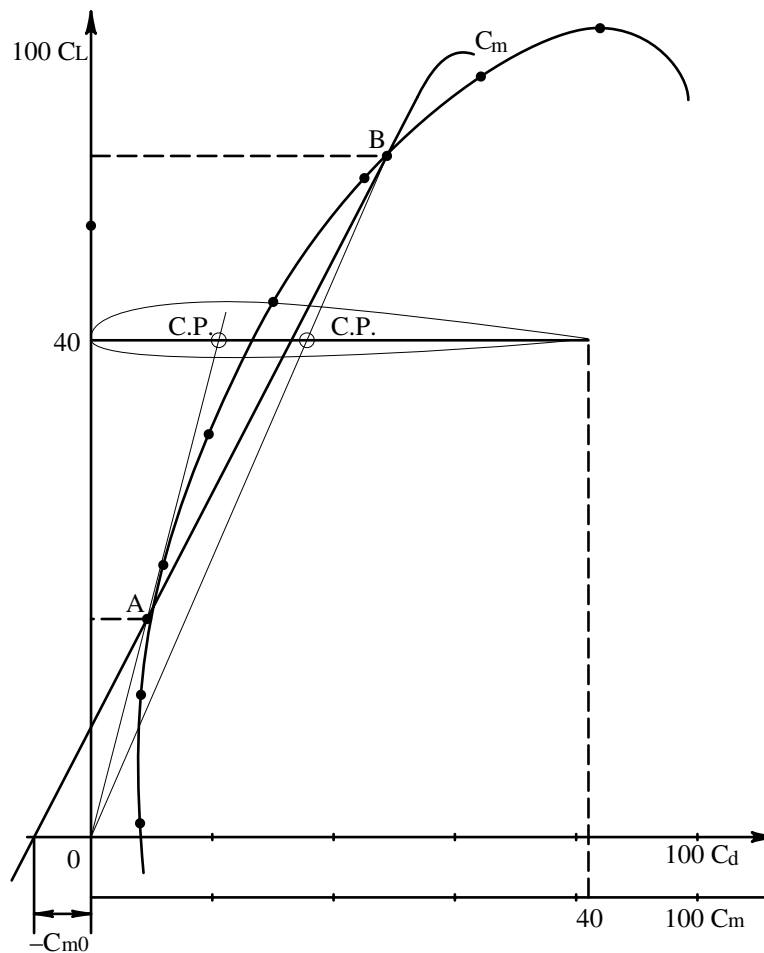


Figure 3-16

Case C. Let's now consider the third condition. For zero lift, C_{m0} is negative. The effect of the center of pressure is therefore opposite the one noticed in Case A. For an increase in incidence, the *C.P.* will move toward the trailing edge, and forward when the angle of incidence is reduced. In these conditions, the airfoil is stable.

All of the airfoils in use, however, are designed as in Case A—they are therefore instable. Airfoils that are unaffected by variations (Case B) are used in tail sections. Their profiles are biconvex and symmetric.

Surfaces that are flat are the one like in Case C, these are stable, but obviously they are not used in the wing construction, both because of the impossibility of obtaining structural strength and because of the low values of lift and efficiency. There are in existence some airfoils that follow the characteristics of these flat surfaces, and these are called autostable, but their use is limited to wing extremities.

The instability is at maximum in concave convex profiles with high degree of curvature, and it diminishes gradually through lesser degree of curvature in the biconvex asymmetric airfoils to, as we have seen, completely disappear in the symmetric biconvex profiles.

The measurement of instability of an airfoil is in conclusion dependent on the movement of the *C.P.* with variation of incidence. In the normal attitude of flight, the position of *C.P.* varies between 25-45% of the wing chord when normal wing airfoils are considered, while for biconvex symmetric profiles found in the tail sections, the variation is 25%.

By studying the moment curve we can thus rapidly establish the instability of a certain airfoil, and say that the closer to the origin the moment curve intersects the horizontal axis (small values of C_{m0}), the flatter the curve is, and the less the instability is.

Moment Arm. Let's suppose we now would like to find the moment, not in relation to the leading edge as we did previously, but in relation to any point on the chord of the airfoil in question, let us say point *G* for an attitude corresponding to the point *A* for the moment curve in Fig. 3-17.

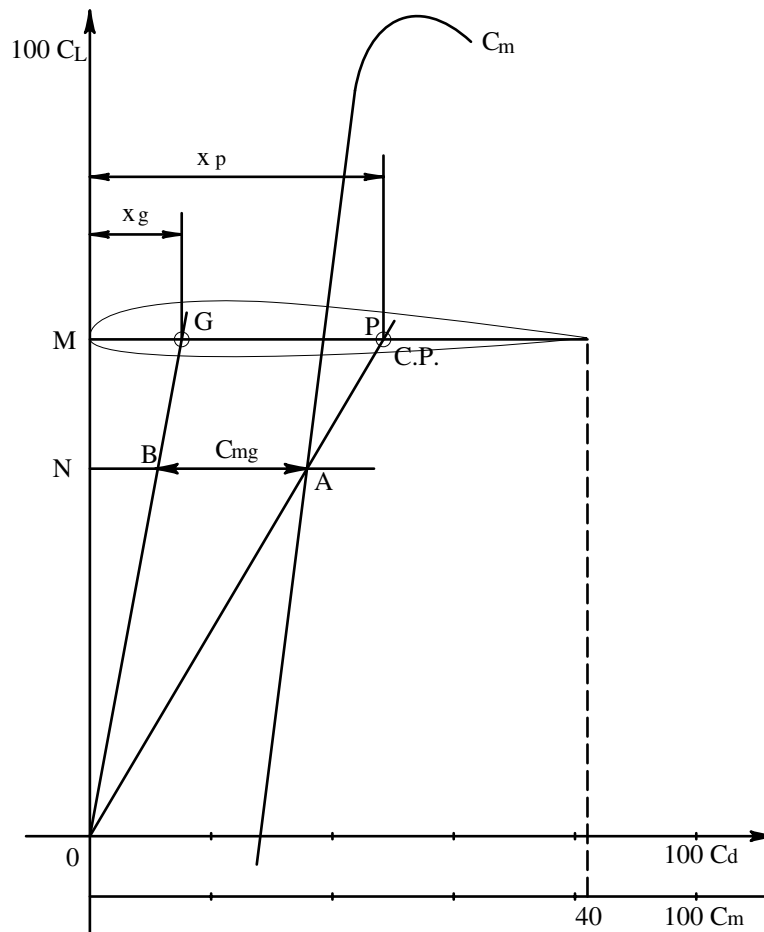


Figure 3-17

Joining points *G* and *A* with the origin *O*, the extension of the line *OA* will determine on the reference line the center of pressure *C.P.*, while the line *OG* will intersect the horizontal line between *A* and *B*. The line *AB* represents, on the C_m scale, the moment of the aerodynamic force for the attitude under consideration in relation to the point *G*.

Thus, if we name x_g the distance of the point G from the leading edge, and x_p the distance of $C.P.$, due to the similarity of the triangles MOG and NOB , MOP and NOA , we have:

$$\frac{x_p}{x_p - x_g} = \frac{NA}{BA}$$

In the chart, NA is the moment C_m in relation to the leading edge and BA is the moment C_{mg} in relation to the point G . If point G happens to be the fulcrum of the aircraft, relative to which we need to determine the moments, these are then found simply by connecting the origin O with the fulcrum G on the reference chord; the horizontal segment found between the said lines and the moment curve will give us the moment fulcrum for that given attitude. This line, which starts at the origin and passes through the fulcrum G , is called the fulcrum line.

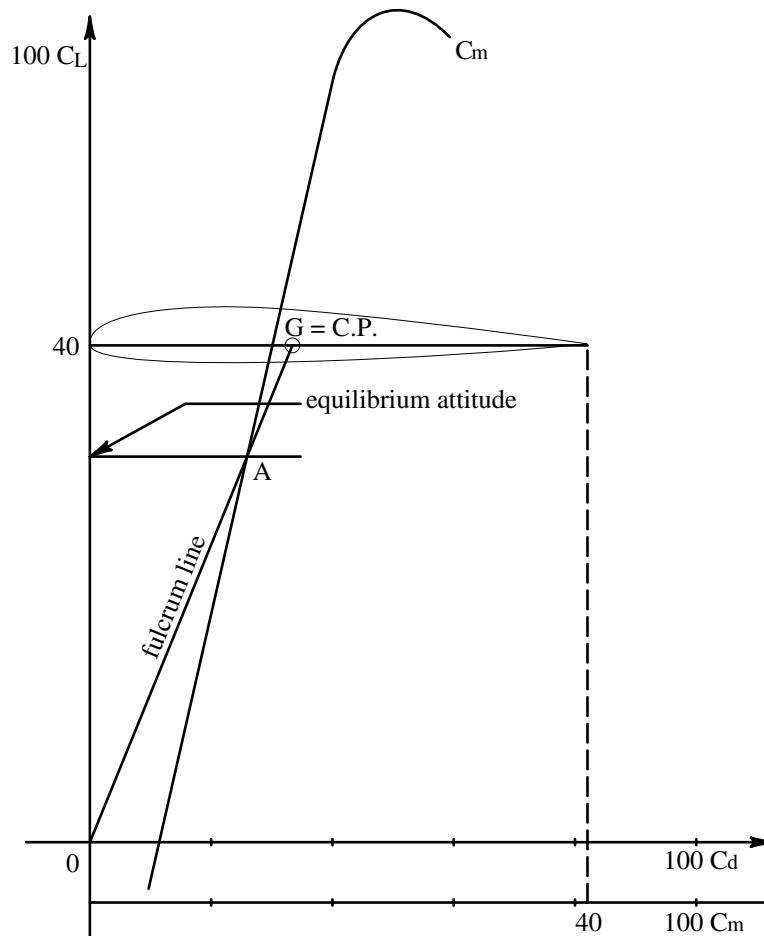


Figure 3-18

Following this we may establish, given the fulcrum G on the reference chord, the equilibrium attitude, by drawing a horizontal line through the intersection of the fulcrum line and the moment curve. (Fig. 3-18) The $C.P.$ of this particular attitude coincides with the fulcrum G . These properties of the chart allow us to study the aircraft's stability graphically, as we will see later on.

16. Wing Aspect Ratio

Thus far we have discussed C_L and C_d without considering one very important factor of the wing, the wing aspect ratio AR . This is the ratio between the wing span and the mean chord:

$$AR = \frac{b}{c_m} \quad [8]$$

where, b is the wing span and c_m is the mean chord, however the following expression is more widely used:

$$AR = \frac{b^2}{S_w}$$

where S_w is the wing area.

To better understand the effect of the aspect ratio on the wing coefficients, let's remember how the lift phenomenon works. We have seen that during normal flight conditions lift depends on pressure below and suction on top of the wing. Thus the air particles will have a tendency to move at the wing tips from the high pressure zones to the low pressure zones by revolving around the wing tips.

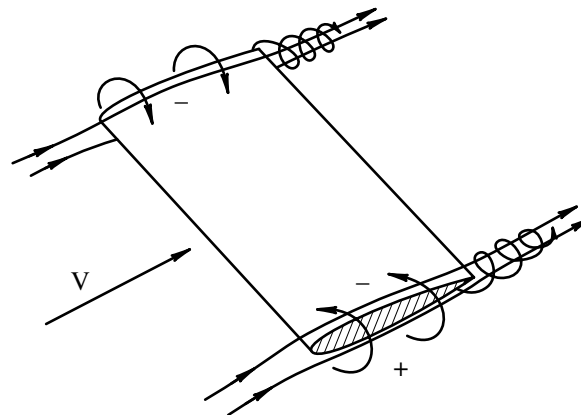


Figure 3-19

Since the air flows in direction V , the air particles at the wing tips will have a spiral motion. This is the so-called vortex, and it produces an increase in drag and a decrease in lift. The larger the wing chord at the tip, the larger are the produced vortices. An increase in the aspect ratio causes a reduction in the wing chord, and thus a reduction of drag, which depends on two factors, profile drag (C_{dp}) and induced drag (C_{di}).

$$C_d = C_{dp} + C_{di} \quad [9]$$

The coefficient of induced drag is given by:

$$C_{di} = \frac{2(C_{dp})^2}{\pi} \cdot \frac{1}{AR} \quad [10]$$

This induced drag is, in fact, the one produced by the vortex at the wing tips.

For a wing with an infinite aspect ratio, AR equals infinity, the induced drag C_{di} is 0, and the drag is only the profile drag. From Formula 10, we notice how the induced drag C_{di} depends on the lift C_L , and this is explainable by the lift phenomenon itself. The larger the C_L , the larger the difference between the pressure and suction, thus the larger the intensity of the vortices. The aspect ratio therefore influences the induced drag while the profile drag remains the same.

The variation of C_{di} with the variation of the aspect ratio is found in the following relationship:

$$\Delta C_{di} = \frac{2(C_L)^2}{\pi} \cdot \left(\frac{1}{AR_1} - \frac{1}{AR_2} \right) \quad [11]$$

where AR_1 and AR_2 are the two values of the aspect ratio. During practical calculations, AR_1 is the experimental value given by tables and generally is equal to 5, while AR_2 is the real one of the wing.

The coefficient C_d' of a wing with aspect ratio AR_2 will be :

$$C_d' = C_d - \frac{2(C_L)^2}{3.14} \cdot \left(\frac{1}{AR_1} - \frac{1}{AR_2} \right)$$

Since the vortices increase drag and destroy lift, an increase in aspect ratio will improve lift as a result. In practice though, these improvements are ignored because they are small values.

Influence of the Aspect Ratio on the Polar Curve. Let us examine the changes to the polar curve with an increase of the aspect ratio.

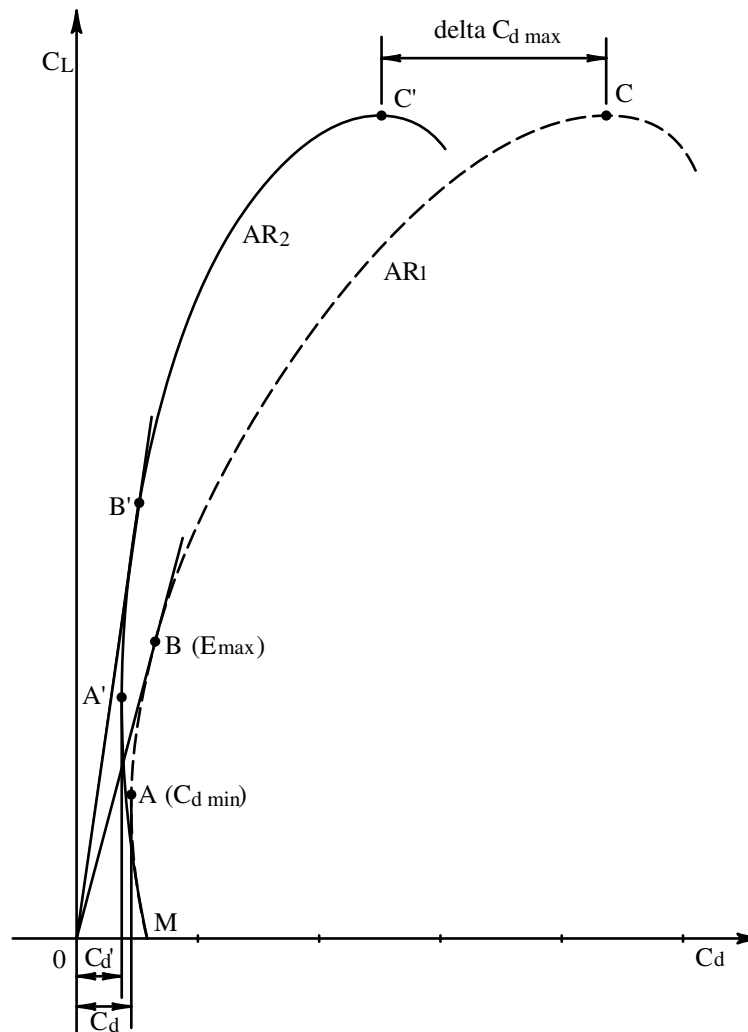


Figure 3-20

Let's consider the polar curve relative to the aspect ratio, AR_1 (dashed line), and let's increase the value to AR_2 . Calculating the values for different attitudes, we establish the values of C_d' relative to AR_2 . This new polar curve (solid line) will intercept the horizontal axis at the point M , this being the same point as the original curve intercepted, since $C_L = 0$ and the variation $\Delta C_d = 0$. For increasing values of C_L , the variation ΔC_d is negative, and it will increase until it reaches its maximum value at the maximum value of lift, a value given by the line $C-C'$.

From this new curve we can see that the attitude of maximum efficiency has moved to greater angles of incidence and a greater minimum value for drag. Thus, increasing the aspect ratio gives a double advantage: (a) a reduction of drag, with subsequent increase in efficiency and (b) movement towards attitudes of greater lift with minimum drag. This very important for gliders which always operate at attitudes of high lift.

We should consider though that the aerodynamic coefficients are also influenced by the shape of the wing itself. The optimum shape would be of an elliptical form that resembles the distribution of lift. As a matter of fact, in fighter planes, where the aspect ratio is rather small, this type of shape is often used. These wings are very complicated to build, so for gliders where the aspect ratio is always high, a linear form with a slight curvature at the wing tips gives optimum results.

17. Wing with Varying Airfoils

It is often of more convenient to build a wing with varying airfoils. In modern planes, this is usually the case. A constant-airfoil wing is rarely used. For structural reasons, the wing is usually thick at the connection with the fuselage. It is here that the greatest forces of bending and shear are applied. As we move toward the wing tips, the airfoil is much thinner to reduce drag and to improve stability and efficiency. For these and other reasons, the wing is almost never of constant chord.

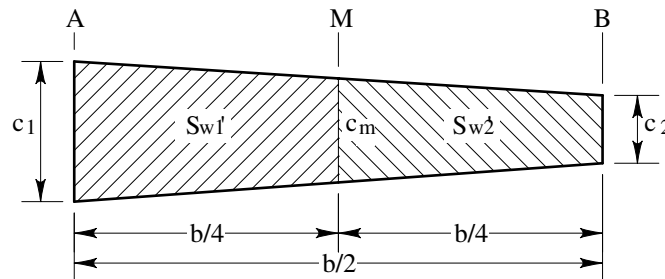


Figure 3-21

Let's see how we can determine the wing characteristics when the airfoil is variable. Let's consider a wing with a shape as shown above, where the airfoils are *A* at the wing root and *B* at the tip. If the variation between *A* and *B* is linear, as is usually the case, then we can accept that the airfoil *M* in the middle would have intermediate characteristics between *A* and *B*. This is not precisely correct due to induction phenomena between adjacent sections, but practical tests show that this hypothesis is close enough to be accepted for major calculations of wing characteristics.

With this hypothesis in mind, where the intermediate airfoil has intermediate characteristics, we can now consider the portion between *A* and *M* to have the characteristics of airfoil *A*, and the portion between *M* and *B* to have the characteristics of airfoil *B*.

The area S_{w1}' of the half wing relative to *A* will be:

$$S_{w1}' = \frac{c_1 + c_m}{2} \cdot \frac{b}{4}$$

and the area relative to *B*:

$$S_{w2}' = \frac{c_m + c_2}{2} \cdot \frac{b}{4}$$

These areas will be doubled for the full wing, thus for the airfoil *A* it will be S_{w1} , for the airfoil *B* it will be S_{w2} . ($S_{w1} = 2 \cdot S_{w1}'$ and $S_{w2} = 2 \cdot S_{w2}'$) The ratio between these areas,

(S_{w1} and S_{w2}) and the total wing area S_w is called the coefficient of reduction. Thus we have:

$$X_1 = \frac{S_{w1}}{S_w} \text{ for airfoil } A$$

$$X_2 = \frac{S_{w2}}{S_w} \text{ for airfoil } B$$

These coefficient of reductions, X_1 and X_2 , are less than 1, and their sum is obviously:

$$X_1 + X_2 = 1$$

The coefficients C_L , C_d , and C_m of the airfoils A and B are multiplied by the respective coefficients of reduction X_1 and X_2 . These new reduced values are then added together to the coefficients C_L , C_d , and C_m of the wing. Summarizing, if we say that C_{LA} , C_{dA} , C_{mA} are the coefficients of the airfoil A , and C_{LB} , C_{dB} , C_{mB} are the coefficients of the airfoil B , then the ones for the complete wing, C_L , C_d , C_m will be:

$$C_L = (C_{LA} \cdot X_1) + (C_{LB} \cdot X_2)$$

$$C_d = (C_{dA} \cdot X_1) + (C_{dB} \cdot X_2)$$

$$C_m = (C_{mA} \cdot X_1) + (C_{mB} \cdot X_2)$$

As an example, let's consider a wing with the following dimensions:

Wing span (b) = 12 m

Wing area (S_w) = 12 m²

Maximum chord (c_1) = 1.2 m

Minimum chord (c_2) = 0.8 m

Midpoint chord (c_m) = 1.0 m

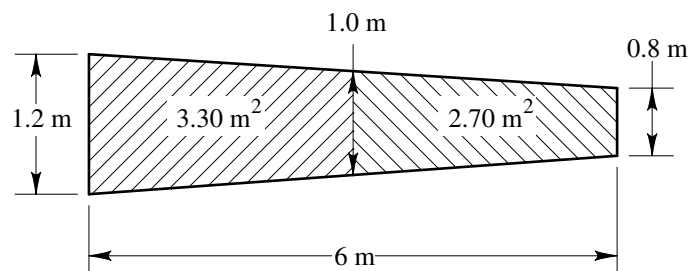


Figure 3-22

Let's suppose that airfoil *A* is the maximum chord, and the minimum chord is airfoil *B*, and the variation between them is linear. The areas for the half wing S_{w1}' and S_{w2}' will be as we have seen:

$$S_{w1}' = \frac{c_1 + c_m}{2} \cdot \frac{b}{4} =$$

$$\frac{1.20 + 1}{2} \cdot \frac{12}{4} = 3.30m^2$$

$$S_{w2}' = \frac{c_m + c_2}{2} \cdot \frac{b}{4} =$$

$$\frac{1 + 0.80}{2} \cdot \frac{12}{4} = 2.70m^2$$

and for the full wing,

$$S_1 = 2 \cdot 3.30 = 6.60m^2$$

$$S_2 = 2 \cdot 2.70 = 5.40m^2$$

the coefficients of reduction will be:

for airfoil *A*

$$X_1 = \frac{S_{w1}}{S_w} = \frac{6.60}{12} = 0.55$$

for airfoil *B*

$$X_2 = \frac{S_{w2}}{S_w} = \frac{5.40}{12} = 0.45$$

Let's suppose now that for a particular attitude we have the following values for C_L , C_d , and C_m .

Airfoil <i>A</i>	Airfoil <i>B</i>
100 $C_L = 50$	100 $C_L = 45$
100 $C_d = 3.5$	100 $C_d = 2.5$
100 $C_m = 15$	100 $C_m = 12$

Multiplying these values by the respective coefficients of reduction, X_1 and X_2 , we will have the reduced coefficients as:

$$100 C_{LA} = 50 \cdot 0.55 = 27.5$$

$$100 C_{LB} = 45 \cdot 0.45 = 20.2$$

$$100 C_{dA} = 3.5 \cdot 0.55 = 1.92$$

$$100 C_{dB} = 2.5 \cdot 0.45 = 1.12$$

$$100 C_{mA} = 15 \cdot 0.55 = 7.5$$

$$100 C_{mB} = 12 \cdot 0.45 = 5.4$$

Therefore the wing coefficients at this attitude will be finally given by the following summation:

$$100 C_L = 100 C_{LA} + 100 C_{LB} = 27.5 + 20.2 = 47.7$$

$$100 C_d = 100 C_{dA} + 100 C_{dB} = 1.92 + 1.12 = 3.04$$

$$100 C_m = 100 C_{mA} + 100 C_{mB} = 7.5 + 5.4 = 12.9$$

By repeating the same operation for different attitudes, we may calculate the polar curve for a wing with varying airfoils.

18. The Complete Airplane

In the preceding paragraphs we have seen how aerodynamic coefficients of the wing are obtained as functions of the wing shape, airfoil and aspect ratio. To obtain the coefficients for the complete airplane, it will be necessary to determine the coefficients for the other parts of the plane, and then add them to those of the wing. Things are not so simple though; the phenomenon of aerodynamic interference comes into play. That is the disturbance that one body in an airstream is subjected to by the presence of another body.

However, due to the simple design of a glider, the coefficients may be derived with good approximation by analytic calculations, but particular care should be given to the intersection axis of the wing and the tail section with the fuselage. In the final calculation, the lift supplied by the fuselage, the tail section and other parts of the plane are never considered due to their small values relative to the lift supplied by the wing.

As far as fuselage drag is concerned, it is not easy to give exact values, since experimental data for gliders is nonexistent. A solution would be to go back and experiment in a wind tunnel, but due to their long wing span, the wing chord of the model would be so small that it would be impossible to make any precise calculation. In practice, for the calculation of the full glider coefficients, the drag from the fuselage, the tail section and other parts, is considered constant, and their lift is nil.

Additional Coefficients. The coefficients of drag of all other parts that are within the flow of air have to be taken in consideration, and these must to be added to that of the wing. To do this, this coefficient C_d , is multiplied by the ratio of the area of the part in question and the area of the wing.

Note however that for the fuselage, tires, etc. the area considered is the largest area perpendicular to the airstream, while for the tail group it is the area in the same plane as the wing.

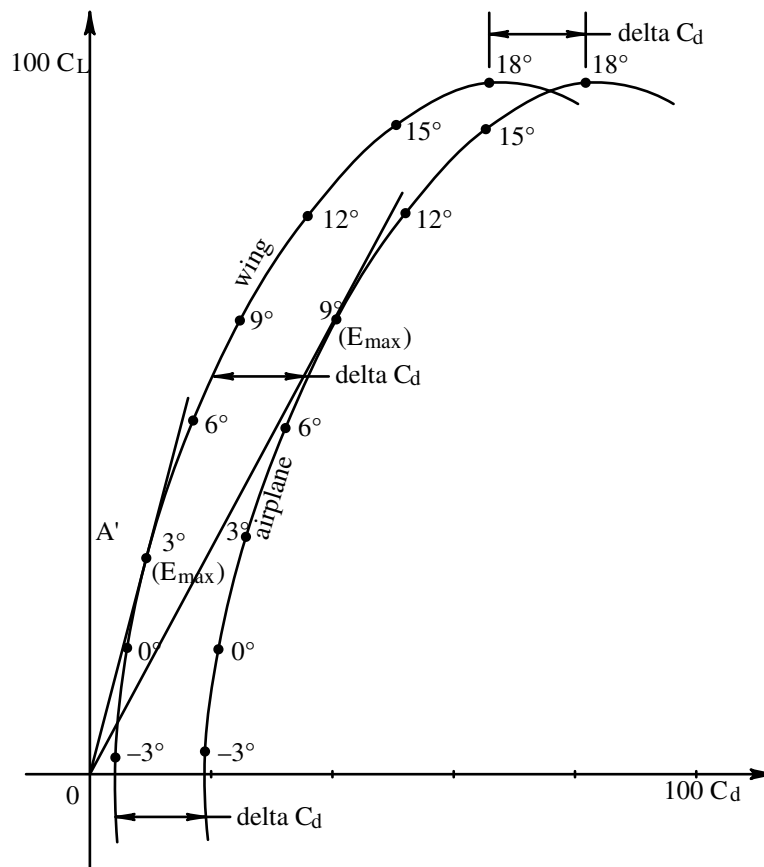


Figure 3-23

These ratios multiplied by the value of C_d will give additional coefficients of drag. Thus, for the fuselage

$$100C_{df} = 100C_d \cdot \frac{S_f}{S_w}$$

and for the tail section

$$100C_{dt} = 100C_d \cdot \frac{S_t}{S_w}$$

and so forth for the other elements.

The coefficient of total drag for the plane (C_{dTotal}) is then the sum of the wing coefficient (C_{dw}) with the ones for the other elements:

$$100C_{dTotal} = 100C_{dw} + 100C_{df} + 100C_{dt}$$

Since lift will not vary, the airplane's efficiency is:

$$E = \frac{L}{D_{Total}} = \frac{100C_L}{100C_{dTotal}} = \frac{100C_L}{100C_{dw} + 100C_{df} + 100C_{dt}}$$

The polar curve of the complete airplane is therefore equal to that of the wing, but it is slightly moved by a line equal to the value of the drag coefficient given by the other elements. (Fig. 3-25) As we have seen, the polar characteristics of the complete airplane has deteriorated, but the maximum efficiency has moved towards a larger incidence, something that could be useful in gliders.

Chapter 4 Flight Stability

19. Static and Dynamic Stability

An airplane has longitudinal, lateral, or directional stability if it will return to its original attitude when disturbed by external forces from its straight-and-level flight by newly generated involuntary forces without the intervention of the pilot. Static stability is when spontaneous forces acting on the airplane will re-establish the conditions that were originally upset by outside forces.

While returning to its original setting, it is possible that the point of equilibrium is passed, thus beginning a number of oscillations. These oscillations may decrease or increase in amplitude. If the oscillations decrease at a fast rate (i.e. are “damped”), it means that the plane possesses not only static stability but also dynamic stability. An airplane requires static stability *and* dynamic stability to quickly reduce any oscillations.

The components for stability and maneuvering are the entire tail section and the ailerons. The tail section is usually characterized by a fixed portion and by a movable one used for maneuvering, in other words, for changing the plane’s attitude or correcting accidental variations. The ailerons are used for lateral maneuvering or to re-establish lateral stability.

20. Longitudinal Stability

We have seen when discussing the various wing airfoils how these are by nature very instable. Their instability is due to the movement of the center of pressure with changes in the angle of incidence. If the lift L is equal to the weight W , when both these forces are at the center of gravity CG , we will have equilibrium because the resolution of the forces is nil, as is the moment of these forces with respect to the CG location.

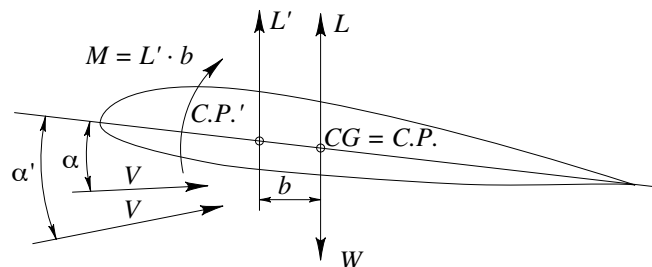


Figure 4-1

Consider what happens if the angle of incidence is increased to α' . The center of pressure will move forward from its original position to CP' . Lift L now has a moment with respect to the point CG , which is:

$$M = L' \cdot b$$

This moment will have the tendency to increase the angle of incidence, thus moving farther away from a position of equilibrium.

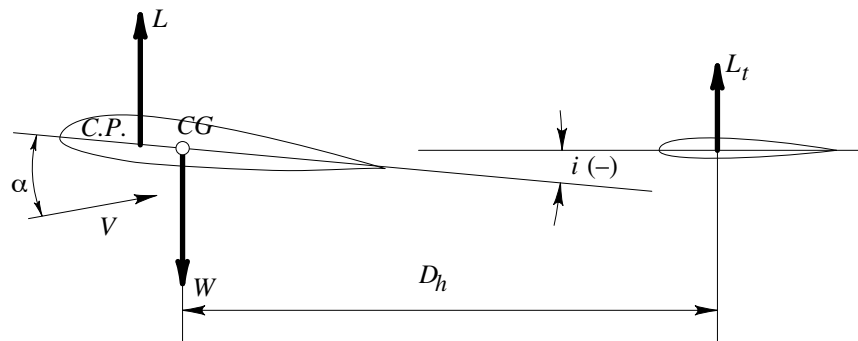


Figure 4-2

An opposite moment will be necessary to re-establish equilibrium. This is achieved by means of the horizontal tail, whose moment with respect to the center of gravity is:

$$M_t = L_t \cdot D_h$$

where

L_t = Total lift (or negative lift) of stabilizer

D_h = Distance of horizontal tail center of pressure from center of gravity CG

With respect to the individual location of the horizontal tail and the wing, the angle between the wing chord and the stabilizer is called the horizontal tail angle. In Figure 4-2, this angle i between the wing and the stabilizer is a negative value.

Moment for the Complete Design. Let us now examine the moment of the complete aircraft design where the horizontal stabilizer is at given angle i . In the polar chart, the moment curve is still a straight line but with a steeper slope than the ones we have seen for the wing itself when only the partial aircraft was being considered—in other words for an aircraft design without considering the tail section.

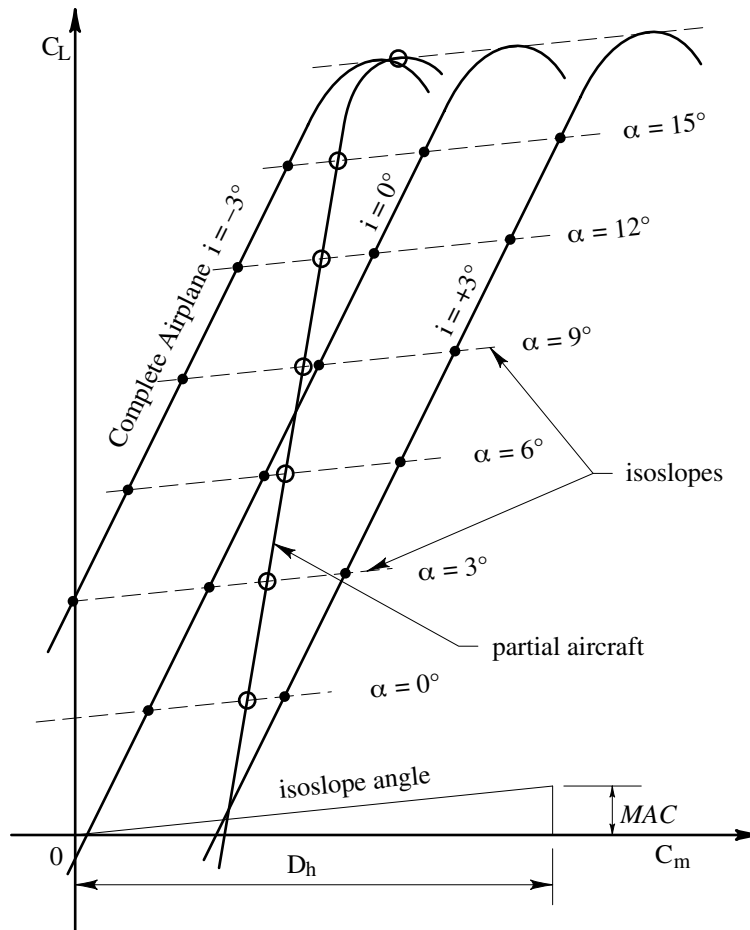


Figure 4-3

By changing angle i , we generate different moment curves, but notice that these curves are essentially parallel to each other. This is because they benefit from the property that the incidence angles—which affect the aircraft attitude when changing angle i —will move on lines of equal slope, lines called isoslopes. The slope is given by the ratio MAC/D_h —the average wing chord over the horizontal tail distance. These isoslope lines are used to determine the moment curves for the complete aircraft design.

We will avoid using the analytical method of establishing these curves because of the many factors involved—factors that are, at times, not easily determined. Therefore we must use a wind tunnel to obtain acceptable results. You run tests by changing the horizontal tail angle and obtain the different moment curves needed for longitudinal stability studies.

Centering. After obtaining the moment curves analytically or by experiment, we can proceed to the study of longitudinal stability.

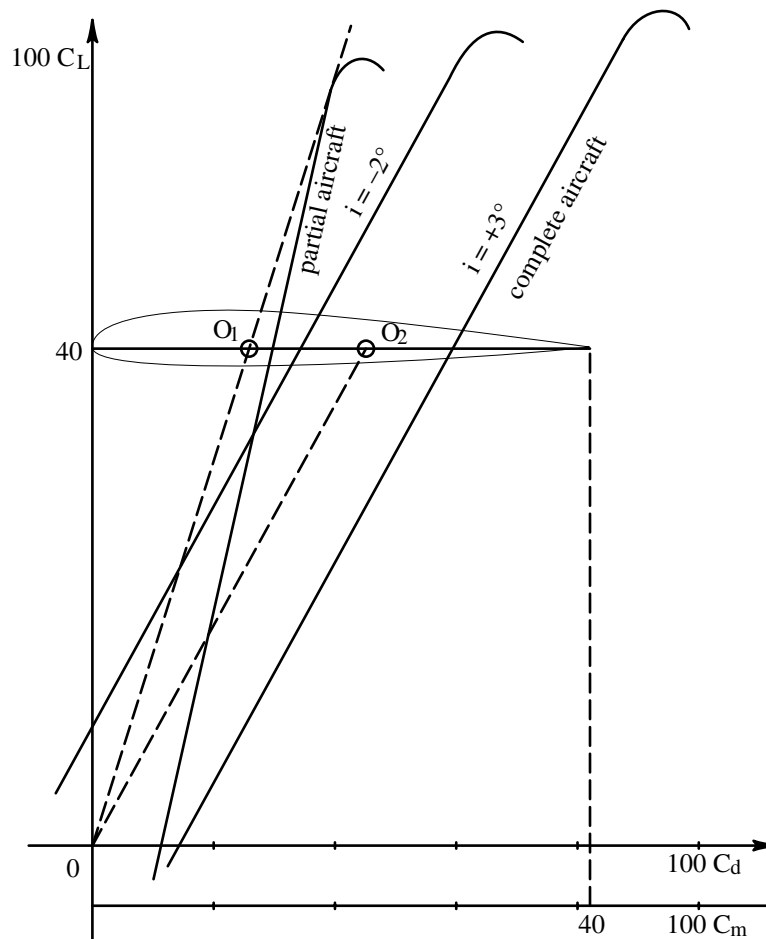


Figure 4-4

As you can see in Figure 4-4, we can establish that the position of the aircraft center of gravity cannot exceed the limits set by the points O_1 and O_2 , where the center of gravity lines drawn are respectively tangent to the moment curve for the partial aircraft and parallel to the moment curve for the complete aircraft.

In fact, in the case where the center of gravity would be ahead of the point O_1 , the center of pressure will result in a farther aft position since its maximum forward position cannot be past O_1 as we have seen when determined graphically. In this condition, we would have a case of auto-equilibrium only for an aircraft design without a tail, while under normal flight conditions the equilibrium would be lost—hence the requirement of a stabilizer anyway. Thus, in all flight attitudes, the tail section will not create lift.

It follows then that the airplane's efficiency will be reduced due to the lower total lift and the increase in tail drag. From what we have seen, we deduce then that, as the center of gravity moves forward, the aircraft will become more stable, even with a small tail section. Its forwardmost position is however limited by the aerodynamic considerations just explained.

In the opposite case, where the center of gravity is aft of point O_2 , we will have instability even with larger tail section surfaces and length, and an attitude of equilibrium will not exist.

The range of the center of gravity will have to remain therefore between these two extremes which may vary between 25% to 45% respectively forward and aft. In reality, however, it is always best to have the center of gravity to the front, between 25-30% of the wing chord.

Angle and Location of the Horizontal Tail Section. To locate and orient the horizontal tail, after determining the center of gravity position, you must determine the attitude of equilibrium without the intervention of any control surfaces, in other words, the normal flight attitude. As in the case of the wing alone, this attitude is the one corresponding to the intersection between the center of gravity line and the moment curve.

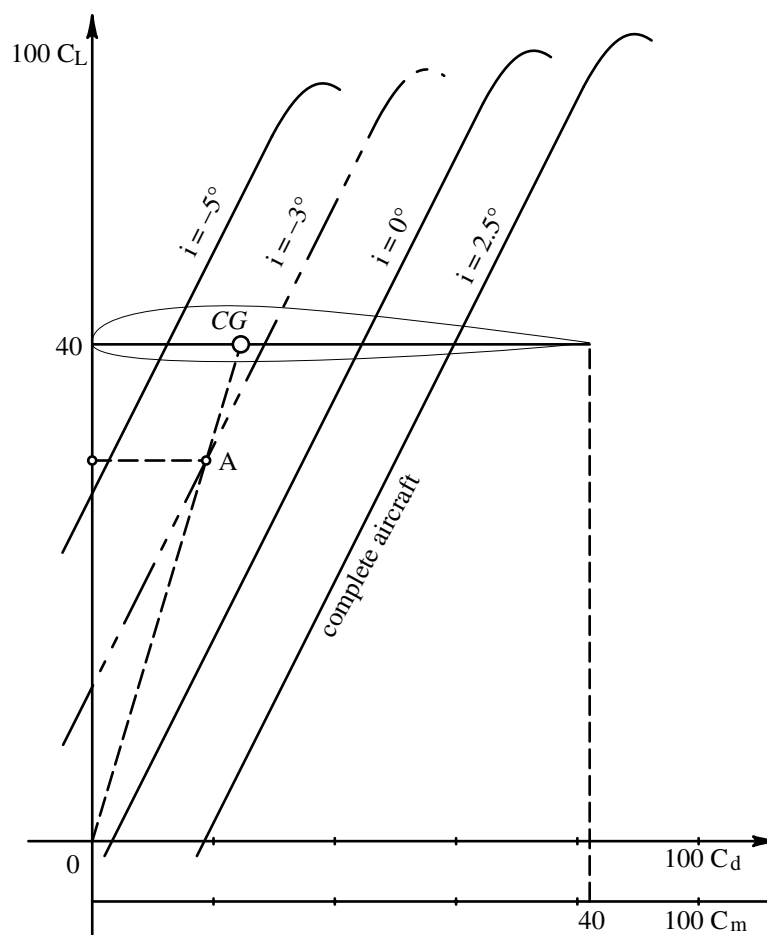


Figure 4-5

Having established this attitude of equilibrium, for example with $C_L = 30$, we draw a horizontal line through this point on the ordinate axis until it intercepts the center of gravity line at point A. This is the point through which the moment curve of the complete aircraft design will have to pass. This curve will give us the angle of the horizontal tail for equilibrium at that particular attitude.

Since high lift is always part of the normal flight attitude of gliders, the angle of the horizontal tail is always negative. At an average equilibrium attitude, we may consider C_L to be varying between

30 and 40.

These procedures are only possible when the moment curves are derived by wind tunnel experiments. Without these, we would have to accept results with a lesser degree of accuracy.

With a glider, you may use a horizontal tail angle between -3° and -4° with a good chance of success.

21. Horizontal Tail Area

In our discussions of the moment for the entire aircraft, we assumed that the area of the horizontal tail was already established, but let's see now how we arrive at the proper dimensions practically. As we have seen, the purpose of the horizontal tail is to create an opposite moment from the one created by the wing in order to re-establish an equilibrium for a particular flight attitude.

The designer could ask questions like: How quick should the action of the horizontal section be to re-establish equilibrium? How large should the stabilizing moment of the tail be over the unstabilizing moment of the wing? These questions are of great importance, but they are difficult to answer with great certainty. This is because the dynamic stability and not just the static stability has to be known. For this reason, it is not sufficient to consider the design by geometric and aerodynamic characteristics alone. Weight and the distribution of masses have to be considered as well.

Also, let's not forget to consider the type of aircraft we are dealing with. Since it exploits air movements for its flight, the glider constantly flies in moving air. Thus it is very important—and natural in a sense—to make sure the airplane has excellent dynamic stability so that the pilot will not become exhausted by making attitude corrections.

Now, let's analyze the factors that influence the determination of the horizontal tail area. We know that its function is to offset the moment of the wing. This moment depends on the movement of the center of pressure along the wing chord. For a wing of given airfoil and area, the longer the span the less the average chord, and the less the total movement of the center of pressure—the destabilizing moment of the wing. Moreover, at equal average chords, the moment depends on the wing area.

The wing area is the main factor used to establish the horizontal tail area.

Finally the third element in the determination of this area is the distance of the horizontal tail from the airplane's center of gravity. The greater this distance, the greater the moment of the tail.

Tail Ratio. We can say that the horizontal tail area S_{ht} depends essentially on three factors: (a) the area of the wing S_w (b) the wing span, or the wing mean aerodynamic chord MAC and (c) the distance D_h of the center of pressure of the horizontal tail from the center of gravity of the aircraft. The relationship that ties these factors is the tail ratio K (also called tail volumetric ratio), the ratio between the moments of the wing area and the horizontal tail area.

$$K = \frac{S_w \cdot MAC}{S_t \cdot D_h} \quad [13]$$

This is a constant characteristic for every aircraft, and accounts for factors that come into play in dynamic stability. Having K , we now can determine from the relationship the value for the tail area S_t :

$$S_t = \frac{S_w \cdot MAC}{K \cdot D_h} \quad [14]$$

Based on analysis of various gliders that have excellent stability, the value of K can be set at 1.8 for small gliders with short fuselages and 2.2 for large gliders with long fuselages. As an average value, we can use a value of $K = 2$.

Horizontal Tail Characteristics. A symmetrical airfoil is always used for the horizontal tail. In its normal position, the horizontal tail establishes the airplane's design attitude. A variation in the horizontal tail incidence will fix the airplane's equilibrium at a different attitude. This change in incidence, or tail lift, is obtained by rotating the aft portion of the tail section up or down. The forward, fixed section is called the horizontal stabilizer; the rear movable section is called the elevator. The angle between the stabilizer and the elevator is the elevator angle. For gliders, the elevator angle is kept between 30° for either climb or dive positions.

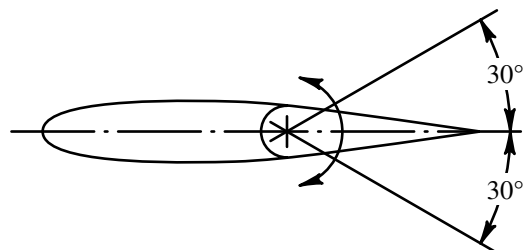


Figure 4-6

The rotational axis of the elevator is called the hinge axis. The hinge moment is the one generated by the aerodynamic reaction on the elevator in respect to the rotational axis. The pilot has to apply a force on the control stick, known as the *stick force*, in order to offset this moment.

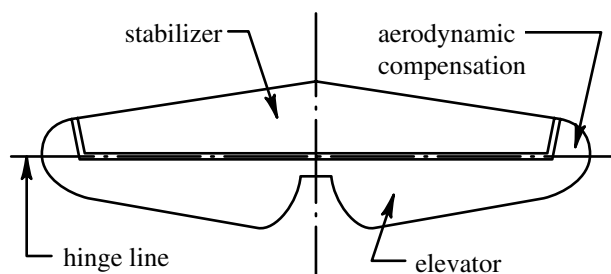


Figure 4-7

To assist the pilot in such task, controls are sometimes aerodynamically balanced, or *compensated*. This is achieved by having some of the control surface in front of the hinge to create a hinge moment opposite to the one generated by the aft section.

However due to the low speed of gliders, the force at the stick is generally very small, therefore a compensated elevator is not required. On the contrary, at times the stick force is artificially increased by means of springs that tend to return the elevator to its normal neutral position. This is

done so the pilot's sensations of control are not lost.

22. Lateral Stability

We must first understand that static lateral stability actually does not exist. After a rotation around the longitudinal axis, lift is always relative to the symmetrical plane, therefore no counteracting forces are present. A difference of lift between the wings is created only by the ailerons, but this is a pilot-generated action, and therefore we may not treat this as stability. We know for a fact however that a plane will have the tendency to automatically return to level flight following a change in attitude, but this because a sideslip motion is generated as an effect of the roll.

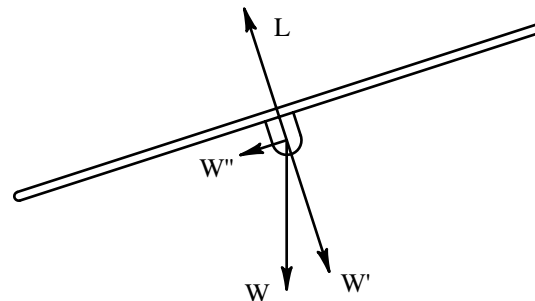


Figure 4-8

Let's suppose for a moment that the center of lift and the center of gravity CG coincide in vertical location, and that a rotation around the longitudinal axis has taken place. Lift L is always on the longitudinal plane of symmetry but now does not coincide with the vertical plane through which CG and the weight force W are found. If we take the components of W , W' and W'' — W' being on the same plane as L , and W'' perpendicular to it—we see that the effect of W'' is to give the aircraft a sideways movement, or slip. If the center of lift and the center of gravity coincide, then there will not be any forces able to straighten the aircraft.

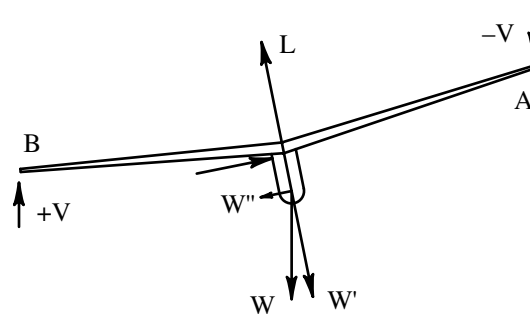


Figure 4-9

If the wings are angled in respect to the horizontal (the *dihedral angle*), we will have a center of lift that is higher than the center of gravity, thus causing a moment that will have the tendency to level the aircraft. Moreover, due to the slip movement, the direction of the relative wind will no longer be parallel to the longitudinal axis, the down-going wing, due to the dihedral, will strike a flow of air at a greater angle of attack than the upper wing. The greater lift produced by the lower wing will roll the airplane back to his original position.

We have to keep in mind that these stabilizing effects are created only by the slippage movement which follows the initial roll movement.

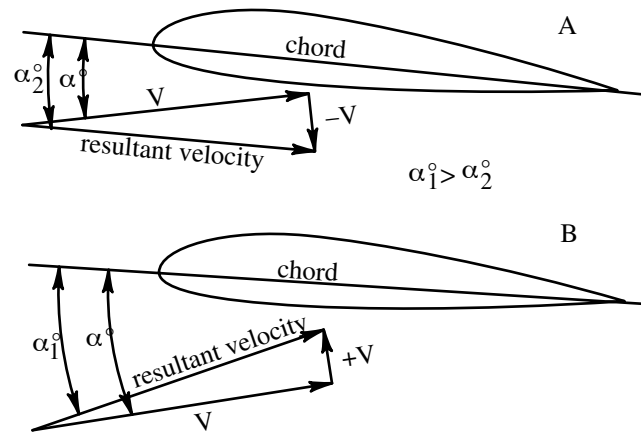


Figure 4-10

Even without dihedral, a wing will have a dampening effect to the roll movement. In fact, when the aircraft rotates around the longitudinal axis, there is a second air velocity that affects the wing, the rotational velocity V . For the upper wing there is a decrease in incidence of the relative air flow, while for the lower wing there is an increase. Consequently we have an increasing lift in the lower wing (B) and a decreasing lift in the upper wing (A). An opposite moment to the original roll is therefore originated that will have the tendency to dampened the starting roll. Notice that as the original roll stops, so does the opposing roll because its origin was dynamic and due to the rotational velocity V . Together with all the factors we have seen that affect lateral stability, inertia due to forces of mass will enter into play as well. It is easy to understand how the analytical study of lateral stability could be a complex one. In practical terms however, to obtain a good lateral stability without exceeding to levels that may hinder handling capabilities, the dihedral may be 2° - 4° for gliders with straight wings and gliders with average taper, the dihedral may be 4° - 8° for the center section and 0° - 1° for the outer panels.

23. Lateral Control Surfaces

To change the airplane's equilibrium in the longitudinal axis, or to return the plane in the original position of equilibrium when the built-in stability is not sufficient, we have control surfaces that move in opposite directions on the outboard wing trailing edge. These are the ailerons, and their rotational movement changes the curvature of the wing and therefore the lift.

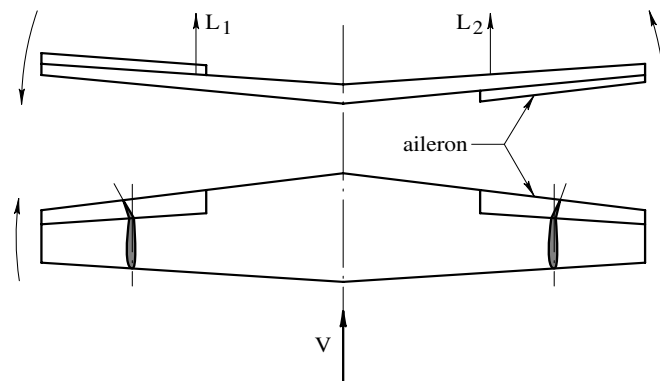


Figure 4-11

The down-aileron will increase lift while the raised one will decrease it, and this produces a rolling movement. However, the down-aileron will produce more drag than the up-aileron, which results in a yaw movement opposite to the one desired. This negative reaction is very perceptible in gliders due to their long wing span and low weight.

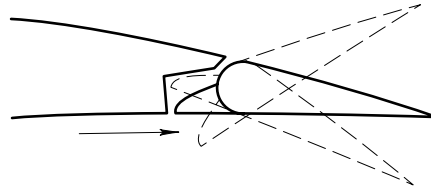


Figure 4-12

To eliminate this, the best method is to increase the drag of the up-aileron to compensate for the additional drag of the down-aileron. This is accomplished by extending the leading edge of the aileron so that it will extend below the surface of the wing when the aileron is up, but which will be inside the wing with the aileron is down. Ailerons on gliders are generally not aerodynamically compensated for the same reasons explained for the elevator.

Wing Twist. As we have seen, the lowering of the aileron will increase wing lift, but this is only true if the flight conditions are for less than maximum lift. If the aircraft is in flight conditions where the wings are producing maximum lift, as it is often the case in gliding, the lowering of an aileron will not increase wing lift. On the contrary, this could cause a sudden wing stall, possibly resulting in an entry into a spiral dive.

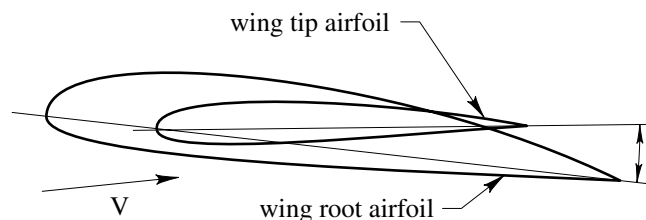


Figure 4-13

It is possible to eliminate such problems by twisting the wing negatively, in other words by building the wing so its extremities have a lower angle of attack than the wing center section. With this design, the ailerons will be more effective, even at a high angle of incidence.

With such a wing, the center portion will stall before the extremities. Because the ailerons are still very effective, there will still be sufficient lateral stability to prevent a spiral dive, even in the critical condition of an imminent stall.

Together with the wing twist, changes in the chord and thickness towards the wing tips are made to increase the overall stability and efficiency. In practice, the aerodynamic twist (relative to the incidence for maximum lift) is kept between 4 and 6 degrees in gliders. The geometric twist (relative to the airfoil chord line) turns out to be between 2 and 4 degrees, since the airfoils adopted for the wing tips generally have a higher incidence relative to the maximum lift than the airfoils used at the wing root.

Aileron Differential Ratio. By increasing the drag of the up-aileron in compensating for the negative moments, we would also worsen the aerodynamic characteristics of the wing. Therefore the idea is to reduce the increased drag of the down-aileron by reducing its angular travel when it is lowered. This is accomplished by designing a differential control system that causes the down-aileron to rotate at a lesser angle than the up-aileron.

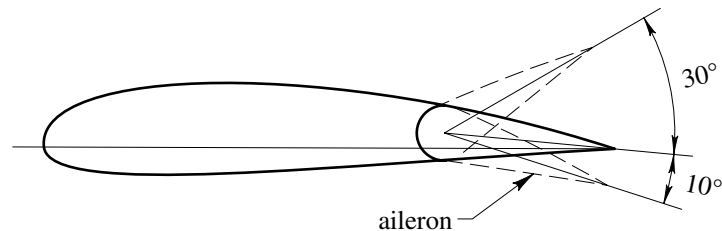


Figure 4-14

This will not necessarily diminish the moment of roll. On the contrary, practice has shown that the up-aileron is more effective than the down-aileron, especially when reaching the conditions of maximum lift as we have previously mentioned. This differential control will give us a double advantage: a full, or nearly full, cancelling of the negative yaw moments, since the drag of the down-aileron with respect to the up-aileron is diminished, and an improvement in the lateral stability, especially at higher incidence, since reducing the movement of the down-aileron also reduces the chance to incurring a loss of wing lift.

In modern gliders, this differential is quite high, 1:3 in the case of one sailplane. For an average value, we can adopt a ratio of 1:2. The maximum rotational angles are 30 degrees for the up-aileron, and they vary between 10 and 15 degrees for the down-aileron.

24. Directional Stability

Directional stability is accomplished by installing a vertical tail surface, or fin and rudder, at the aft end of the fuselage. This location puts the resulting center of side-force lift behind the center of gravity, thus if the aircraft is turned about its vertical axis, a resulting stabilizing force will be generated that will return the aircraft to its original position.

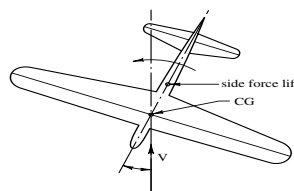


Figure 4-15

We have to keep in mind, however, that a center of side-force lift that is too far behind the center of gravity is detrimental to the lateral stability, since a drop of the aft fuselage will result and a corrective action will be required, like increasing tail lift. But in such conditions an increased dihedral will be required also to prevent aircraft slip. Lateral and directional stabilities are therefore related to each other, and each has an effect on the other. Thus a large dihedral requires a larger vertical surface and vice versa.

The dimensions of the vertical surface are also dependent on the shape of the fuselage. The larger the keel effect of the fuselage, the smaller the required size of the vertical surface. On this subject we should remember that a fuselage of circular, or nearly circular, cross-section will have a rather a

low keel effect. It is not convenient for the fuselage to have a small circular section, and it is better to have a taller and flatter section for structural reasons. For the correct size of the vertical surfaces that insures static stability, you must rely on wind tunnel experiments for the particular model in question, try different sections and choose the most appropriate one. These results will not enough to guarantee stability; our concerns are with dynamic as well as static stability.

Since wind tunnel tests are not very practical for these kind of aircraft, the only avenue left is a comparison with similar existing aircraft that are known to have good flight characteristics.

25. Vertical Empennage

From the examination of various gliders, we have obtained an empirical formula for the determination of the area of the vertical tail that may be used as a first approximation. This formula takes in account the wing span, the distance of the surface hinge from the center of gravity and the total weight of the aircraft.

$$S_{vt} = K \frac{W \cdot b}{D_h^2} \quad [15]$$

where S_{vt} is the area of vertical tail in square meters, b is the wing span in meters, W is the total aircraft weight in kg, and d_h is the distance of rudder hinge line from the center of gravity. The coefficient K may have the following values: 0.0035 for small gliders with short wing spans, 0.004 for medium-size gliders, and 0.0045 for large gliders with long wings.

Vertical Tail Features. As in the case of the horizontal tail, symmetrical airfoils are always used to produce the same aerodynamic reaction on both sides of the aircraft from the same amount of angular movement. In the vertical empennage, the fin is a fixed forward part, and the rudder is a moveable surface.

Rudder Area. In gliders, the area of the rudder is always a large percentage of the vertical tail area, generally between 60%-75%, and the rudder is normally the only control surface that is aerodynamically compensated. The percent of compensating area is normally between 15%-20% of the rudder. The angle of movement is generally 30 degrees to either side.

Chapter 5 Mechanics of Flight

26. Glide Angle and Glide Ratio

To understand the flight of a glider, we will set up a simplified situation. Let's stipulate that the flight is performed in calm air, in a straight line, and at a constant velocity. In these conditions, we have a flight path that follows a linear slope at angle φ , called the glide angle.

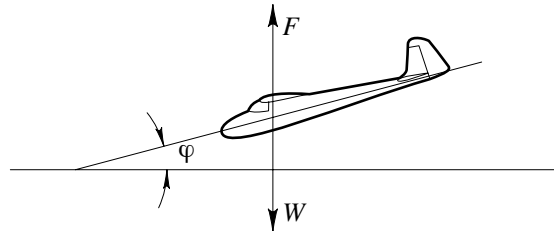


Figure 5-1

The forces that act on the airplane are the weight W and the aerodynamic force F . For any attitude, we will have equilibrium when these forces are on the same vertical line (W is always vertical), intersect the center of gravity CG , are opposite, and have the same magnitude. Consequently, the moment of these two forces in relation to any point in space will be nil. For simplicity, we will further suppose that the point where force F is applied is also the center of gravity CG .

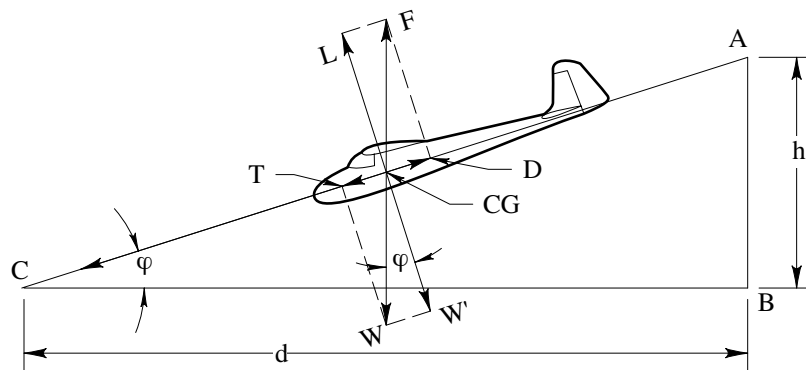


Figure 5-2

Let's consider the components of the forces F and W in relation to two directions, one vertical and one parallel to the flight direction. The F components are the lift L and the drag D . The components for W are W' and thrust T , and they will be opposite to L and D . The thrust T determines the motion along the trajectory and depends on the glide angle φ and the weight W . In the diagram, we can see how the triangles $F-CG-L$ and $W-CG-W'$ are equal and similar to the triangle ABC . Consequently,

$$\frac{L}{D} = \frac{d}{h}$$

knowing that

$$\frac{L}{D} = \frac{C_L}{C_D} = E$$

we also know that

$$\frac{d}{h} = E \quad [16]$$

The ratio d/h is called glide ratio, and its value represents the aerodynamic efficiency E as well. Its reciprocal, h/d , represents the trajectory slope p .

$$p = \frac{h}{d} = \frac{1}{E} \quad [17]$$

which is trigonometrically expressed as

$$p = \frac{h}{d} = \tan \varphi \quad [17']$$

To summarize, the greater the efficiency E , the smaller the trajectory slope. Therefore, for a given altitude loss, the distance travelled d is proportional to the efficiency E .

27. Horizontal and Vertical Speeds

Velocity V on the trajectory is due to the thrust T , a component of the weight W , in the direction of motion. In equilibrium conditions, $T = D$, thus

$$T = D = C_d \cdot \rho \cdot S_w \cdot V^2$$

from which we have

$$V = \sqrt{\frac{T}{C_d \cdot \rho \cdot S_w}}$$

which can be calculated from the other equation as

$$L = C_L \cdot \rho \cdot S_w \cdot V^2$$

therefore

$$V = \sqrt{\frac{L}{C_L \cdot \rho \cdot S_w}}$$

Since $L = W \cos\varphi$, we have the more practical equation that will give us the velocity as a function of the wing loading W/S_w .

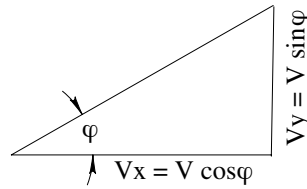


Figure 5-3

$$V = \sqrt{\frac{W}{S_w} \cdot \cos \varphi \cdot \frac{1}{\rho \cdot C_L}} \quad [18]$$

From the velocities triangle we can see that the horizontal and vertical velocities are

$$\begin{aligned} V_x &= V \cdot \cos \varphi \\ V_y &= V \cdot \sin \varphi \end{aligned}$$

therefore, from formula 18 we know that the horizontal velocity V_x is

$$V_x = V \cdot \cos \varphi = \cos \varphi \cdot \sqrt{\frac{W}{S_w} \cdot \cos \varphi \cdot \frac{1}{\rho \cdot C_L}} \quad [18']$$

and V_y , the vertical component of V , is

$$V_y = V \cdot \sin \varphi = \sin \varphi \cdot \sqrt{\frac{W}{S_w} \cdot \cos \varphi \cdot \frac{1}{\rho \cdot C_L}} \quad [18'']$$

or

$$V_y = \frac{V_x}{E} = \frac{1}{E} \cdot \cos \varphi \cdot \sqrt{\frac{W}{S_w} \cdot \cos \varphi \cdot \frac{1}{\rho \cdot C_L}} \quad [18''']$$

On normal flight attitudes though, angle φ is very small. For an example, given a standard value of efficiency for a glider of $E = 20$, we know that $1/E = \tan \varphi$ or $\tan \varphi = 1/20 = 0.05$. From trigonometric tables, we find the value of angle $\varphi = 2^\circ 50'$, which corresponds to a value of $\cos \varphi = 0.99878$. For normal flight attitudes, we can use a value of 1 for $\cos \varphi$ without introducing too much of an error. The equations will then be

$$V_x = \sqrt{\frac{W}{S_w} \cdot \frac{1}{\rho \cdot C_L}} \quad [19]$$

$$V_y = \frac{1}{E} \sqrt{\frac{W}{S_w} \cdot \frac{1}{\rho \cdot C_L}} \quad [20]$$

These are the formulas of current use for the calculation of both the horizontal and vertical speeds of a glider in a linear and uniform flight.

28. Minimum Horizontal and Vertical Velocities.

From the previous relation, for the wing loading W/S_w and the air density at a constant altitude, at any given value of attitude C_L , we have velocities V_x and V_y . Of all these values, the only ones of interest in the case of the glider are the minimum horizontal speed, the minimum vertical speed, and the top speed in a dive. The minimum horizontal speed can be easily calculated from formula 19 with the maximum coefficient of lift C_{Lmax} .

$$V_{x \min} = \sqrt{\frac{W}{S_w} \cdot \frac{1}{\rho} \cdot \frac{1}{C_{L \max}}} \quad [21]$$

To determine the minimum speed of descent, formula 20 is written

$$V_{y \min} = \left(\sqrt{\frac{W}{S_w} \cdot \frac{1}{\rho}} \right) \cdot \frac{1}{E \cdot \sqrt{C_L}}$$

In this equation, we know that the factor that is rooted is constant for a certain altitude. It follows that velocity V_y is dependent on the factor $E \cdot \sqrt{C_L}$.

The Power Factor

The velocity of descent V_y will be lowest at an attitude where the factor $E \cdot \sqrt{C_L}$ is at a maximum value. This is because

$$E = \frac{C_L}{C_d}$$

thus

$$E \cdot \sqrt{C_L} = \frac{C_L}{C_d} \cdot \sqrt{C_L} = \frac{C_L^{3/2}}{C_d}$$

In other words, the velocity of descent will be at its lowest when the factor $C_L^{3/2}/C_d$ is at its maximum. This is called the power factor, since the power required to maintain horizontal flight at any given attitude is inversely proportional to it.

29. Top Speed in a Dive

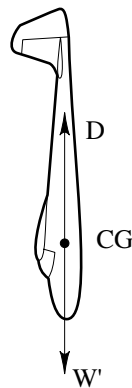


Figure 5-4

In the flight attitude shown above, the aerodynamic force F is in the direction of the trajectory since $C_L = 0$. Thus F is directly in line with D and equals the weight W . The equations are $W = D$ and $L = 0$, thus

$$W = C_d \cdot \rho \cdot S_w \cdot V^2$$

The velocity on the trajectory coincides with the velocity of descent V_y , so $\varphi = 90^\circ$, $\cos\varphi = 0$, and $\sin\varphi = 1$, therefore

$$V_y = V \cdot \sin\varphi = V = \sqrt{\frac{W}{S_w} \cdot \frac{1}{\rho} \cdot \frac{1}{C_{do}}} \quad [22]$$

where C_{do} is the coefficient of drag at zero lift.

This top speed is important for safety considerations of the airplane's structure. Aerodynamic brakes have been used, if the top speed reaches a value that can compromise the glider's structural strength.

Chapter 6

Applied Aerodynamics

30. Airfoils. Criteria for Choosing Them.

Wing airfoils can be classified in three categories from the geometric point of view: thick airfoils with relative thickness greater than 15%, medium airfoils with relative thickness between 12% to 15%, and thin airfoils with relative thickness less than 12%.

When choosing an airfoil, we should not consider the aerodynamics characteristics alone. We also have to take into account the requirements of the construction.

In the case of gliders, the wing span is always considerable, thus the selection would be made from medium, or even thick, airfoils. It is important that the airfoil be of sufficient thickness so that the strength-to-weight ratio of the spar is not compromised—particularly at the point where the wing meets the fuselage.

The airfoil's thickness is therefore established by considering both the aerodynamics as well as the construction.

Among these, we particularly take into consideration the following:

1. Maximum value of the lift coefficient $C_{L_{max}}$. This is the factor that directly influences the minimum velocity.
2. Maximum value of efficiency $E = C_L / C_d$. As we have previously seen, this is of utmost importance, especially for gliders.
3. Maximum value of the power factor. $C_L^{3/2} / C_d$. This index measures the quality of climb and the velocity of sink. The higher the value, the lower the power required to maintain flight. Therefore, the higher the value the lower the sink velocity V_y .
4. Minimum value of the moment's coefficient for zero lift C_{M0} . This factor is the index of stability of the airfoil, and it gives the movement of the center of pressure. If its value is negative, it means that the airfoil is stable.

It is not necessary to find an airfoil that simultaneously satisfies all these requirements, and some of them offset each other. For example, airfoils with a high value of $C_{L_{max}}$ have generally a high value of C_{M0} , that is they have a considerable movement of the center of pressure.

Therefore to obtain the best compromise between the various characteristics we turn to a combination of different airfoils. The wing is seldom of constant airfoil, particularly in gliders. At the fuselage as we have seen, even for construction reasons, a thick airfoil with high lift will be convenient. At the tips, however, a thinner and more stable airfoil, with low drag and small pitching moment, will be necessary to reduce losses and increase stability and handling qualities.

Let's understand that, if there is doubt in selecting a single airfoil for the wing, the doubt will be greater when selecting more than one airfoil. For this reason it is not possible to tell which will be the best airfoil for a glider. To all these factors that may influence the selection, such as the particular type and use of a glider, we have to add the designer's own preferences.

As we saw in Chapter 1 when considering the characteristics of the various gliders, there is a great variety in the design of the wing airfoils. We go from the concave convex airfoil to the biconvex asymmetric airfoil for gliders with same architecture and same use. Until ten years ago the most common design were the concave convex airfoil, which presented optimum characteristics of efficiency and minimum sink speed, but lower horizontal speed and little longitudinal stability. On the contrary, today we see the use of airfoils with little curvature or even biconvex asymmetric. In concluding, we can say generally that thick, curved airfoils constant throughout the full wing span, are the most convenient for recreational gliders.

For training gliders, the curved airfoils but with varying extremities to the biconvex asymmetric or symmetric, are still preferred. For competition gliders, the preference goes to the semi-thick, and much faster, airfoils. For the tail section, there is not much doubt, since the biconvex symmetric design is always used with thicknesses ranging from 10% to 12%.

31. Airframe Components and Drag.

We will now discuss the coefficients of drag of some of the airframe components. As stated earlier, these coefficients are based on the largest cross section perpendicular to the flight direction.

Flat Rectangular Sections. The drag coefficient C_d of a flat surface is a function of its length and Reynolds number. For isolated flat surfaces, $C_d = 0.65$. For flat controlling surfaces, (considering the wing interference), $C_d = 0.85$ as an average value for normal Reynolds numbers found in such aircraft.

Wires, Cables and Extrusions. For round wire normal to the wind, the drag coefficient is $C_d = 0.60$. For cables of non-regular section, $C_d = 0.72$. Due to the high drag generated by wires and cables, they are often substituted with extrusions, generally with lenticular section, which is a good aerodynamic shape and also rather easy to fabricate. The coefficient for such an extrusion is $C_d = 0.20$.

Shaped Supports. In gliders, all of the supports could be made of round steel tubes, but generally in order to reduce the drag, an extrusion or a wood shape with a metal core is used. We will show the drag coefficients for various cross sectional shapes.

As we can see, if the length of the section is increased in relation to its thickness, the drag coefficient also increases. The optimum value for the section's length is three times its thickness. In the following table, the values for sections with their major axis at incidence angles of 0° , 5° and 10° are shown. As you can see, the drag increases with the incidence angle.

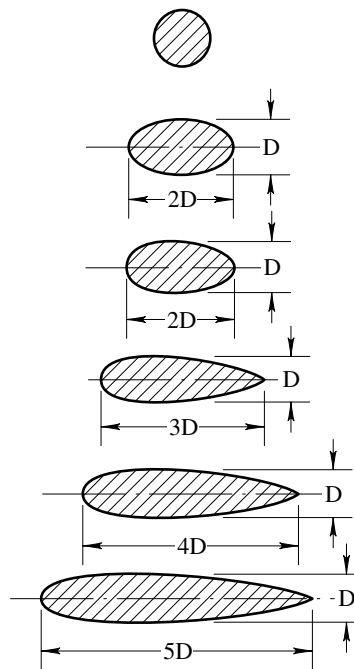


Figure 6-1

The Fuselage. Due to the large number of possible fuselage designs, it is very difficult to establish the drag of a new design without conducting wind tunnel tests, however as a rough approximation, you can establish the drag coefficient of a fuselage by comparing it to a similar one with known characteristics.

The shape of the fuselage is rather simple from the standpoint of construction, but experimental results are lacking. The drag coefficients that we show here do not pertain to any particular glider, but they could be used as a reference to understand the magnitude of these values.

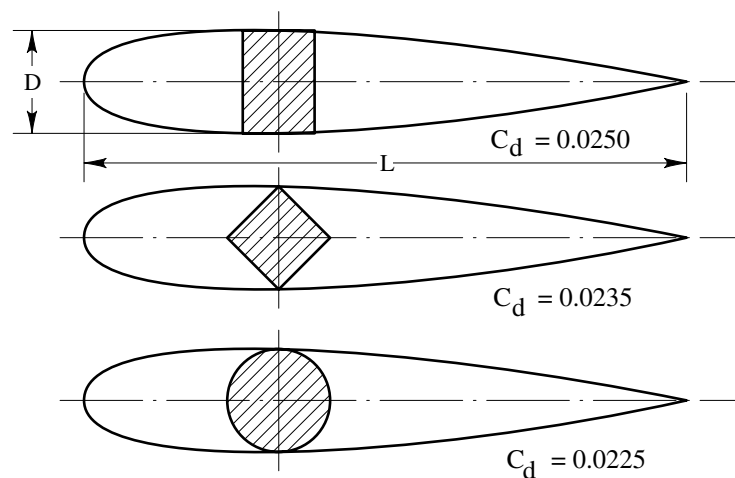


Figure 6-2

In these three shapes, note that there is little difference in the minimum drag. You could assume that the section design has no bearing on the outcome. But let's notice the importance the shape of section assumes once the angle of incidence is increased—with an angle of 10° in respect to the fuselage axis, there is an increase of the minimal drag of 230% if the section is square, while it will not reach 33% if the section is circular. Drag coefficients values for fuselage with open cockpit can vary from 0.09 to 0.18.

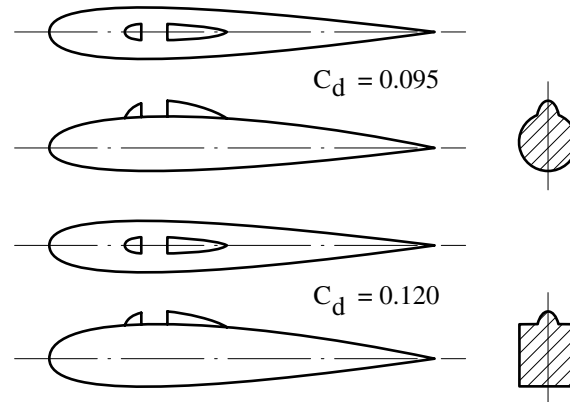


Figure 6-3

Two types of fuselage with open cockpits are shown above, one with a rectangular section, the second with a circular section. For a fuselage with a closed cockpit, drag coefficients can be achieved from 0.045 to 0.050.

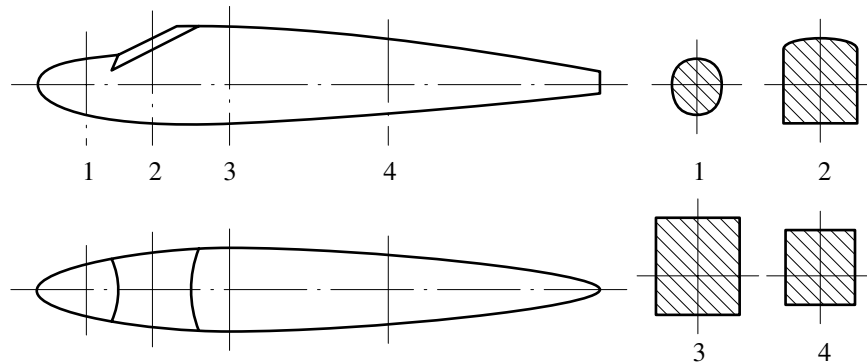


Figure 6-4

For the fuselage here above, the following drag coefficients were found: 0.044 at 0° incidence, 0.071 at 10° incidence, and 0.1545 at 20° incidence. As you can see, the drag increases considerably with an increase of the angle of incidence, especially with a fuselage of square or polygonal shape.

As an approximation, we can establish the coefficients of drag of 0.08 to 0.10 for a polygonal shape fuselage with open cockpit, 0.07 to 0.08 for the same but with a closed cockpit and 0.04 to 0.05 for a curved, plywood-skinned fuselage.

Wheels. For drag coefficient for low pressure wheels that are usually used in gliders, we can use $C_d = 0.15$ where the section considered is obtained by multiplying the wheel diameter by the largest wheel width. In gliders, the wheels—normally one—are always

partly masked by the fuselage, but we can assume the drag for the wheel in its entirety considering the interference with the fuselage.

32. Summary

Sample of an Aerodynamic Calculation for a glider. Let us try a simple example of the aerodynamic calculation of the flight characteristics of a glider. The aircraft will be a glider with a 15 meter wing span. The basic data is:

Wing	
Span	15 m
Area	15 m ²
Aspect ratio	15
Chord, root	1.4 m
Chord, tip	0.6 m
Airfoil, root	NACA 4415
Airfoil, tip	NACA 2R ₁ 12,
Angle of incidence	
Root	0°
Tip	-3°
Tail	
Horizontal area	2.1 m ²
Vertical area	0.9 m ²
Airfoil	NACA M3
Fuselage	
Max cross-section	0.48 m ²
Total weight	250 kg.
Wing loading	16.7 kg/m ²

The architecture is for a glider with high wing with trapezoidal shape, and a monocoque fuselage with plywood skin. The cockpit is closed, well-streamlined and faired to the fuselage. The glider has a ski and a wheel that is partially protruding.

Aerodynamic Characteristic of the Wing. Let us start our calculation with the most important component both aerodynamically and by construction, the wing. From the data we see that the airfoil is the NACA 4415 at the wing root and NACA 2R₁12 at the tip with a 3° twist. The wing has, in other words, a negative twist of 3°. The airfoil variation from the fuselage to the tips is linear. From the airfoil tables, we get the values of the aerodynamic characteristics C_L , C_d , C_m for an aspect ratio of 5.

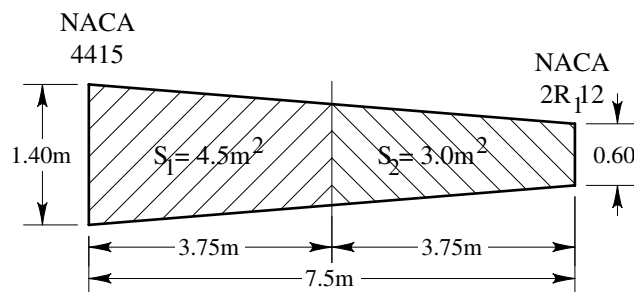


Figure 6-5

Let's consider the wing by disregarding any tip radiuses. Let's obtain the reduced coefficients for the two airfoils. The partial areas S_1' and S_2' are:

$$S_1' = \frac{1.40 + \left(\frac{1.40 + 0.60}{2}\right)}{2} \cdot 3.75 = 4.5m^2$$

$$S_2' = \frac{\left(\frac{1.40 + 0.60}{2}\right) + 0.60}{2} \cdot 3.75 = 3m^2$$

The wing area is:

$$S = 15m^2$$

Therefore the reduced coefficients are, for NACA 4415:

$$\frac{2 \cdot S_1'}{S} = \frac{9}{15} = 0.60$$

and for NACA 2R₁12

$$\frac{2 \cdot S_2'}{S} = \frac{6}{15} = 0.40$$

For clarity, let's make a table with the values of C_L and C_d for an aspect ratio of 5 for the two airfoils and include the new calculated values with reduced coefficients.

α°	C_L	C_d	$.6 C_L$	$.6 C_d$
-3	.055	.0055	.033	.0033
0	.137	.0075	.082	.0045
3	.245	.0128	.147	.0077
6	.359	.0210	.215	.0126
9	.465	.0330	.279	.0198
12	.572	.0482	.343	.0299
15	.658	.0650	.395	.0390
18	.740	.0855	.445	.0513
20	.785	.1096	.472	.0657

NACA 4415

α°	C_L	C_d	$.4 C_L$	$.4 C_d$
-6	-.15	.0048	-.06	.0032
-3	-.06	.0044	-.024	.0018
0	.040	.0044	.016	.0018
3	.118	.0075	.047	.0030
6	.275	.0140	.110	.0056
9	.380	.0238	.152	.0096
12	.485	.0362	.194	.0145
15	.591	.0535	.236	.0214
18	.685	.0725	.274	.0290

NACA 2R₁12

We now know the reduced coefficients C_L and C_d . To obtain the coefficient for the complete wing, all we have to do is add these together taking into account that the airfoil at the tip, NACA 2R₁ 12 is twisted at -3° in relation to the airfoil at the wing root, NACA 4415. For example, at 0° we have

$$C_L = 0.082 + (-0.024) = 0.058$$

$$C_d = 0.045 + 0.018 = 0.063$$

The values obtained and the one for efficiency $E = C_L/C_d$ are shown in the following table

α°	C_L	C_d	E
-3	-.025	.0067	—
0	.058	.0063	9.2
3	.163	.0095	17.2
6	.262	.0156	16.8
9	.389	.0254	15.3
12	.495	.0395	12.5
15	.589	.0535	11.0
18	.681	.0727	9.3
21	.746	.0947	7.9

In these calculations, great precision is not important. Calculating to the third or fourth decimal place is useless if you think of the number of unknowns caused by the interference of various elements, all of which would be impossible to take into account. For example, establishing that the plane's minimum sink rate is of 0.6784 m/s or of 0.68 m/s is exactly the same thing. Therefore as you have probably already noticed, the values are rounded off.

We have calculated the values for C_L , C_d and E for an aspect ratio of 5.

We must now calculate the change in these values for the aspect ratio of our example. We'll disregard the variation relative to C_L , because it's too small to be of consequence. But let's calculate the change in the drag

$$\Delta C_d = \frac{2C_L^2}{\pi} \left(\frac{1}{AR_1} - \frac{1}{AR_2} \right)$$

where AR_1 and AR_2 are the values of the aspect ratio between which the variation exists. In our case, $AR_1 = 5$ and $AR_2 = 15$, we have

$$\Delta C_d = \frac{2C_L^2}{3.14} \left(\frac{1}{5} - \frac{1}{15} \right) = 0.085C_L^2$$

at each value of α , thus for C_L , we have the value of correction for drag.

For example at $\alpha = 0$, $C_L = .058$ so we have:

$$\Delta C_d = 0.085 \cdot 0.058^2 = 0.0003$$

and the value for C_d' for $AR = 15$ is:

$$C_d' = C_d - \Delta C_d = 0.0063 - 0.0003 = 0.006$$

All the ΔC_d are therefore calculated for all the values of C_L .

In the following table we see the coefficients C_d for $AR = 5$, the change ΔC_d , and the resultant values C_d' .

α°	C_d AR = 5	ΔC_d	C_d' AR = 15
-3	.0067	.0001	.0066
0	.0063	.0003	.0060
3	.0095	.0022	.0073
6	.0156	.0058	.0098
9	.0254	.0118	.0136
12	.0395	.0208	.0187
15	.0535	.0295	.0240
18	.0727	.0395	.0332
21	.0947	.0472	.0475

As a result we may now have the characteristics C_L , C_d , and E for the complete wing for an aspect ratio of 15.

α°	C_L	C_d	E
-3	-.025	.0066	—
0	.058	.0060	9.7
3	.163	.0073	22.3
6	.262	.0098	26.7
9	.389	.0136	28.6
12	.495	.0187	26.5
15	.589	.0240	24.5
18	.681	.0332	20.5
21	.746	.0475	15.7

Characteristics of the Complete Glider. To obtain the aerodynamic characteristics of the complete aircraft, you must add to the wing's lift and drag values those of the various other elements that make up the glider, such as the fuselage, empennage, landing gear, bracing struts, etc. In our example, we will ignore the lift components of these elements.

Additional Coefficients. To determine the additional coefficients of drag, let the fuselage with skid be $C_d = 0.05$ and since the fuselage cross-section s is 0.48m^2 , its coefficient to be added will be

$$C_{df} = C_d \cdot \frac{s}{S} = 0.05 \cdot \frac{0.48}{15} = 0.0016$$

where the wing area $S = 15\text{m}^2$.

The minimum drag coefficient of the empennage airfoil NACA. M.3 is $C_d = 0.004$ and since the empennage surface S_t is $2.10 + 0.9 = 3\text{m}^2$, the additional C_{dt} will be

$$C_{dt} = 0.004 \cdot \frac{3}{15} = 0.0008$$

And for the wheel, let its dimension be 300×100 and the drag coefficient $= 0.15$. Since its calculated cross-sectional area is 0.03m^2 , the additional C_{dlg} is

$$C_{dlg} = 0.15 \cdot \frac{0.03}{15} = 0.0003$$

that we will use in its entirety even though the wheel is only protruding half way. This is to take into consideration the interference drag with the fuselage.

The additional total coefficient C_{dT} will then be $C_{df} + C_{dt} + C_{dlg}$

$$C_{dT} = C_{df} + C_{dt} + C_{dlg}$$

$$C_{dT} = 0.0016 + 0.0008 + 0.0003 = 0.0027$$

that we will slightly increase to allow for interferences and set it at

$$C_{dT} = 0.003$$

By adding this constant value to the value of C_d of the wing in the various configurations we are left with the coefficient of drag for the total aircraft.

As we have previously mentioned this procedure is not exact, since it does not take into account for the additional changes in drag caused by interference.

These changes, while almost negligible at small angles of incidence, will increase at higher angles of incidence and may even double at angles of incidence over 15° . Since you cannot obtain exact data on fuselages, it is simpler to proceed in this manner, even if it is not precise and add a constant value for additional drag.

The characteristics of the complete aircraft are thus

α°	C_L	C_d	E
-3	-.025	.0096	—
0	.058	.0090	6.4
3	.163	.0103	15.8
6	.262	.0128	20.5
9	.389	.0166	23.6
12	.485	.0217	22.8
15	.589	.0270	21.9
18	.681	.0362	18.8
21	.746	.0505	14.8

We can observe how the value 23.6 for maximum efficiency E is similar to the total efficiency of other gliders of this category, which average around the 24 mark.

Flight Characteristics Determination. Let us now calculate the horizontal and vertical velocity, V_x and V_y , at different aspect ratios at sea level. These velocities are given by the following relations:

$$V_x = \sqrt{\frac{W}{S} \cdot \frac{1}{\rho} \cdot \frac{1}{C_L}} \text{ m / sec}$$

$$V_y = \frac{1}{E} \sqrt{\frac{W}{S} \cdot \frac{1}{\rho} \cdot \frac{1}{C_L}} \text{ m / sec}$$

where:

$$W/S = \text{wing loading} = 16.7 \text{ Kg/m}^2$$

$$\rho = \text{air density} = 0.125 \text{ at sea level}$$

therefore the horizontal velocity will be:

$$V_x = \sqrt{16.7 \cdot \frac{1}{0.125} \cdot \frac{1}{C_L}}$$

where

$$V_x = 11.5 \cdot \frac{1}{\sqrt{C_L}} \text{ m / sec}$$

then in Km/h

$$V_x = 11.5 \cdot 3.6 \cdot \frac{1}{\sqrt{C_L}}$$

or

$$V_x = 41.4 \cdot \frac{1}{\sqrt{C_L}}$$

For instance for $\alpha = 3^\circ$, the $C_L = 0.163$, therefore

$$V_x = 41.4 \cdot \frac{1}{\sqrt{0.163}} = 102 \text{ Km / h}$$

In this manner, you calculate all of the horizontal speeds for the various angles of incidences and put them in a table.

Then to obtain the sink rate V_y , all you have to do is to divide the horizontal speed by the respective efficiencies E . However, since the sink rate is expressed in m/sec, and the horizontal speed is in Km/h, we will have to divide by 3.6. We'll then have:

$$V_y = \frac{V_x}{E \cdot 3.6}$$

for the previous example of $\alpha = 3^\circ$, we have $V_x = 102 \text{ Km/h}$ and $E = 15.8$, thus

$$V_y = \frac{102}{15.8 \cdot 3.6} = 1.89 \text{ m / sec}$$

The results are tabulated together with the horizontal velocities.

α°	E	V_x	V_y
0	6.4	172	7.5
3	15.8	102	1.80
6	20.5	81	1.10
9	23.6	66.5	0.78
12	22.8	59	0.72
15	21.9	54	0.68
18	18.8	50.5	0.74
21	14.8	48	0.90

The characteristics of E and V_y , for our glider are reasonably good; not because of their absolute values, but because of their relation to the horizontal speeds. For example, at a velocity of 81 Km/h, the efficiency is 20.5 and the sink rate is 1.10 m/sec. These are good for the gliding distance. At the efficiency's maximum value, $E = 23.6$ we still have a substantial horizontal velocity and a low sink rate; while at the minimum sink velocity, $V_y = 0.68$ we still have an optimum efficiency value.

To get a quick view of the glider's characteristics the results are plotted in the diagrams shown in Figures 6-6 and 6-7.

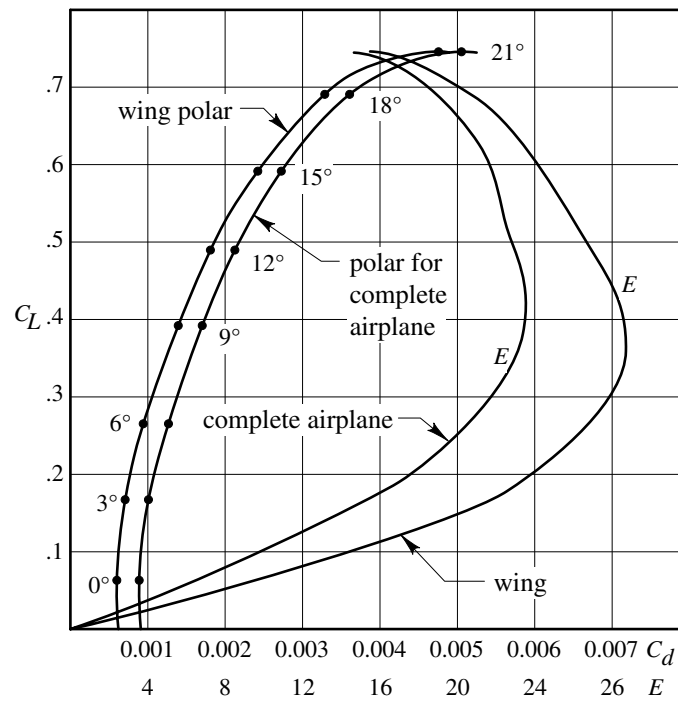


Figure 6-6

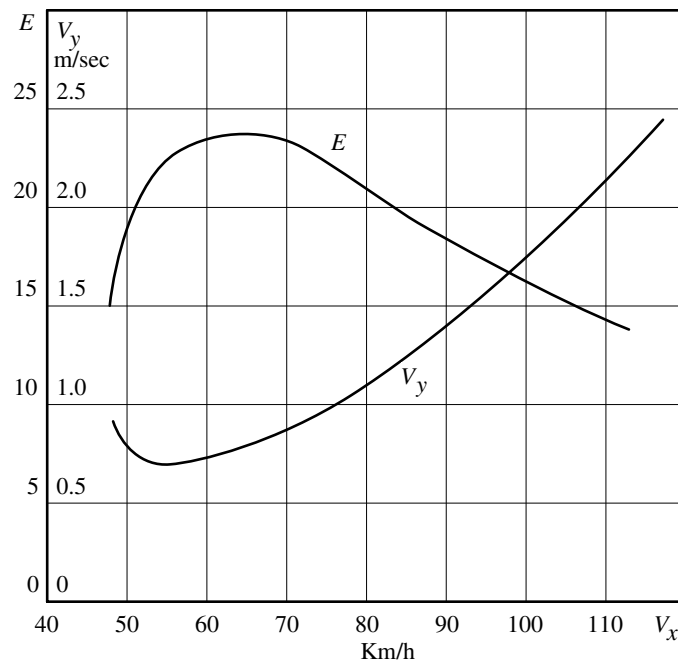


Figure 6-7

Maximum Speed in a Dive. Let us calculate now the maximum speed that the glider will reach in a prolonged dive. As we have seen this is given by the equation:

$$V_{y \max} = \sqrt{\frac{W}{S} \cdot \frac{1}{\rho} \cdot \frac{1}{C_{do}}}$$

expressed in m/sec, where C_{do} is the coefficient of drag at zero lift. From the chart, at $C_L = 0$, $C_{do} = .0096$, where

$$V_{y \max} = 11.5 \cdot \frac{1}{\sqrt{0.0096}} \cdot 3.6$$

expressed in Km/h, therefore:

$$V_{y \max} = 425 \text{ Km / h}$$

which is a very dangerous high speed if reached in actual flight.

Sizing of Wing Spoilers. From an aerodynamic point of view, the proper sizing of the spoilers is very important, since the spoilers are used as brakes to limit the speed in a dive. In our previous calculation, we have determined the maximum speed in a dive, and we can see that this speed is very high for this type of aircraft, and if it is reached in actual flight, the overall structural integrity of the glider would be compromised. Therefore we must be able to limit this speed, which at times might be reached inadvertently or unavoidably. In normal gliders, the speed is kept to around 200-220 Km/h for safety reasons, and spoilers are used as brakes.

To calculate the size of the spoilers, we return to the equation given for the maximum speed:

$$V_{y \max} = \sqrt{\frac{W}{S} \cdot \frac{1}{\rho} \cdot \frac{1}{C_{dt}}}$$

where C_{dt} is the total drag of the aircraft plus the spoiler's drag, which is yet to be calculated, while $V_{y \max}$ is the never-exceed speed set by the designer. Since the aircraft's drag at zero live, C_{L0} is known, from the previous equation we can calculate the total drag. The difference between the values will be the spoiler's drag. Then knowing the drag coefficient for the spoilers, their surface area can be calculated.

Let's calculate the size of the spoilers for the glider in our example, keeping in mind that we want to limit its speed in a dive to 200 Km/h. We have

$$\frac{1}{\sqrt{C_{dt}}} = V_{y \max} \cdot \frac{1}{\sqrt{\frac{W}{S} \cdot \frac{1}{\rho}}}$$

or

$$\sqrt{C_{dt}} = \frac{\sqrt{\frac{W}{S} \cdot \frac{1}{\rho}}}{V_{y \max}} \cdot 3.6$$

expressed in Km/h. Substituting with numeric values:

$$\sqrt{C_{dt}} = \frac{11.5 \cdot 3.6}{200} = 0.207$$

squaring this we find that $C_{dt} = 0.0429$. Since we know that the drag coefficient of the aircraft at zero lift is 0.0096, the drag for the spoilers will be $C_{ds} = 0.0429 - 0.0096 = 0.0333$. This coefficient of drag is additional and is a coefficient of the wing area therefore:

$$C_{ds} = C_d \cdot \frac{s}{S}$$

where:

$S = 15 \text{ m}^2 =$ Wing area

$s =$ unknown area of the spoilers

$C_d = 0.0085 =$ drag coefficient of a rectangular plate

The total area s for the spoilers is then:

$$s = \frac{C_{ds} \cdot S}{C_d} = \frac{0.0333 \cdot 15}{0.0085} = 0.59 \text{ m}^2$$

With a spoiler surface on the top and bottom of each wing, we'll have four elements, therefore the area of each spoiler will be $0.59/4$ or 0.148 m^2 , so we can use spoilers measuring $165 \times 900 \text{ mm}$. We can see how the effect of these surfaces as true brakes is remarkable, and the design of the controls for such spoilers is also very important in order to prevent excessive loading on their deployment.

Chapter 7 Design Plan

33. General Considerations

In the design process, it is extremely important to know in advance where the machine is going to be used. Poorly defined plans will always bring mediocre solutions.

Therefore in designing a glider, we should have a precise understanding of its use, and thus the desired aerodynamic characteristics and construction features. When defining these, the designer's biases are naturally present, and it is in this phase of the design that it is preferable that common sense be combined with lots of experience. A mistake at this stage will hurt the quality of flight or the overall production cost.

When the designer has little experience, it's a good idea to follow the example of existing designs and learn from the experience of others in this phase of the project. It is not a good idea to attempt something new if you have little experience. The 'new' always brings unknowns, even with expert designers.

And you should consider the practicalities of construction. It is better to build a well-constructed basic design than a poorly-constructed competition sailplane, which would be totally useless and would cost at least three times as much.

34. Wing Span

We have seen how the wing span is an index of the classification of gliders, which may be put into the following categories: (a) basic low-performance gliders with a wing span of 10 meters, (b) medium-performance gliders with a wing span of 15 meters, and (c) high-performance sailplanes with a wing span of 18 to 20 meters and above.

Another very important factor in classifying a glider is the wing aspect ratio.

The total weight of the proposed glider should be established using similar existing gliders that have good performance.

Knowing the wing span and the aspect ratio, we can then determine the wing area S and the wing loading W/S . We see therefore how the preparation of the design depends almost exclusively on the determination of the wing span and aspect ratio.

Practical considerations and economics also come into play at this point. You can achieve high performance with a long wing span, however this comes at the expense of ease of handling due to the inertia of the wings. Moreover, large dimensions are less practical when it comes to construction, transport, assembly, and especially with the difficulties that come with off-field landings.

And finally, any aircraft with larger dimensions will cost more to build, because of the size itself and also because of all the extra requirements a high-caliber machine requires, like retractable gear, special instrumentation, etc.

Thus we can say that various factors come into play when making the choice of the wing span, and the economics are determined by the conditions that the aircraft will be subjected to. For example, when designing a competition sailplane, greater importance should be given to the aerodynamic performance. A long wing span will certainly be called for, as this offers a large wing area with improved efficiency and sink rate due to

the reduction in the ratio between passive area and wing area, as we have seen in the determination of the characteristics for the complete aircraft.

Thus, in a competition sailplane more importance is given to the aerodynamic characteristics, even if this results in increased costs, higher probabilities of damage while attempting an off-field landing, and handling difficulties. These inconveniences—excluding cost naturally—will be compensated for by the pilot’s expertise, since this type of aircraft will not be entrusted to beginners.

In any case, a compromise has to be reached between the various factors that will determine the aircraft’s characteristics, giving preference to one or the other depending on the requirements. A good rule therefore is not to push oneself towards extreme solutions. The middle road is always the best. Only in experimental designs can you try extreme solutions, with the understanding that it requires thorough knowledge. This was the case with the famous glider of the Center of Polytechnics at Darmstadt, 30 Cirrus, with an aspect ratio of 33. The aerodynamic characteristics are without a doubt very high, but so was its cost.

Considering the cost, which is the determining factor of the construction for aircraft to be purchased by individuals, we can say that as a general rule, the aircraft with larger wing spans (18 to 20 m) are three to four times more expensive than the one with shorter span (10 to 12 m). It is clear that the cost factor is a decisive importance at the start of the project.

35. Aspect Ratio and Wing Loading

Having established the wing span, we can now consider the other factor that determines the aircraft’s performance—the wing aspect ratio. We know that increasing the aspect ratio diminishes the induced drag, therefore we increase efficiency. However, with equal wing spans, when we increase the aspect ratio, the wing area is reduced and wing loading is increased.

But the wing span L , the aspect ratio AR , and the wing area S , are bound by the relation:

$$AR = \frac{L^2}{S}$$

Having determined L and AR , S is also determined and so is the wing loading W/S , which is always referred to as the total weight, pilot included. Pilot weight may vary within restricted set limits.

Going to the actual practice, we can give approximate values to these factors for the gliders of the category we have discussed:

Low performance gliders: $L = 10$ to 12 m.

Wing loading15 to 17 kg/m²

Aspect ratio.....8 to 12

Wing area.....10 to 15 m²

Medium performance gliders: $L = 13$ to 15 m.

Wing loading16 to 18 kg/m²

Aspect ratio.....13 to 16

Wing area.....14 to 16 m²

High performance sailplanes: $L = 17$ to 20 m.

Wing loading16 to 22 kg/m²

Aspect ratio.....18 to 22

Wing area.....18 to 20 m²

This are nominal values for standard gliders. Of course, there are gliders with greater aspect ratios and modest wing spans, and others with modest aspect ratios and longer spans, but these are special cases for particular conditions.

The limits that the wing loading varies between is fairly restricted—on an average between 15 and 18 kg/m²—and this is restricts the sink rate and landing velocity. But since the wing loading does not influence the glide ratio, water tanks are added to serve as ballast on gliders designed for long-distance flights to increase the horizontal velocity, and the water dumped in flight once the higher speed is no longer required and a low sink rate is desired to exploit slowly rising thermals, or to obtain a slow speed for landing.

36. Fuselage

The most important factor that defines the fuselage of a glider is its length, with consideration given to the aircraft's stability and handling ease, however many factors influence its dimensioning.

We can achieve the same static stability with a short fuselage and larger empennage, or with long fuselage and smaller empennage. The wing aspect ratio also influences the longitudinal stability.

In the case of a long fuselage, we have a smaller empennage area, and thus a lower weight and drag, but this is offset by the larger weight of the fuselage and the higher drag due to the increase surface friction. Under this condition there wouldn't be much difference between longer or shorter fuselages.

However, if we consider the dynamic stability, we conclude that a longer fuselage is preferable since the longitudinal inertia moments are increased and the empennage is less influenced by the wing turbulence because the wing is much farther away, and thus is more effective. However the fuselage cannot be excessively lengthened, or the glider will be sluggish.

As a good approximation, we can set the fuselage length with the formula based on the wing span L :

$$f = (0.30 \cdot L) + 2.5$$

This is the total length from the nose to the tail in meters.

37. Empennage

In dimensioning the empennage, it is important first to determine the area necessary to maintain good stability. The area of the horizontal tail S_{ht} can be established using the formula in Chapter 4 (§ 21), as a function of the wing area S for the average wing chord, and the distance a of the airfoil from the aircraft's center of gravity.

We have:

$$S_{ht} = \frac{S \cdot L}{K \cdot a}$$

where the coefficient K may vary between 1.8 and 2.2. Also for the vertical tail we have seen in Chapter 4 how its surface can be dimensioned (§ 25).

38. Basic Three-View Drawings

Having established with approximation the overall required elements, we follow with the preparation of the general schematic design of the plane, thus drawing in the appropriate scale the three basics views, making provision for the loads and their required space.

First we draw the side view in 1/10 scale, drawing the fuselage shape, providing for the various loads allocation but also considering aerodynamics and aesthetics.

In this phase, we can take care of the so-called aesthetic aspect, in such a way that the design and the relationship between the various components results in a shape that is pleasant to the eye. Nature itself teaches us that generally designs that are aesthetically pleasing are also aerodynamically shaped.

Obviously, however, judgment should be left to the expert who knows and understands the nature of the phenomena associated with flight. At all the times, keep in mind the structural and aerodynamic requirements and reach a compromise to obtain the best of all factors.

The design of the fuselage is influenced almost entirely by the arrangement of the cockpit. Indeed, we can say that the fuselage of a glider is tailored around the pilot, with the need to reduce the cross-section to a minimum.

In a single-seat design or with two seats in tandem, the maximum width of the flight deck can be 60 cm on the outside. The interior dimension should not be less than 54 cm. The same can be said for the height, which may vary from 100 to 110 cm as a minimum. We have therefore established the preliminary requirements of the fuselage as a starting point.

We will sort out later the location of the wings, the horizontal empennage, the forward skid and eventually the landing gear.

39. Centering

Having established the location of the various elements and that of the loads, before we continue to define the aircraft's design, we have to verify its centering. That is, we must make sure that the total of all the aircraft's weights, fixed and moveable, will fall within 25-30% of the mean aerodynamic chord of the wing. This location for the center of gravity of the aircraft is essential for good stability.

Remember that the mean aerodynamic chord is the wing chord at the geometrical center of the wing.

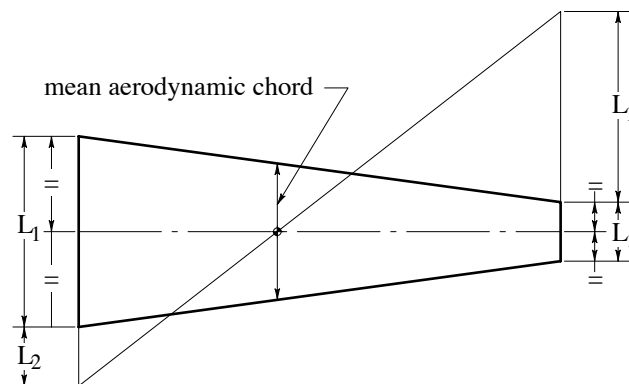


Figure 7-1

In gliders, there is no variation in the load during flight therefore centering is a singular operation. It is obvious that the determination of the center of gravity does not require the pilot's presence. However in a two-seat side-by-side configuration, it is necessary to determine the centering with one and two people to check if the center of gravity fluctuation falls within the allowable limits (25-30% of the wing chord for longitudinal stability).

The determination of the center of gravity location can be found either analytically or graphically.

In both cases, we first design the longitudinal section and the location of the various loads are established. The determination of the location and values of the various loads is not a simple matter at this stage since it's not always possible to know in advance the weight distribution of the aircraft's structure.

It is essential that the estimates of the weight of the components be made with great care, because the accuracy of these estimates will determine whether there will be a good or bad outcome in the design.

This analysis will be easier for the experienced designer who may use data from previous projects. It is very difficult to obtain detailed data on weight from aircraft built by others.

Analysis of Partial Weights. To help you with this difficult task, we will give you some average values of structural weights for various components for gliders.

Wing. For wings with a single spar and a torsion box at the leading edge, fully covered and complete with aileron controls and with wing root fittings, we have the following weights per m^2 of wing surface: for a wing of small aspect ratio (8-10), with external bracing: 4.5-5 Kg/m^2 , cantilever: 5-5.5 Kg/m^2 ; for a cantilevered wing of medium aspect ratio (12-15): 5.5 to 6.5 $Kg./m^2$; for a cantilevered wing with high aspect ratio (18-20): 6.5 to 8 $Kg./m^2$.

Empennage. For the horizontal empennage with plywood-covered stabilizer and fabric-covered elevator, complete with all the attachments and controls, the weight varies from

3 to 4 Kg/m² respectively for aspect ratios of 3.5 to 4.5. The position of the center of gravity for monospar wings can be placed at about 30% the wing chord. In the horizontal empennage instead the position is 40% of the chord.

Fuselage. The determination of the fuselage weight by empirical methods is more difficult. We can give some values relative to the total weight \bar{W} (in Kg.) of the fuselage in relation to its length L , measured in meters; but as far as the longitudinal distribution of weights, it will have to be considered according to the internal arrangements and will vary from type to type.

For a single-seat and polygonal truss type fuselage without landing wheel, or for monocoque fuselage with landing wheel and plywood covering, complete with vertical empennage and canopy, we have

$$W = 6L + 20$$

For a two-seat design (side-by-side or tandem) with dual controls and complete as described above:

$$W = 6L + 50$$

The pilot with parachute is considered to be 80 Kg.

Center of Gravity Determined Analytically. Based on the partial weights, let's now proceed to determine the location of the center of gravity.

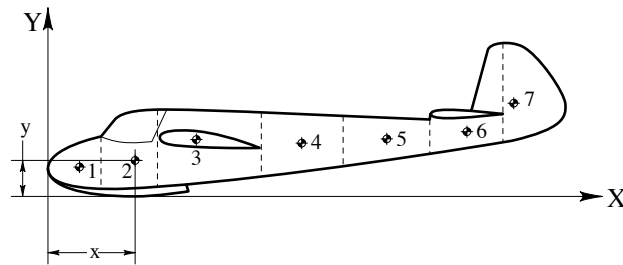


Figure 7-2

The longitudinal section of the glider is subdivided in stations, and to each we fix its weight and the position of its center of gravity.

We select two reference points on the two axes of coordinates. Typically, we will select the tip of the nose as the 'zero point' in the horizontal (X axis), and this is usually called the 'datum'. We'll use the bottom of the skin or wheel as the 'zero point' in vertical (Y axis), often designated 'W.L. O' for 'water line zero'.

Let's call x the distance from the datum, and y the distance from W.L. O. Multiplying this distance by the weight gives us the static moment of the station relative to each axis and referred to as index M_x and M_y respectively for the X and Y axes:

$$M_x = W \cdot y \quad M_y = W \cdot x$$

All the moments for each axis are the summed and there are referred to as Σ (sum).

Dividing then the summation of the static moments, ΣM_x , and ΣM_y by the summation of the weights, ΣW , which is the total aircraft weight, we get the respective distances x_{cg} and y_{cg} from the X and Y axis for the center of gravity CG.

This distances are expressed by the following relationships:

$$x_{cg} = \frac{\Sigma M_y}{\Sigma W} = \frac{\Sigma(W \cdot x)}{\Sigma W} \quad [24]$$

$$y_{cg} = \frac{\Sigma M_x}{\Sigma W} = \frac{\Sigma(W \cdot y)}{\Sigma W} \quad [25]$$

For convenience the values of the individual operations are summarized in a table. We show as an example the calculation to determine the center of gravity for a glider in the 15 m. category.

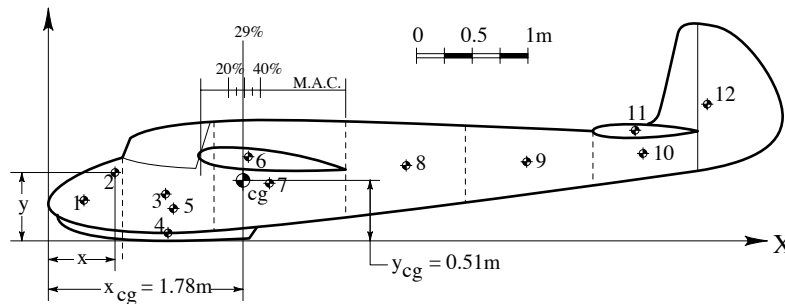


Figure 7-3

Sta.	W(Kg)	x (m)	M_y	y (m)	M_x
1	6	0.35	2.10	0.32	1.92
2	5	0.61	3.05	0.58	2.90
3	19	1.05	19.95	0.39	7.40
4	5	1.08	5.40	0.04	0.20
5	80	1.12	99.60	0.27	21.60
6	90	1.75	157.50	0.77	69.30
7	18	1.96	35.30	0.51	9.17
8	7	3.10	21.70	0.62	4.34
9	5	4.25	21.25	0.70	3.50
10	4	5.25	21.00	0.78	3.12
11	7	5.20	36.40	0.97	6.79
12	4	5.85	23.40	1.23	4.92
$\Sigma W = 250$			$\Sigma M_y = 446.65$		$\Sigma M_x = 135.16$

$$x_{cg} = \frac{\Sigma M_y}{\Sigma W} = \frac{446.65}{250} = 1.787m$$

$$y_{cg} = \frac{\Sigma M_x}{\Sigma W} = \frac{135.16}{250} = 0.54m$$

Center of Gravity Determined by Graphical Means. In order to determine the location of the center of gravity graphically, the polygon method is used. Using the side view of the aircraft, we draw vertical lines through the already pre-established partial center of gravities. These lines represent the direction of the weight-forces applied to them.

On one side, the *polygon of the forces* is constructed. All the individual weights are reported according to a selected scale and drawn one after the other in a continuous line. The ends of each segment are then connected to a randomly chosen point. These connecting lines are indicated as s_1 , s_2 , etc. The parallels of these lines, s_1 , s_2 , etc. are reported and intersected with the previously drawn vertical lines.

On the resulting vertical line R drawn from the intersection of the extension of the first and the last of the polygon lines, will be the location of the center of gravity CG longitudinally. Repeating the operation but now using the horizontal lines, line R' will be determined. The intersection of this line with line R will be the location of the center of gravity, now established in height as well.

Normally, knowing the location of the center of gravity CG in height is not necessary, therefore only the location of the line R is sufficient. The determination of the horizontal line R' graphically is not very precise—all the lines constructed horizontally are very close to each other making the process very confusing.

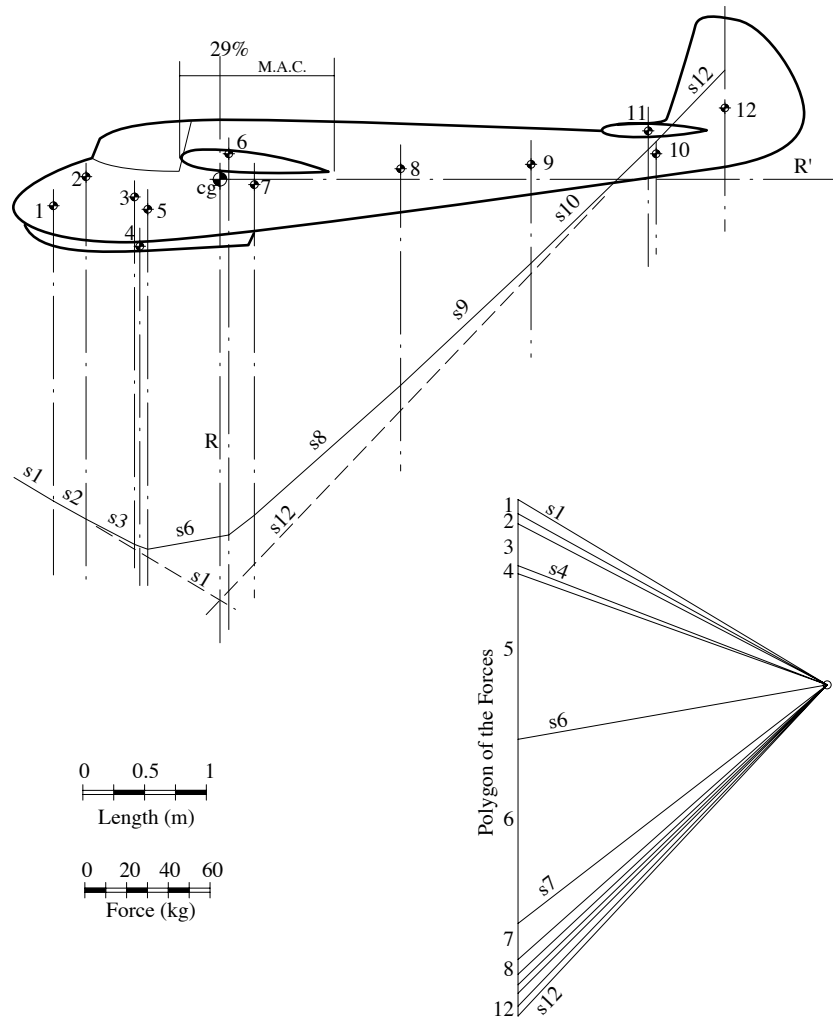


Figure 7-4

Once the center of gravity has been found, its position may not be what one would have expected. In this case a relocation of weights may be necessary. In our sample case, it is necessary to vary the position of the pilot in relation to the wing. After few changes and with the center of gravity location fixed in the desired location, the project may proceed with the determination of the aircraft shape, dimensions and general arrangements.

40. Side View

Cockpit. The first consideration is the location of the cockpit. For stability and optimal visibility, the cockpit is located as forward as possible.

For an average pilot (1.70 m), the cockpit will have the following dimensions: From the edge of the seat's shoulder rest to the pedals' rotational: 98-100 cm. Internal minimum width: 54-56 cm. From the edge of the seat to the control column: 45 cm.

In gliders, the seat is ergonomically shaped in order to offer maximum support to the body all the way past the pilot's knees. This is done to diminish leg fatigue, since in most gliders the control pedals are set very high, almost at the same level of the seat.

In the canopy, it is best if the windshield and the side windows are at a small inclination from the vertical axis, otherwise even a light mist may produce a mirroring effect that will reduce visibility. Canopies that are flared to the fuselage with a high degree of inclination are better aerodynamically but offer poor visibility—and are therefore not recommended.

The windshield also should not be close to the pilot's eyes: the optimum distance is approximately 60 cm, which is well over the minimum human focusing distance.

The instrument panel should be at a distance of 60-70 cm from the pilot and lightly inclined forward. Attention should be given to avoid having the panel located too low to prevent interference with the pilot's legs. The seat should be elevated 8-10 cm from the bottom of the fuselage to allow proper clearance for the ailerons and elevator control cables that run under it. The rudder bar cables are run instead in the inner side walls so not to disturb the pilot. The following sketch shows the cockpit arrangements in a standard glider.

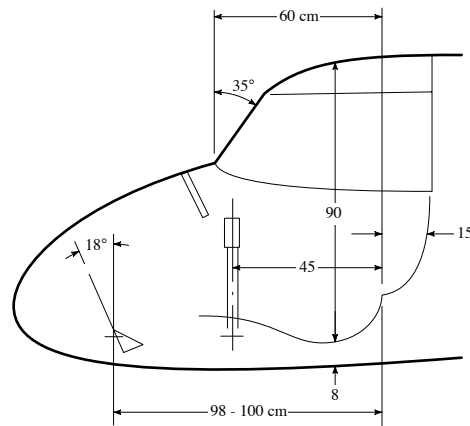


Figure 7-5

There is a space allocated for the parachute, usually 15 cm in thickness and placed behind the headrest. When designing a completely new glider, it is a good practice to first build a prototype of the cockpit. For this a forward section of the fuselage is built, then in it are placed the seat, the control stick, the rudder bar and all the various components. Finally the pilot with parachute will take a seat inside and check for possible interferences, practicality and comfort. If necessary, changes are made until you are satisfied with the design, recorded and transferred to the actual project.

The prototype is constructed with available materials. It does not require an outside aerodynamic shape or need a skinned fuselage. Its function is only to determine the location of the various controls and to finalize the shape and form of the seat for comfort and practical purposes.

Fuselage Shape. Once the various arrangements are established, and it comes the time to design the fuselage shape, there are no specific rules or formulas to allow the designer to get the best fuselage design. It is obvious that from the aerodynamics stand point, curved shapes are more efficient, but they are also more complicated and expensive to build.

As we mentioned before, at this stage in the project the personality of the designer has a lot to do with it. It will be up to him to find the best compromise between the aerodynamic requirements and the available resources.

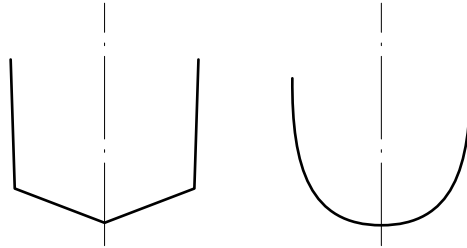


Figure 7-6

Only a few general considerations are mentioned here. It will be up to the designer to decide which will be the best solution. For the forward fuselage section in the cockpit area, it is best to use a uniform width all the way from the shoulder height to the bottom of the seat. If the cross-section is a polygon, it is best if the sides are kept parallel or slightly inclined. If the cross-section is curved, it should be flattened at the bottom.

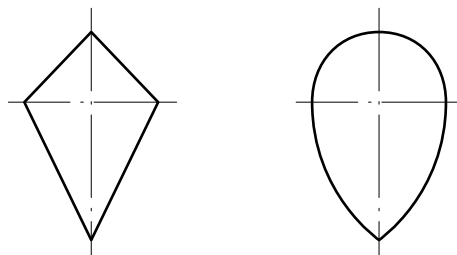


Figure 7-7

This is done in order to locate the seat position as low as possible in the fuselage, therefore reducing the fuselage's overall height. Towards the rear, it is necessary to flatten the fuselage on the sides and create a sharp edge at the bottom. This helps the aircraft's lateral stability since a sharp keel retards and actually opposes lateral slippage.

On occasion, we find that a sharp edge even in the upper portion of the fuselage and the dorsal area, further increases the lateral stability, particularly in flight conditions of high angles of incidence. This design also facilitate the application of plywood skin to the fuselage.

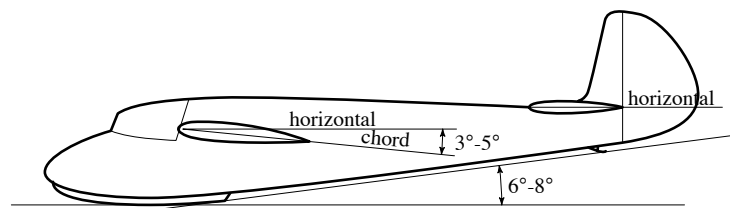


Figure 7-8

In the side view, we have to take into account the planing angle, which is the angle formed by the tangent to the landing carriage when the glider is in flying configuration and the ground. Due to their lower landing speed, the value of the planing angle is not as

important for gliders as it would be for powered airplanes, but it is recommended for this angle not to be less than 6 to 8°.

In the side view, the wing chord angle and the stabilizer angle should be defined. The horizontal empennage is usually set at 0° to the horizontal plane of the fuselage; for the wing chord that angle is set between 3 and 5°.

Wing to Fuselage Connection. The relative position of the wing in respect to the fuselage takes quite an importance in gliders. An interference between these two very important components may increase the total drag up to 15-20% if a bad design choice is made.

An analytical study of the wing-fuselage relationship is not possible. The only way to obtain proper data would be from wind-tunnel testing. But this is always a very laborious and difficult undertaking, especially when dealing with gliders

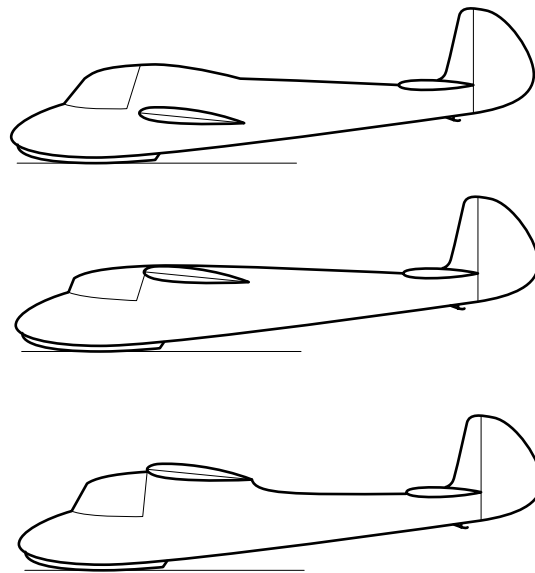


Figure 7-9

The wing position may be: (a) middle wing, (b) high dorsal wing, or (c) high elevated wing (above the fuselage).

In the wing-fuselage connection, the following conditions should be adopted: The angle formed between the wing's upper surface and the fuselage's tangent at the point of intersection should be 90° or higher. The distance between the intersection lines should be constant all the way from the wing leading edge to trailing edge. Understandably, these conditions are difficult to maintain, especially for the middle wing configuration.

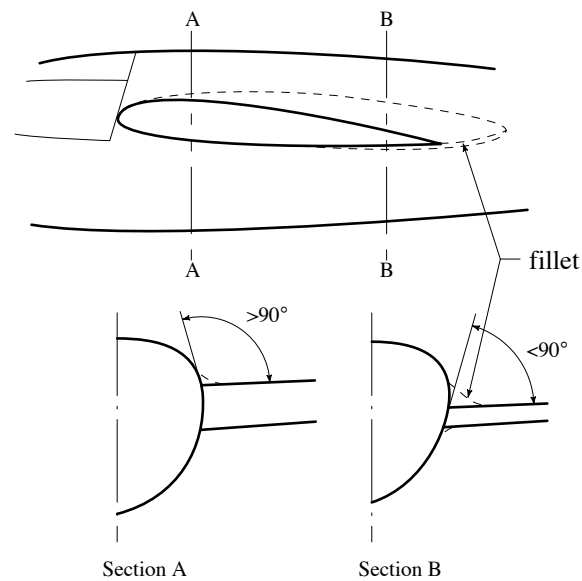


Figure 7-10

The use of a fairing helps the condition by filling those locations where the increased area would reduce the laminar layer's speed. This reduction in speed induces eddies and therefore increases drag. The fairing also assures that the intersection line be in areas of relatively high pressure if at all possible.

It is important to mention that if the wing airfoil is bi-convex or plano-convex (flat bottomed), the connection to the fuselage is quite easy, while in cases of a wing airfoil having deep camber and high lift, it is difficult to obtain a good connection, both constructively and aerodynamically. This is because in a fairly short distance, all the high lift has to be eliminated and reduced to zero at the connection of the wing to the fuselage. It is common to gradually vary the airfoil and reduce the lift as it approaches the fuselage thus facilitating the fairing.

When the wing is high on the fuselage, or above and connected by a dorsal fin (as was often done in the past), the airfoil is left unchanged even if heavily cambered. It is important to note that the fairings used for gliders are different from the ones for powered planes. This is because gliders usually fly in heavy lift conditions, contrary to what happens in regular airplanes.

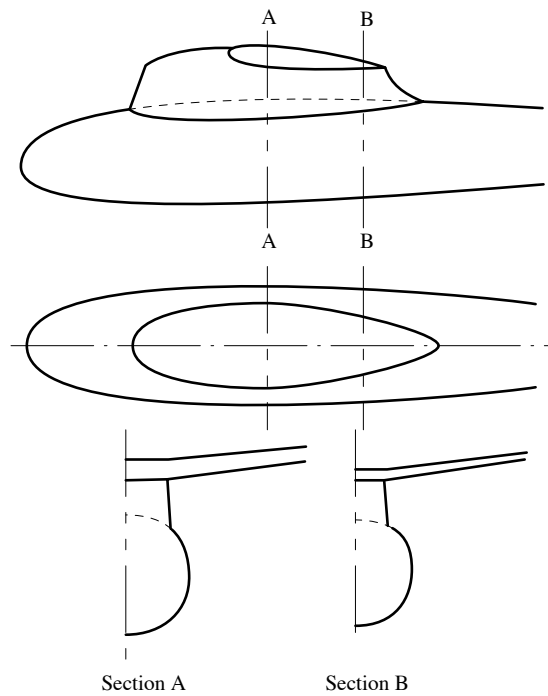


Figure 7-11

From all this, you may conclude that the high-wing configuration is the best solution for wing-fuselage coupling in gliders. The fairing in this case is simple both in design and in construction, consisting generally of a fin with vertical walls that attached at the cockpit.

41. Frontal View

There is little to say in regards to the frontal view design. In a mid-wing design, it is convenient to make it as a M-configuration. This is to raise the wing tips as far as possible from the ground and to increase lateral stability by increasing the aircraft's keel effect. In this type of wing the dihedral is between 4 to 8° for the central section and of 0 or 1° from the formed elbow to the tips.

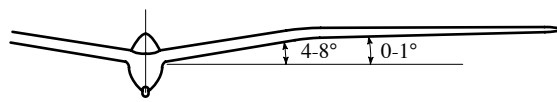


Figure 7-12

In the case of the high wing, the M shape is not necessary, and a dihedral of 2 to 3° is sufficient to give good spiral stability.

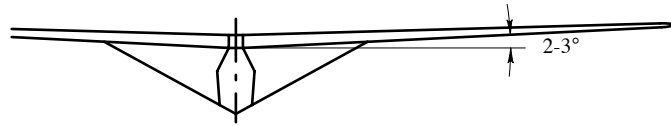


Figure 7-13

Having so determined the position and shape of the wing from the frontal view, it's now important to check the position in height of the horizontal empennage. With the aircraft in a rest condition, that is with the wing and both landing skids on the ground, the horizontal empennage should not touch the ground, or even worst, it should not touch before the wing. In such case the empennage would have to support portion of the aircraft weight. It's desirable that at rest, the horizontal empennage be at least 8 to 10 cm. from the ground.

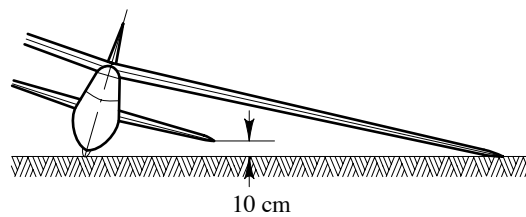


Figure 7-14

42. Top View

In the top view, we are going to define the shape of the wing, the fuselage and the horizontal tail. For the wing we had already established, at the beginning, the opening, and the surface, therefore the mean chord and the span. What is required now is to establish the actual shape. In gliders, the wing could be tapered, rectangular, or a combination of both, rectangular for a central portion and then tapered.

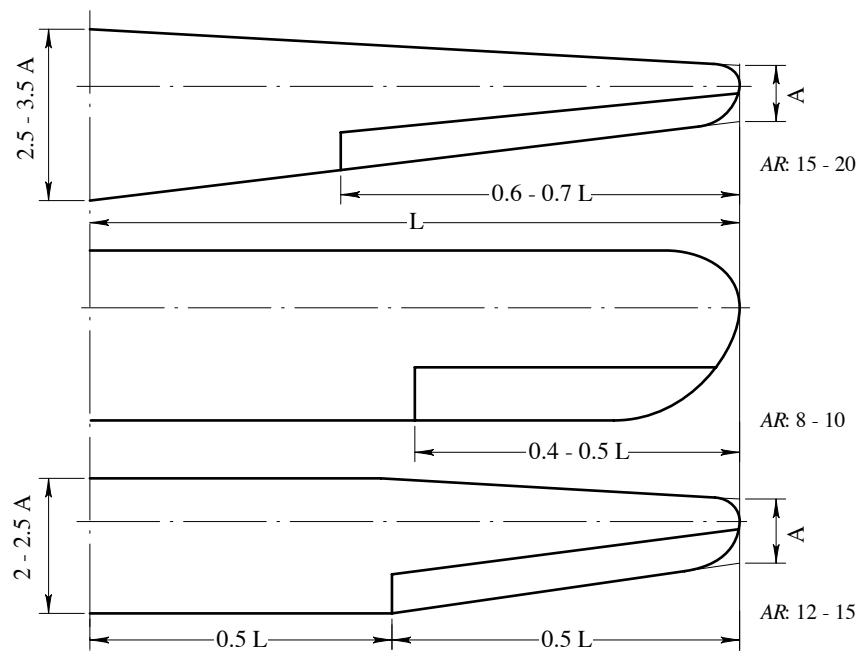


Figure 7-15

For wings of greater span, the first design is preferable, since a greater chord is possible at the fuselage thus allowing for a thicker spar. The tapering ratio, the ratio between the maximum and minimum chord, may vary between 2.5 and 3.5, with greater ratio for longer span.

The rectangular wing is more suitable for smaller gliders with a short wing span, mostly used in trainer gliders, due to the relative simple construction. Furthermore the rectangular wing presents troublesome design characteristics in regard to sturdiness, in fact, at equal span and surface to a tapered wing, the chord and therefore the spar thickness at the fuselage connection is much smaller. Also the maximum bending moment is much greater in the rectangular wing due to its geometrical center being much further away from the fuselage junction than the one in the tapered wing. This type of wing is therefore not suitable for serious gliders or gliders with longer wing spans.

The third design in Figure 7-15 shows a compromise between the trapezoid wing and the rectangular, a square wing up to the center portion and tapered from there to the tip. This shape is suitable in the case of wings with external strut supports, since the maximum bending strain is not longer at the fuselage, but it coincides with the strut mountings. In the center portion the wing airfoils remains constant, while in the tapered portion the airfoil varies.

The fuselage top view should offer the largest width corresponding to the pilot seating area and have a minimum width of 60 cm. The width of the fuselage at the tail should be at least 15-18 cm. to offer sufficient support and attachment for the tail itself.

43. Control Surfaces

Having designed the plane in its complexity, it is now necessary to determine the dimensions of the control surfaces, such as ailerons, elevators and rudder. In gliders, these surfaces have to be fairly large due to the aircraft's low speeds.

For the ailerons, based on numerous practical experiences, it has been found that their maximum efficiency is reached when their chord is approximately 25-30% of the corresponding wing. Practically though, the chord is kept constant with the wing span and with little tapering, but at its extremities should never be more than 40-45% of the corresponding wing. The length of the aileron may vary between 45% to 70% the length of the half wing span, while its surface may vary between 18% to 22% the one of the half wing.

The ratio between the ailerons and the wing span is greater in gliders with longer wing span.

The elevators area is kept at 45% to 50% the area of the horizontal stabilizer. The area of the rudder is kept between 60% to 75% the area of the vertical fin.

44. Landing Apparatus

There is a great difference between gliders and motorized aircraft in their landing gear designs.

In gliders, due to the lack of a propeller, the low wing loading, therefore low landing speed, the landing gear may be just a simple ski or sliding block that may or may not be

shock-absorbed. The application of a small wheel with low pressure tire is very common and its location is just aft the center of gravity. Lateral stability when the craft is stationary is not there. As it's commonly known, at the beginning of the takeoff run a person runs along side, holding one wing until enough velocity is reached and stability from aerodynamic forces through aileron control is obtained.

It was mentioned that the ski may or may not have shock absorbers. In training gliders, the ski is a wooden rail, rigidly attached to the fuselage. Generally though, the ski is attached by interposing rubber pads, tennis balls, or even metal springs.

The use of a wheel, does not mean that it replaces the ski, it is only an aid. It reduces friction at the start and facilitates the takeoff, and also it's very useful for ground maneuverings. Generally it is placed just aft the center of gravity, and it should protrude at least 5 cm.

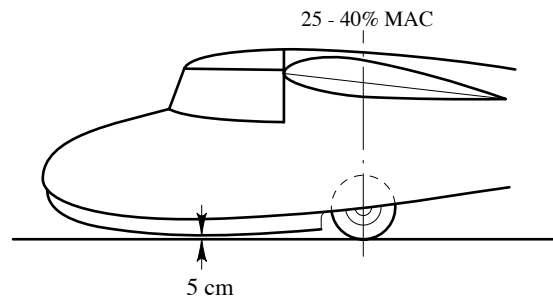


Figure 7-16

This is a preferable location because it gives the pilot some freedom in choosing landing rolls, long or short as required. With elevator control, at touch down, one could ride on the wheel for a lengthy and smooth landing, or vice versa, drive the ski to the ground in order to brake the run.

In better gliders, the wheel is completely retractable. In this case, its position is slightly ahead of the center of gravity and is equipped with a brake. The ski in this case is nonexistent. This solution, brings some complications to the construction design and adds weight, but also makes the fuselage more aerodynamic, not having protruding parts, such as the ski and the fixed wheel, which add drag and deteriorate flight efficiency.

The disadvantage of not having a front ski is appreciable when having to perform forced landings; plowed fields, river beds, or any other uneven field can easily damage the fuselage undercarriage.

To determine the type of the landing gear to be used, it is necessary to pre-determine the the use of the aircraft and the type of person that will be flying it.

Such daring construction designs as retractable gear, are then only used in high performance gliders, used by experienced pilots, where the risks of sustaining possible damage are offset by the possibilities of winning races or establishing new records.

45. Control of Maneuvering Surfaces

The development and design of these controls is very important on any type of aircraft, but more so on gliders. Their controls have to be "very sweet". Because of the light

aerodynamic loads exerted to the control surfaces, due to low speeds encountered in this type of flying, and the modest wing loading on these aircraft, the mechanical resistance found in the transmission's linkages should not mask the reactions to the controls and prevent the pilot from "feeling" the aircraft at all times. Since the various linkages must be mechanically sound, it is necessary to reduce to the minimum all the possible friction causing apparatus such as pulleys, levers and elbows.

The simpler the transmission the better it works. The development of the aircraft's structure and the development of its various controls should be carried out simultaneously, and if necessary, adapt the aircraft's design to the design of the controls, not the other way around. If it's necessary, in the end, it may be more convenient to design a more complex fuselage section, in order to facilitate the implementation of the control assemblies, rather than doing it the other way around.

Let us briefly point out the most common methods in use to control the movable surfaces. The ailerons, elevators, and rudder, are controlled by the pilot via linkages that may be made up of cables, rods or a combination of both.

The Control Stick. The ailerons are activated with a lateral movement of the control stick, while a longitudinal movement controls the elevators. The rudder is controlled with the pedals. In most gliders and powered aircraft, the stick movements are transmitted to the control surfaces with steel cables.

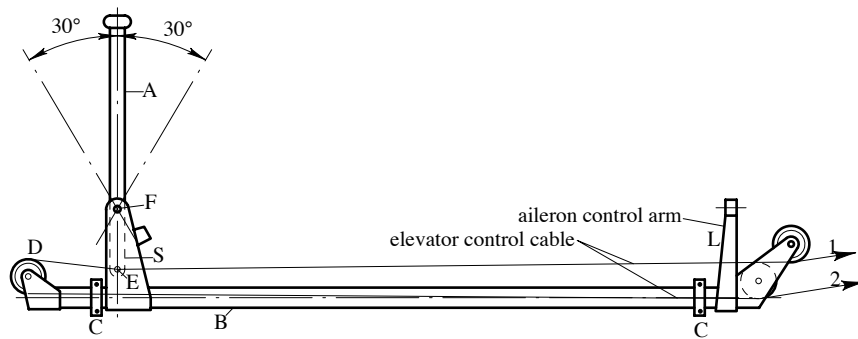


Figure 7-17

In high-performance gliders, the use of solid rods is becoming acceptable, these give a better feel to the pilot because of the low friction. These types of controls, though, are expensive and present fussier tune-ups. For these reasons, the cable method is more popular. The diagram on Figure 7-17, shows the most common method used for the transmission of movements by cables.

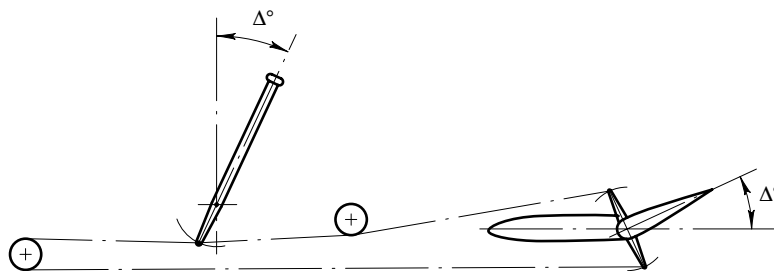


Figure 7-18

The control stick A is hinged at F on a supporting bracket S which in turn is fixed to rod B that liberally rotates on bearings $C-C$. The control stick rotates at F in a longitudinal plane, and it extends beneath as a lever to which at point B the control cable for the stabilizer is connected. From here, one end of the cable (1), goes directly to the upper stabilizer lever, the other end (2) through a pulley situated in front of the control stick, returns and is attached to the lower stabilizer lever.

Pulling the bar backwards, the connection E moves to E' pulling on the control cable (1) and the stabilizer moves up. The aircraft pitches up. On the contrary, if the control stick is pushed forward, the pull is now on the cable (2), the stabilizer moves down and the aircraft pitches down.

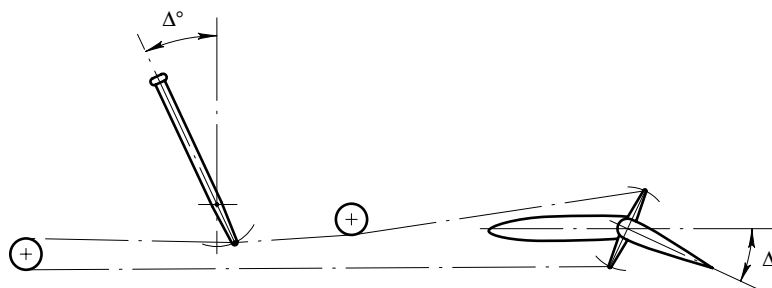


Figure 7-19

The control to the ailerons is obtained through a lateral movement of the control stick, which in turn rotates rod B . On rod B there are attached two levers L , and attached to them there are two rods T that transmit the movement via a three-arm lever to a cabling system connected to the ailerons.

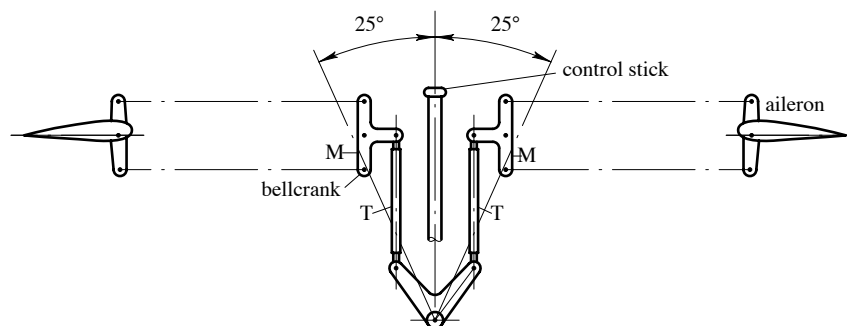


Figure 7-20

The three-arm lever is fixed to a wing longeron. By disconnecting the lever T from it, it allows the disassembling of the wings. In standard gliders the radius of the lever is kept between 80-120 mm. If space is not a concern, it is better to adopt the larger radius in order to reduce the system resistance.

Pedals. The pedal system in gliders is different from the ones used in powered aircraft. In powered aircraft, the rudder movement is achieved by the longitudinal movement of the pilot's leg. This rotates a bar around a vertical support or the footboard moves entirely forward.

In gliders, in order to diminish pilot fatigue, due to occasionally lengthy flights, and also because the forces required in the controls are not that big, the command is achieved by the rotation of the pilot's foot by pressing the pedal with the toes; the pedal is pivoted at the bottom, and the foot rests on it.

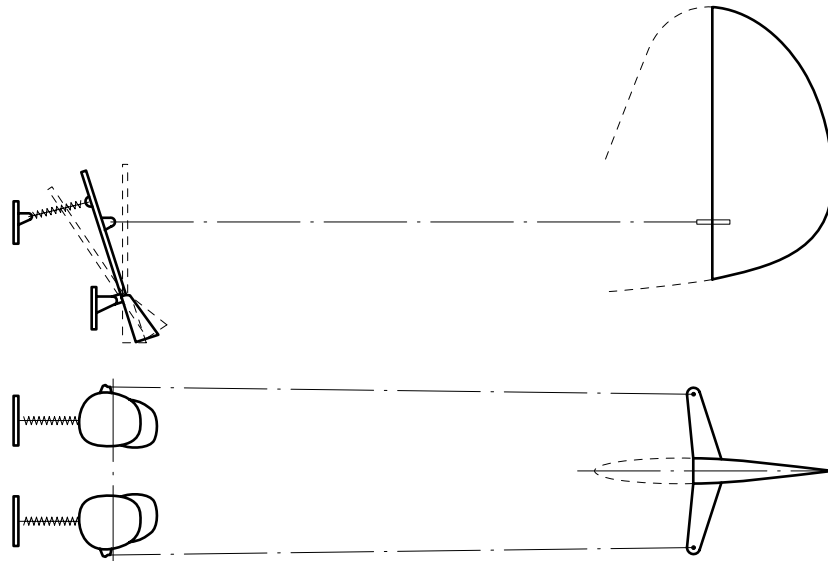


Figure 7-21

On the pedal above the rotational axis are attached the control cables that run to two levers connected to the rudder. Behind the pedal there are springs for proper tensioning of the cables.

The diagram on Figure 7-22 shows the location of the controls, the levers, and the distribution of cables as generally used in gliders.

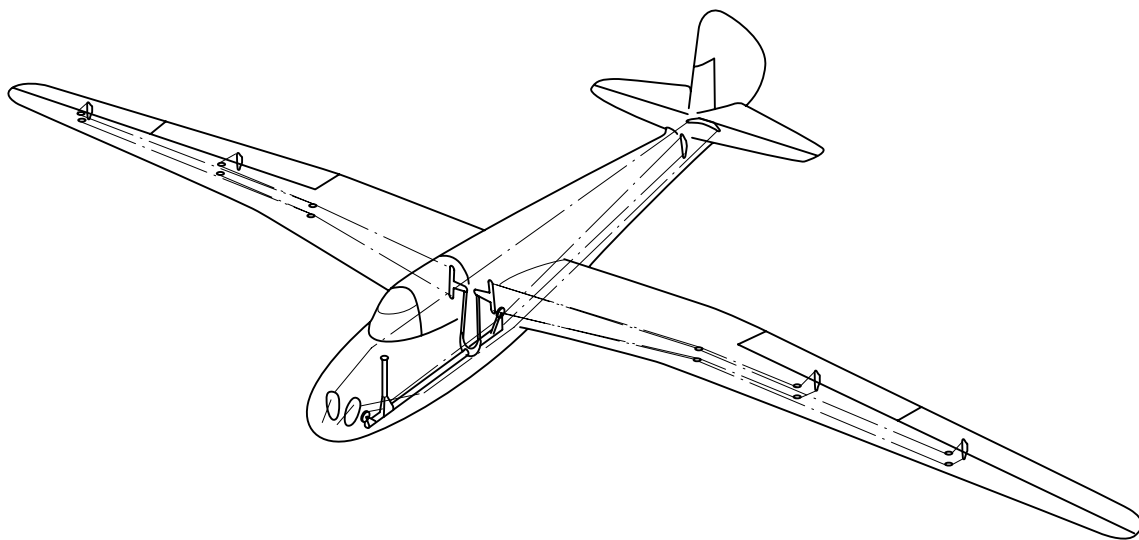


Figure 7-22

46. Options

Spoilers. For years now, the use of spoilers has become essential. By design, they are generally flat surfaces, that when deployed by the pilot they open in a position perpendicular to the wing's surface.

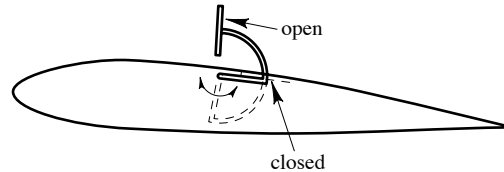


Figure 7-23

Their purpose is that of disturbing or spoiling the airflow over the wings surface, thus their name. This causes a loss of lift, therefore a decrease in efficiency and speed. This is a must for landing to reduce the landing roll especially in forced landings, situations that are very frequent in soaring. Spoilers are always placed on the dorsal side of the wing to get the maximum disturbance effect.

It is obvious that their size is related to the characteristics of the glider they are installed on. It is recommended, though, not to oversize them in order to increase their efficiency, because their deployment would require too much force. Their location should be such that once deployed their effect does not pose interference with other control surfaces and cause unwanted vibration, that, even if not dangerous definitely not welcomed.

With the increased popularity of the sport and its extreme ranges, such as flying into thunderstorms as well as into clouds, it has become necessary to be able to reduce the maximum achievable speed when in a dive. One may find himself in a situation, sometimes unavoidable, or without knowledge, where dangerous speeds are reached that could even compromise the integrity of the aircraft.

The thinking of limiting the maximum speed in a dive, increasing the aerodynamic drag, by designing oversized spoilers was entertained. (We have shown previously by a numeric example how to calculate the surface size of such air brakes.)

But in order not to exert an excessive strain when deploying such a large surface, designers have decided on dividing the calculated surface in two, locating one on the upper side of the wing and one on the lower side. The two sections are connected in such a way that the deployment of one is aerodynamically compensated by the other. In fact, the resistance encountered on the deployment of the upper spoiler is balanced by the wind assisted opening of the lower spoiler.

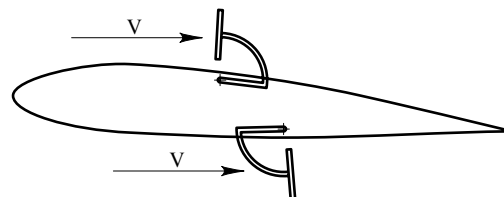


Figure 7-24

The use of a double spoiler systems has become widespread in the soaring. Their duty is twofold: Lessen the aircraft efficiency and descending speed, and bring the maximum speed attainable within the safety values of the aircraft structure. The speed with the double spoiler deployed in modern gliders is within the 200 and 250 km/h.

Towing hooks. In the first chapter, we discussed the various methods used in the towing gliders. These methods may be divided in two distinct categories: ground tow (elastic cable, winch, towing car) and towing in flight by aircraft.

The hooks, and their location on the aircraft, have to be consistent with the particular method used in towing. In the ground tow, the aircraft trajectory is sloped upwards in order to reach elevation quickly. In this condition it is necessary to place the hook much lower than the center of gravity and not too much forward of it.

Also the release has to happen automatically at the very end of the pull. For these reasons the hook employed in such systems has to be located under the front ski and has to be of the open type.

To prevent premature cable release, due to the higher inclination the glider presents in relation to the pulling cable, it is necessary for the hook to have an angle of approximately 25° from its vertical when the glider is in straight attitude.

For flight towing, the glider is usually slightly higher than the towing plane: therefore the hook should be just a little lower than the center of gravity but as forward as possible.

It is important to note that when towing this way, the towing cable is not always under tension. At times, due to different flight conditions between the two aircrafts, some caused by external effects, or caused by pilot's inexperience, it may happen that the cable slacks. It is understandable then, that, to prevent premature release, the hook cannot be of the open type, but closed with pilot control on its opening.

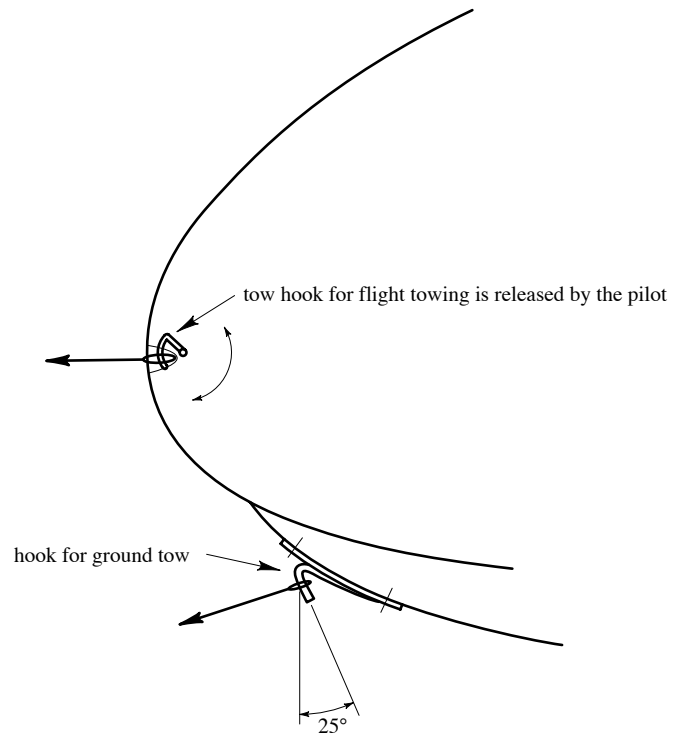


Figure 7-25

The two type of hooks are shown in Figure 7-25. In most gliders both types of hooks are installed in order to accommodate the use of either system.

Chapter 8 Aircraft Design

In this chapter we will try to offer some comments about the design of the aircraft and its components, and in particular the geometric section of these elements. And in the design process, we have to constantly be aware of the construction demands. For instance, when designing the wings and fuselage, it is done in such a way that the various components may be developed into surfaces that are straight and flat. Since these will be covered with plywood, we know that plywood does not adapt well to shapes that have double curvature. Only a slight amount of shaping is permissible, but even this requires very specialized work.

47. Wing Design

For simplicity of construction, it is preferable that the design be made with straight outlines except for the tip. Here, for aerodynamic reasons as well as for aesthetics, the contours will be curved. To lay out these wing tip curves, which are also used in the tail section, the most practical method is to draw a parabola by using tangent lines.

Generally the curves of the wing tips and tail section are drawn on paper to scale and free-handed. The difficulties arise when the same curves have been reproduced in the construction stage. Even in the case of a simple curve like a circular arc, drawn simply with a compass at the design stage, we realize the task may well be difficult, not to mention the difficulties encountered when trying to use other irregular curves. Laying out of parabolic lines by tangent lines is, however, practical and the reproduction at any scale is feasible, therefore it is possible to get harmonious and very pleasing curves.

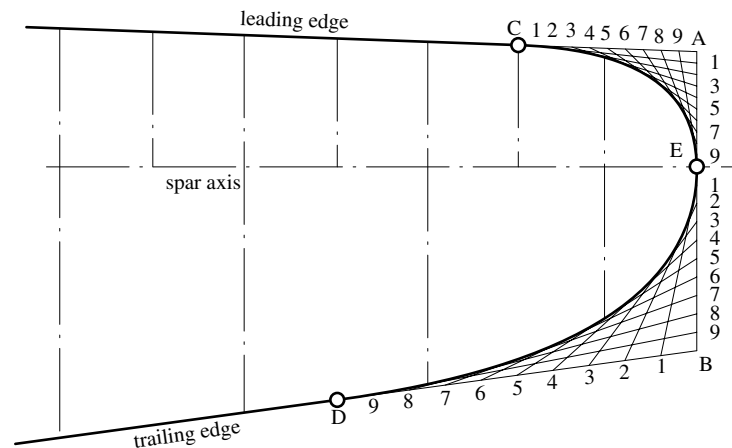


Figure 8-1

Let's look at, for example, the outline of a wing tip. The first step is to design a square wing, like the line AB in Figure 8-1. On the leading edge, a point C is selected at a distance of about one half the length of AB . On the trailing edge, a point D is selected at a distance of about 1.2 times the length of AB . A third point E is chosen at the intersection of the line AB with the spar axis. Points C , E , and D are the tangent points of the curve that will be drawn from the leading edge, to the wing tip, and to the trailing edge.

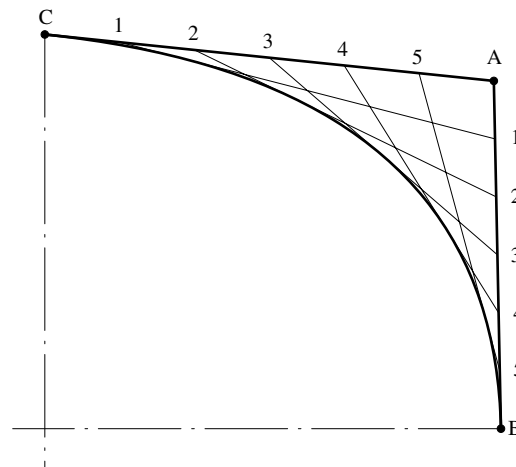


Figure 8-2

To draw the curve, we must first divide the segments CA and AE into equal parts, in our example six, and these points are then joined as we can clearly see in Figure 8-2. If we draw a curve tangent to all of these lines, these will result in a parabolic arc. The operation is repeated for points E, B , and D . For design simplicity, points C and D are made to correspond to the wing ribs, or at a distance from A and B of an integer value. Point E , as we mentioned, can be on the axis of the spar. It is possible that the points C, E , and D , following the first design, may be adjusted in order to give a more pleasing curve to the eye. It may take a few attempts to find the right location that gives the best results. The tail section and even the fuselage may be drawn using the same methods.

48. Design of Wing Airfoil

In the design of the wing, the airfoil is of fundamental importance.

Wing with constant chord. In a wing where the airfoil is kept constant throughout the full span, the design of the various airfoil sections is relatively simple. A section of Chapter 6 Applied Aerodynamics is dedicated to the design of the proper airfoils. [The tables of the 1946-era airfoils are omitted here.] In each table, there are three columns of numbers: X, Y_s and Y_i , and these values relate to a unit length of the airfoil. In other words, they are percent values of the airfoil length.

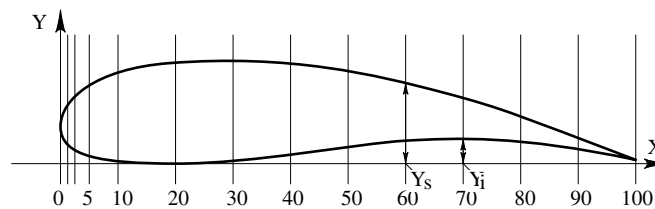


Figure 8-3

The X -values are the horizontal distance (abscissa) and the Y -values are the vertical distances (ordinate). The length of the airfoil is subdivided into ten parts, and the first part is again subdivided into five to six parts in order to obtain greater precision near the leading edge. We have, therefore, values of X at 1.25% to 2.5%...10% to 20%...100%. From these points we draw perpendicular lines, and on these we trace the values for Y_s and Y_i , (Figure 8-3). By connecting the newly found points, we obtain the shape of the airfoil. To determine the values for X, Y_s and Y_i for a particular length, all we have to do

is multiply the values found on the table by the desired length and divide by 100. This way we can obtain the proper airfoils in relation to their length.

Wing with varying airfoil and angle of incidence. As we have seen, the wings of gliders rarely are of constant airfoils, and they vary from section to section. At the fuselage, for reason of construction, the airfoils are thick and designed for greater lift, while at the tips, for increased efficiency and stability, the airfoils are much thinner and may even be at a negative incidence angle in respect to the sections near the fuselage.

If we are given the two fundamental airfoils, we can design the intermediate ones. Only wings with a linear sweep will be considered, this way, the airfoil variation will be linear, and this linear variation can be determined either analytically or graphically.

Graphic Method. On an horizontal reference line T , we trace the location of the ribs in a selected scale (1:10, 1:5). If A and B are the location of the ribs at the extremes, which have a known airfoil, we mark on them the upper, Y_s , and lower Y_i , values for a chosen percentage of the chord, let's say 30%. We connect these points with a line.

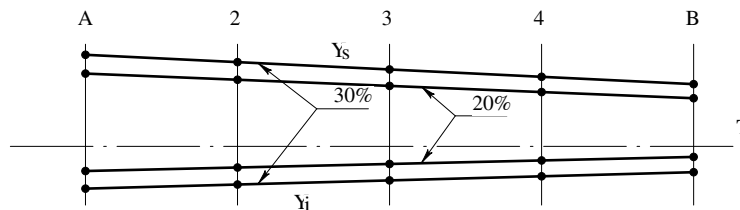


Figure 8-4

The intersection of this line with the previously traced lines representing the ribs location, will give the upper and lower values of all the intermediate ribs at that particular percentage of chord. The schematic seen on Figure 8-5 show this type of construction. Repeating this operation for all the percentage on X , we'll have all the required values for all the intermediate ribs.

Since the process has to be repeated a number of times, (usually 14), if we continue the use of the same line T to generate the expected values, a lot of these will be too close together and even coincide, making the operation very difficult and cumbersome.

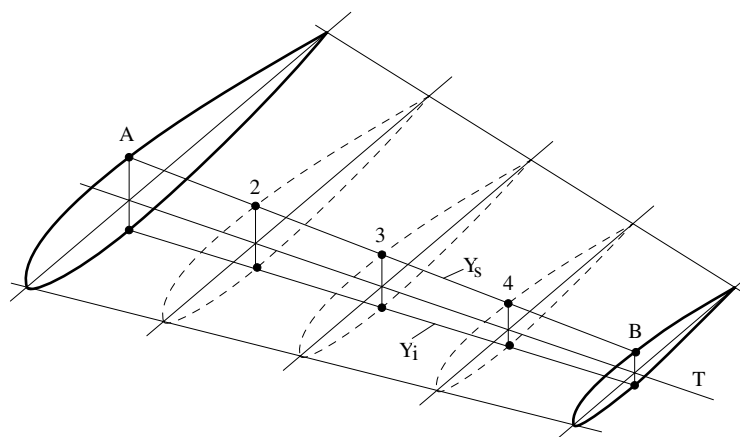


Figure 8-5

In order to eliminate this, and the possibility of errors, the design will have to be repeated separately for every percentage value. We understand how long and laborious the operation will become.

For this reason and also for the poor precision expected from the graphic method, it is preferable to calculate the required values by means of the analytical method.

Analytical Method. Let us consider again the airfoils *A* and *B* and the intermediate airfoils 2-3-4. At each percentage value of *X*, (30% for instance), we find the difference between the value of *A* and the value of *B*. Dividing this difference by the number of ribs less one, which is the same as the number of spaces between the ribs, we find the difference in value that exists between adjacent ribs. This is only true if the distance between the ribs remains constant, if not a difference may be calculated proportionally. Adding this difference to the value of rib *B*, or subtracting this difference from the value of rib *A*, the same amount of times that there are spaces, we obtain the value for each intermediate rib.

Example. Let's use a practical example to better understand the principle. Let us consider the upper value Y_s at 20% of the chord. For *A*, $Y_s = 40\text{mm}$. For *B*, $Y_s = 20\text{mm}$. The difference between the two is $40 - 20 = 20\text{mm}$.

This divided by the number of spaces, four in our case, gives us the increment between two adjacent ribs:

$$20 / 4 = 5\text{mm}$$

Adding to the value *B* or subtracting from the value *A* we have the values for ribs 2-3-4:

$$\begin{aligned} Y_s \text{ for B} &= 20 \text{ mm} \\ Y_s \text{ for 4} &= 25 \text{ mm} \\ Y_s \text{ for 3} &= 30 \text{ mm} \\ Y_s \text{ for 2} &= 35 \text{ mm} \\ Y_s \text{ for A} &= 40 \text{ mm} \end{aligned}$$

To verify we see that the value of Y_s for *A* = 40mm. With the same procedure we obtain all the other required value at all the percentages of the chord.

49. Wing Twist and the Wing Reference Plane

We have seen how to obtain the various airfoils of the intermediate ribs between the root and tip ribs, but we have done this without consideration of their relative orientation to each other, created by the twist in the wing.

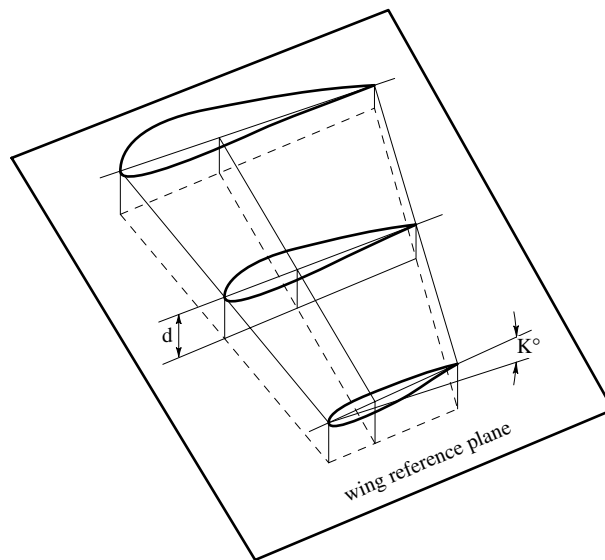


Figure 8-6

For the proper wing construction, we need to have the exact orientation of each airfoil in relation to the other. It is useful therefore to refer to each airfoil, not to its chord, but to a common plane that we call the wing reference plane.

This arbitrary selected plane is chosen outside the wing. This is done in order to keep all the dimensions of the various airfoils positive, and thus to simplify the calculations.

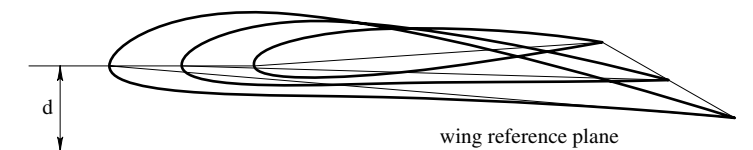


Figure 8-7

To obtain the desired twist, generally, the airfoil sections are rotated around their leading edge so the leading edge remains straight.

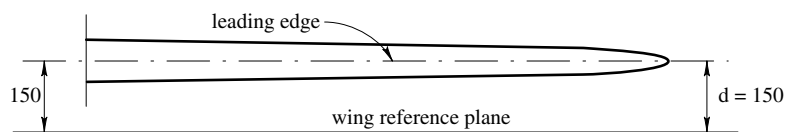


Figure 8-8

The wing reference plane is generally fixed at a distance of 15-20 cm below the leading edge.

The airfoils for the wing root and tip are drawn in reference to their chord or tangent depending on the type of airfoil table used.

It is now necessary to refer to the angle of incidence of the wing in relation to the fuselage axis.

For this we draw a horizontal reference line at a distance from the leading edge by the same amount of the earlier chosen distance to the wing reference plane, and at an angle equal to the angle of incidence.

To clarify this let's use an example.

Let the wing reference plane be parallel and at a distance of 150 mm from the leading edge. Let the wing twist be -5 degrees, and the angle of incidence of the wing in relation to the fuselage be 3 degrees. The airfoil at the wing tip will then be -2 degrees in relation to the fuselage.

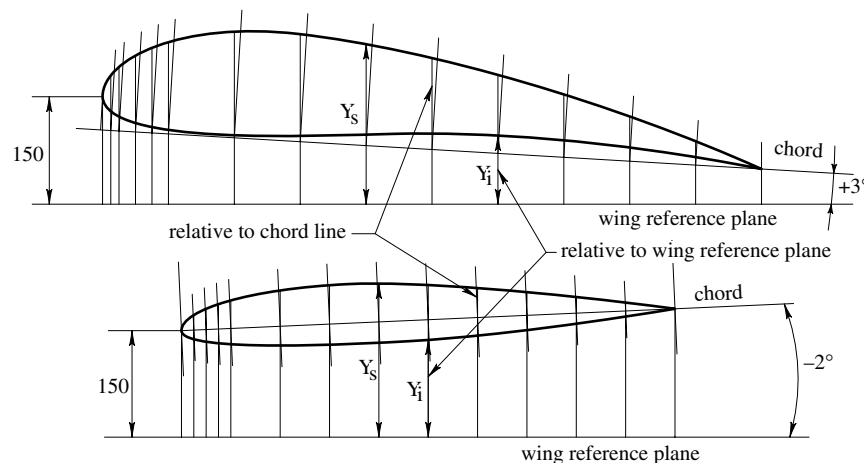


Figure 8-9

Having drawn the basic airfoil in relation to its chord, we trace a horizontal reference line at a distance from the leading edge of 150mm and having an inclination of 3 degrees at the fuselage and -2 degrees at the wing tip.

We reference all of the airfoil data to this line.

We then trace from each point of division of the chord lines perpendicular to the horizontal reference line. On this line, we read the Y_s and Y_i values of the airfoil in relation to the horizontal reference line.

The basic airfoils are therefore then defined by the exact points.

For the basic linear variation between them we proceed as we seen earlier. The intermediate airfoils will all be referred to the wing reference plane with an angle of incidence based on the wing twist.

Virtual and Real Airfoil for the Wing Tip. Up to now we have only considered a straight wing all the way to its tip. We know that the wing tips are rounded for aerodynamic reasons as well as for aesthetic design, and we have already seen how these curves are designed.

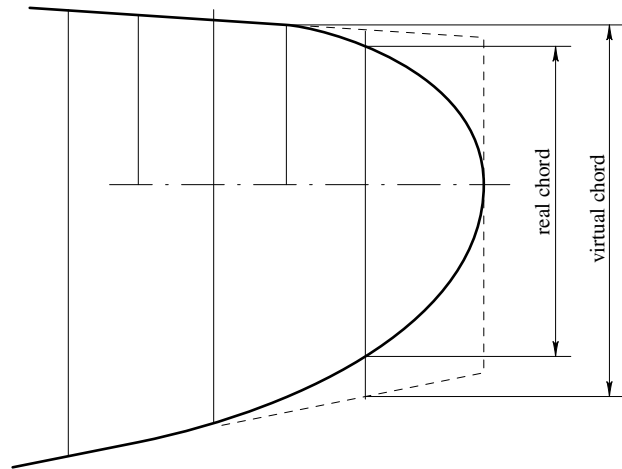
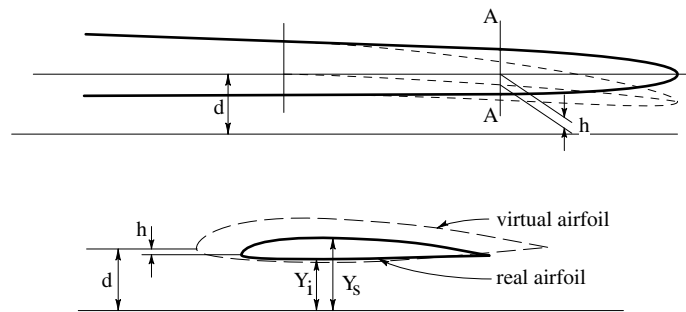


Figure 8-10

We will now look at how the airfoils in this region have to be modified.

The values Y_s and Y_i of these airfoils need to be multiplied by the ratio of the real and virtual chords. This ratio will diminish towards the tip, and it will always be less than one.



Section A-A

Figure 8-11

We thus obtain airfoils with the chord, thickness and angle of incidence desired, but closer to the wing reference plane. The leading edge therefore in this region is no longer straight. We need to adjust this distance back to the original distance. To do this all that is required is to add to the values Y_s and Y_i the difference h found between the leading edges of the virtual and real airfoils.

50. Fuselage Design

Having approximately designed both the top and side views of the fuselage at the beginning of the project, we should now sort out the shape of the various sections required for construction. Having fixed the fundamental shape, considering all the space needed by accessories, it is now the time to proceed with the streamlining of the fuselage, in other words to design a fuselage that is aerodynamic and still compatible with the construction requirements.

We should first explain the process of streamlining. If we consider a body of revolution—a body obtained by rotating a curved line around an axis—its sections will

be circles. In a case like this, it will be sufficient for the single generating line to be streamlined in order for the entire body to be streamlined.

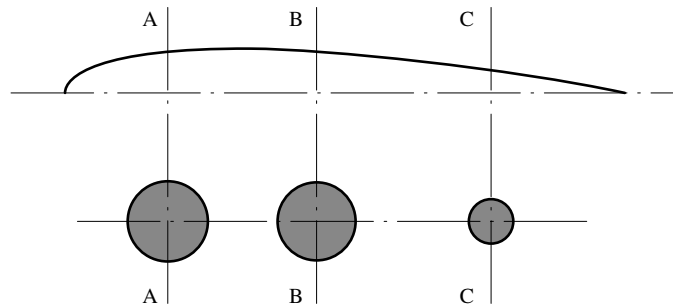


Figure 8-12

Similarly, a body whose sections are of any shape but similar to each other, and aligned on a common straight axis passing through a fixed point in each section, the body will be streamlined if any of the generating lines are streamlined.

Therefore a fuselage of an elliptic shape, where the ratio of the axis of the ellipses of the various sections is constant, and these ellipses are aligned on an axis drawn through a characteristic point to them (for example one of the foci, or its center) will be streamlined as long as any of the parameters, such as one axis, is streamlined. The same stands true for a fuselage of rectangular shape, where there is a constant ratio between the two sides and where the sections are aligned at the intersection of the diagonals.

Generally though, the various sections are not similar and the ratio of the axis of the ellipses or the sides of the rectangular are not constant. Also the line to which the sections are referred to is not linear, but curved downwards, like in the front part of the fuselage.

In such cases, is no longer sufficient that only one of the parameters, like a generating line, to be streamlined. We have to verify the streamlining of different parameters and of the sum and the ratio on all of them.

In practice, this type of design work is accomplished in this manner: First the top and side views of the fuselage are drawn, taking into account all the necessary space requirements. Then the fundamental shape of the cross-section and the longitudinal variation is fixed. Then a simple solid body of the desired shape is defined, where its sections are geometrically determined. To this base body, other simple shaped bodies, for cockpit, wing connections, etc., are superimposed.

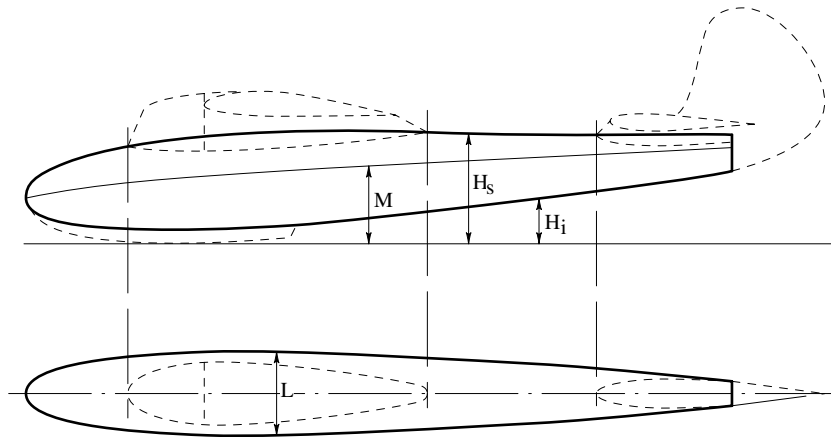


Figure 8-13

Thus having outlined the fuselage, that is, having defined the various parameters, width L , and the various heights, relative to a common base line or ground plane, we now proceed with their streamlining.

We verify the process by means of a design trick, where the curves are exaggerated. Thus, we design the fuselage with a scale of 1:10 longitudinally and 1:4 or 1:5 transversally.

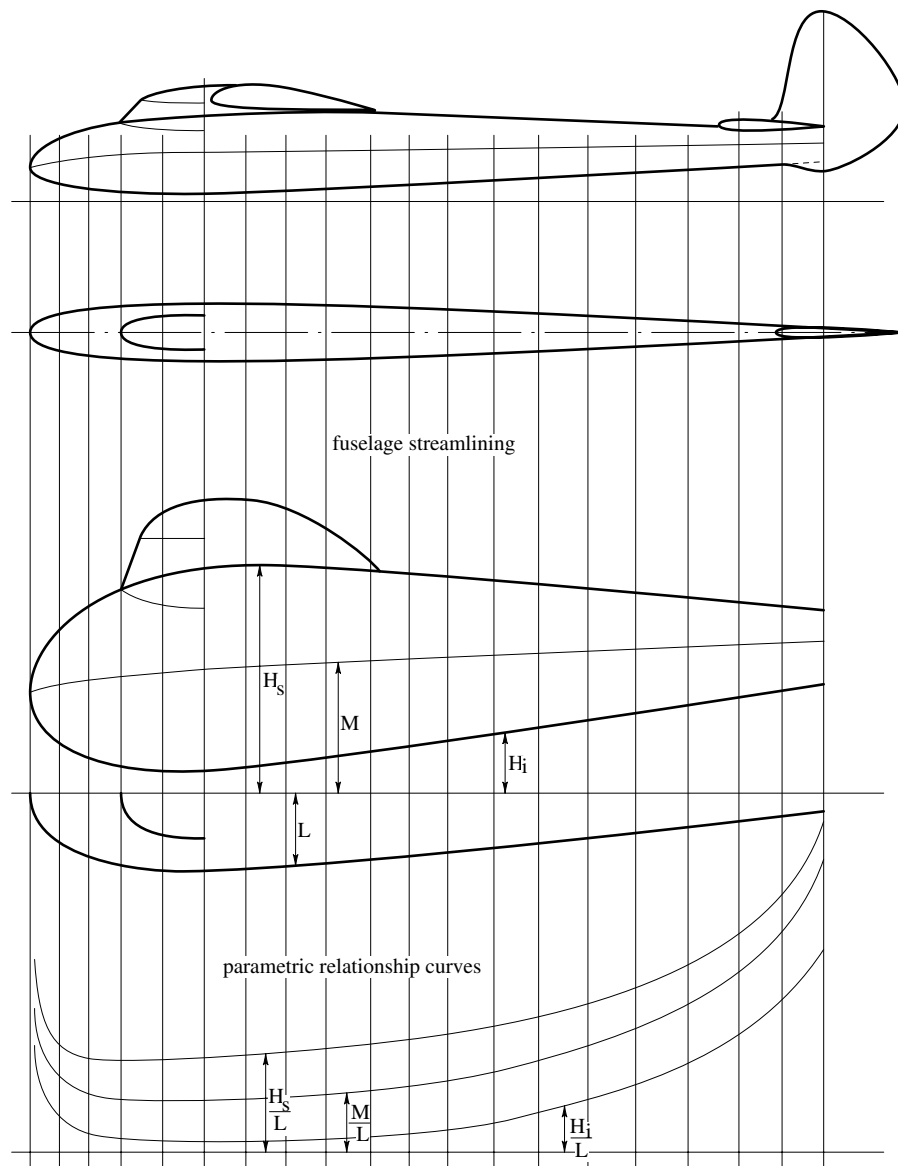


Figure 8-14

In any case the ratio between the two scales will be adopted on a case-by-case scenario, according to the particulars of the design. Generally, these curves will exaggerate any irregularity or errors in the data points, and corrections will then be made.

We will return to the design of the sections, once more, with these corrected values, to check that we are still meeting the necessary requirements of space and aerodynamics. The same streamlined design of the various parameters will also serve to extract the changing dimensions for the outline of the cross-sections of the fuselage itself.

Streamlining of fuselages when the sections are not geometrically defined. When the sections of a fuselage are not geometrically defined, a streamline study is no longer possible since the required parameters are missing.

We then turn to the *water line* concept, so called because of its extensive use in boat design and construction.

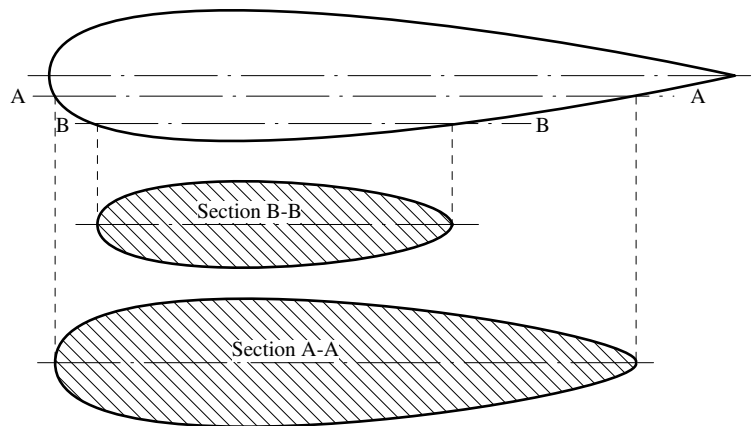


Figure 8-15

This consists in slicing off parallel sections of the body under study, and verifying that the intersection shape is streamlined.

It's not necessary for the sections to be aerodynamic, as in the case of Section A-A, because the laminar flow around the body is not parallel to the axis.

Design of the Sections. We have seen that the easiest method of streamlining the fuselage is achieved when the shape of its sections are geometrically identifiable. We are not going to describe all the various sections employed in fuselage design, since the designer will adopt the best suited design for the requirements at hand and based on the best aerodynamics, construction methods and space requirements.

We will like to point out though, a type of section, that is simple and practical, both in its design form and in the streamlining of its parameters. This type is brought about by means of parabolic curves, constructed with the tangential method, seen earlier in the design of the wing tips. With this kind of construction, we can achieve most types of fuselage shape sections, from almost circular rounded shapes to ones that are sharp-cornered on the lower section or even on both sections, as it occurs in the aft portion of the fuselage.

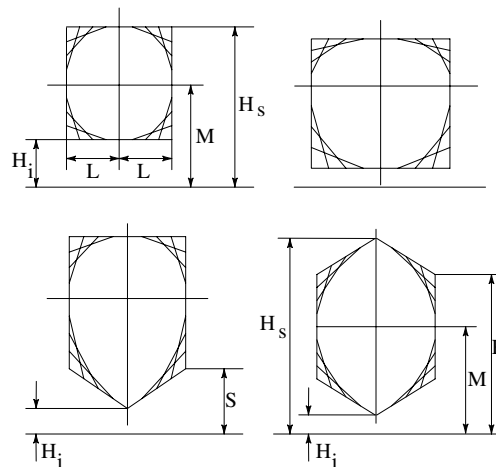


Figure 8-16

To streamline a fuselage with such sections, it is necessary to streamline the various parameters that define the section, such as the width L and the various heights H in relation to the plane of construction, and the ratios of these with the width itself. We can easily see that it is not possible to give a fixed rule for this type of design, since one would have to study in specifics the most convenient and necessary streamlining of the parameters for each fuselage type.

In the case, as an example, where the sections are the arcs of a circle, one would have to streamline the circle's radii, their centers and the ratio among them. It will then be the design itself that will suggest, case by case, which will be the parameters to be examined.

What we have briefly described is not to be used as a rule, but rather as a basis for the study of this very important work of fuselage design.

51. Empennage Design

What we have seen in the wing design also applies in the empennage design. Even in the tracing of its airfoils, the procedure used is similar to that one of a wing with a constant airfoil. The empennage's airfoil, in fact, is always symmetric and bi-convex, and also it never has a twist.

In reality, it is often convenient to taper the airfoil in thickness, but the variation is on the same airfoil. Generally the thickness goes from 10% - 12% where it attaches to the fuselage to 6% - 8% at the tips. The variation has to be linear for both the horizontal and vertical section.

52. Design of Movements of the Mechanical Controls

We have seen in the last chapter how to lay out the various controls. The actual movements of these controls is of fundamental importance and should now be considered. Let's have a few examples that will allow us to make some observations.

Let's suppose we have two levers, l_1 and l_2 , hinged on their axis at their half-way point, and placed at a distance L . The levers are straight, of equal length and connected to each other at their extremes by cables of equal length, in such a way that the angle between the cables and the lever's axis is 90° . Under these conditions, the levers will then be parallel to each other.

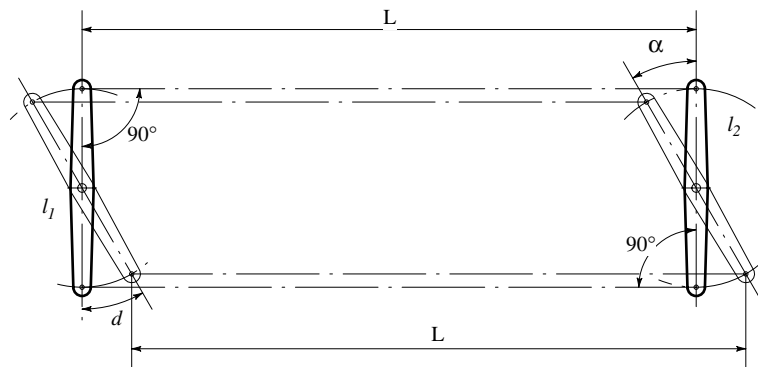


Figure 8-17

Let's rotate lever l_1 in the direction show by an angle α . The amount of movements for both the cables is the same, since the lever's arm are the same. Therefore the other lever, l_2 will rotated by the same angle α , and the tension of both the cables will remain the constant since the distance L did not change.

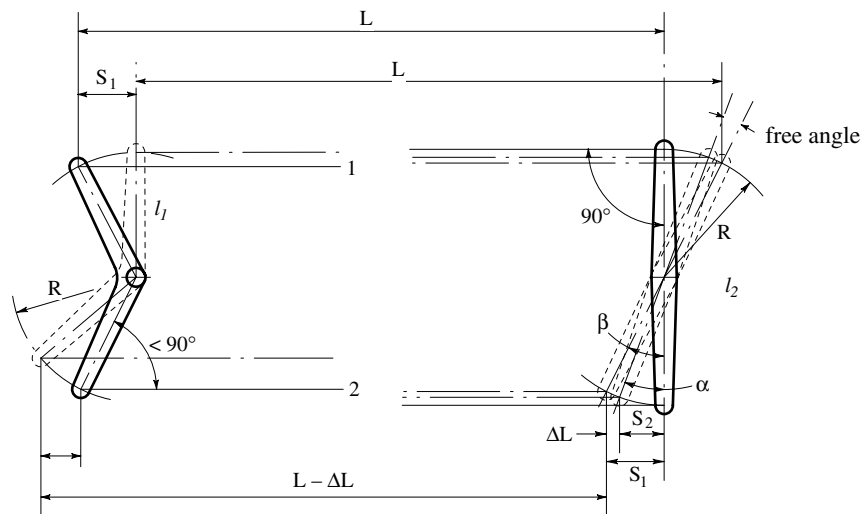


Figure 8-18

Let's now consider lever l_1 bent backwards as in Figure 8-18, with the angle between the cable and the lever's arm is less than 90° , and the second lever still being straight, with its arm being of equal length to the first lever. Rotating the first lever clockwise by a certain angle, we notice that the lever's movements at its extremes, in the direction of the cables, is not the same but is greater for the top cable, S_1 than it is for the bottom cable S_2 .

Since lever l_2 , is controlled by the lower cable which moves by S_2 , its rotation angle will not be equal to the one for lever l_1 . Also, and more importantly, the top cable will slack, since the movement S_1 of lever l_1 is greater than the top movement of lever l_2 . Consequently, the top cable will slack by a quantity equal to the difference between the movements of lever l_1 , S_1 and S_2 :

$$\Delta L = S_1 - S_2$$

Due to this slack in the top cable, lever l_2 has freedom to further rotate even though lever l_1 remains stationary. It will rotate until the top cable is taut—resulting in the bottom cable becoming slack.

In conclusion, we can say that at every position away from neutral of lever l_1 , there is no single corresponding position for lever l_2 , but lever l_2 may rotate between angles α and β that correspond to movements S_1 and S_2 . Similarly, if lever l_2 is kept stationary, lever l_1 can rotate by the same angles.

If we would use this system in the control system of an aileron, for instance, the aileron, when off its neutral position where both the cables are equally taut, will be free to move back and forth by a certain angle even though the control lever is kept secured. Under these conditions, the aileron will start to vibrate with consequences that are easy to appreciate.

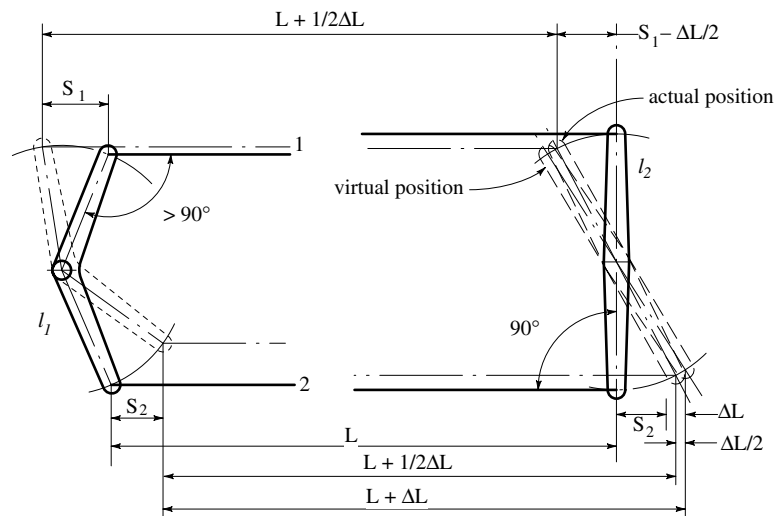


Figure 8-19

A third consideration is having a lever l_1 bent forward, with an angle between the lever's arm and the cables greater than 90° as shown in Figure 8-19.

In this case, a rotation of lever l_1 off its neutral position will result in a movement S_1 greater than S_2 , and since the top cable is controlling lever l_2 , l_2 will move by the same amount S_1 in both its top and bottom arm. This will have the tendency to also move the bottom cable by the same amount, S_1 , but the bottom portion of lever l_2 only allows that cable to move by S_2 .

This will follow with an over-tensioning of both cables, resulting in a general hardening of the entire system.

From this examples we can draw an important conclusion. *In a closed-circuit cable transmission system, in order not to experience slacks or over-tensioning in the system when off its neutral position, it is necessary that the angle between the cable and the lever's arm, to which the cables are attached, be of 90° , when in the neutral position.*

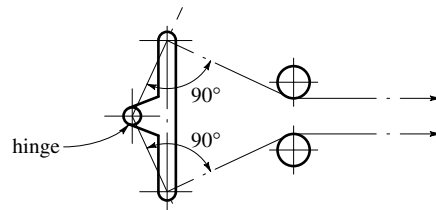


Figure 8-20

It is important to notice that at times, due to the construction, the hinged portion of the lever is not on the lever's axis itself, but placed outside. Therefore, in a more generic way, we can say that the 90° angle has to be between the cable and the radius drawn from the center of the lever's rotation to the point in the lever to which the cable is attached.

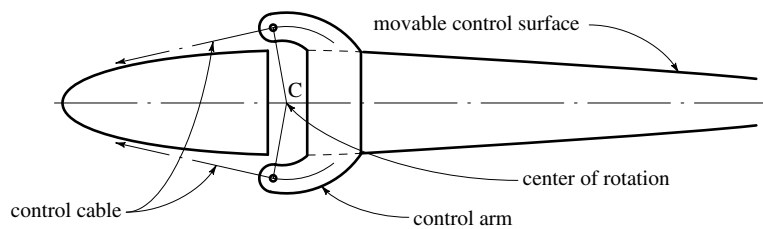


Figure 8-21

For this reason, the levers that control the various moveable surfaces assume strange forms at times.

Rigid Controls. So far we have talked about controls where the transmission of movement is accomplished by means of cables. If instead, the transmission of movement is obtained by means of rods, since these can work in tension as well as compression, the system is not required to be closed, with two arm levers and two cables, but a single arm lever is sufficient to transmit the movement in both directions.

With rigid controls we also eliminate the inconvenience of having slack or hardening of the systems in the conditions we have seen when the angles between levers and cables are not at 90° . The inconvenience of the non-equal angular rotation, between the moving lever and the moved lever does remain, if the angle is not 90° . This inconvenience though, does not lead to serious consequences as we have seen earlier.



Figure 8-22

Often, there is the requirement of not having equal angular rotation of the moving lever in respect to the moved lever. Such is the case in the differential controls of the ailerons. As we already know, in the case in the lateral handling of an aircraft, it is necessary to have the up-going aileron move at a greater angle than the down-going aileron. This is accomplished by having angles, between levers and connecting rods, different from 90° . A simple, and very commonly-used scheme of this type of control is shown in Figure 8-23.

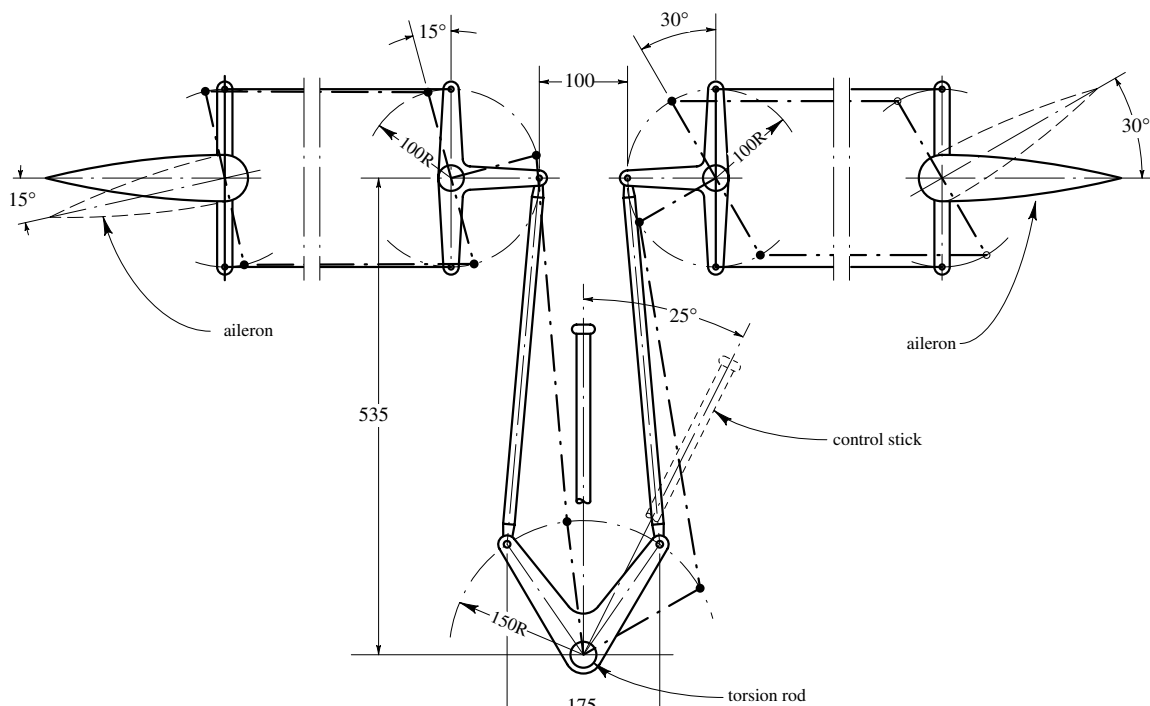


Figure 8-23

To the torsion rod there are attached two levers forming an angle of 30° and with a turning radius of 150mm. The angle of movement of the control stick, also attached to the torsion rod, is 25° on both sides. The angular movement of the ailerons results in a down-position of 15° and in an up-position of 30° . The differential ratio is 1:2, a normal value for gliders.

We will not elaborate too much on these topics, even though they are of fundamental importance. What is important is that an idea was given that may serve useful in the orientation of the study of these mechanisms. Also we cannot give many examples, since each aircraft requires its own particular study. These mechanisms are tied to the particular architecture, construction demands and the final use of the aircraft. This is an area, in a way, where the designer can indulge in his own whims, and because of this, we have at times seen solutions that are very ingenious, but also often which are more complicated than necessary.

Chapter 9

Applied Loads and Structural Design

53. Flight Loads

The design of the airframe is carried out in three distinct phases: (1) analysis of all the flight loads to which an aircraft may be subjected, and the analysis of the stresses caused by these conditions, (2) determination of all the strains on the various structures under different conditions, and (3) testing the strength of the various elements.

The first phase is the most difficult analysis due to the number of flight conditions and atmospheric conditions. These stresses are very difficult to foresee.

Today, based on years of experience we can accurately establish the loads that are applied to the various elements of an airplane in various flight conditions. The results of these experiences are common to the majority of aircraft with appropriate adjustments for individual type.

Every country has adopted regulatory engineering standards for the design of the structures, and which establish the loads that affect the components of every aircraft. These standards have been established to help the designer in his work, and also to establish a discipline and regulate the aeronautical design so as to not leave the structural strength and safety of the aircraft at the sole judgment of the designer.

In their standards, each country considers all of the possible flight conditions, and among these have determined and examined the ones that calculations and experience have shown to be the most dangerous ones. In the beginning these standards were very simple, but various countries had a considerable difference of opinions.

Today however while improving they also have become complicated, since not only the weight of the plane and its dimensions are considered and examined but also the aerodynamics. Countries have therefore reached a standardization, especially in the civil sector of aviation.

From tests performed on aircraft under various atmospheric conditions the following conclusions were established: (a) the greatest flight loads occur in sudden pull-ups, (b) the flight loads in rough air generally do not exceed the value of 2.5 g and (c) maximum acceleration withstood by men is roughly 7-8 g for short durations, and 3.5-5.4 g if continuous. With gliders it has been established that the maximum acceleration does not exceed 3.5 g.

From these conclusions the regulatory standards have established a load factor for various categories of aircraft, a value that is equal to the ratio of the maximum load applied to a specific structure and the airplane's maximum weight. In a steady horizontal flight, the lift is the applied load and equal to the weight, and the load factor is equal to one.

In Italy there are two authorities that regulate aeronautical production: one for civilian aircraft and one for military aircraft. The military airworthiness standards are more complete and complex than the civilian standards, however we will discuss only the civilian regulations.

In these regulations there are three load factors used: gliders: 3.5 *g*, normal category aircraft: 3.5 *g* and acrobatic category aircraft: 4.5 *g*. The civilian standards use these load factors to calculate the loads applied to the components of the airframe. To make sure that the structures are not subjected to loads that exceed the elastic limits of the construction materials, the airframe components are designed to a greater load.

In mechanical or civil engineering, structures are designed for loads that are 3 to 5 times greater than the anticipated loads. This is the same as saying that the factor of safety is 3 to 5. These safety factors are fairly high, and they are adopted to insure against all possible dangers, including the deterioration of the materials over time, the possibility of errors in the calculation of the loads, and also for unforeseen accidental causes. Adopting a safety factor this high results in a heavy structure. Generally this is not very important in terms of cost or the quantity of material used.

In aircraft construction, however, weight is very important and extra material cannot be used. For this reason, the factor of safety in aircraft construction is relatively low, and a safety factor of 2 is required by civilian airworthiness standards for all types of aircraft, with some exceptions, thus the structures are designed for a load factor of twice the flight loads. [*Today, the standard factor of safety is 1.50.*]

54. Static Tests

Because aircraft use a lower factor of safety, the calculations of the strength of the aircraft structure must be done with a greater degree of rigor than for civil and mechanical engineering. We must also verify the airframe's strength with static tests. Civilian and military airworthiness standards require that every aircraft prototype has to undergo a static test. Once the aircraft passes this test, it is allowed to continue with flight tests and normal flight.

These static tests check the strength of the most important components, such as the wings, fuselage, control surfaces, landing gears, controls, etc. During these tests, the components are attached to a test rig to duplicate the flight loads and conditions. The test rig should be quite strong so that the internal deflection may be ignored or at least measured. This allows controlled forces to be applied to the structure and the failures documented.

The static tests consist of a limit load test and an ultimate load test. The limit load test is performed with limit loads which are imposed for an indefinite period of time, and it should result in no permanent set. The ultimate load test is carried out following a successful limit load test. In this test, ultimate loads are applied for a short duration and failure may not occur. After this, the loads are increased until failure occurs, and the

designer may collect data in order to study any divergence of the calculation from the results of the test.

In gliders, since they are manufactured in limited numbers and at times are based only on the prototype, static tests to ultimate loads or failure are never conducted, since an airframe loaded to such extremes, even if it never shows signs of failure, is no longer suited for flight since the structure has gone beyond the limits of elasticity and would be over-stressed.

Static tests to limit loads are used for the main structural components, however tests to ultimate loads and failure may be performed on individual components and assemblies where appropriate and practical.

55. Flight Conditions

Let us see then how to determine the loads affecting an aircraft during various flight conditions. With gliders we consider four fundamental flight conditions for the wing: (1) maximum lift, (2) maximum speed, (3) zero lift, and (4) hard landing.

Maximum Lift. The condition at maximum lift occurs during a sudden pull-up or when a strong vertical gust is encountered during high-lift conditions. The limit load factor is 3.5 *g* for gliders and normal category aircraft, and 4.5 *g* for acrobatic category aircraft. Under these conditions, we have the maximum bending of the wing.

The forces that are acting in this case are: aerodynamic forces (lift, drag, moment), aircraft weight, centrifugal reactions, and the reaction of all the linkages that transmit the forces of the rest of the aircraft to the wing.

The load applied on the wing is:

$$L = 2 \cdot N \cdot (W_{total} - W_{wing})$$

where

2 = factor of safety [*today, 1.50 is used*]

N = load factor (3.5, 4.5, ...)

*W*_{total} = aircraft total weight

*W*_{wing} = wing weight.

As we see in the formula, the load applied to the wing is reduced by the weight of the wing itself. This weight, being distributed with the same laws of aerodynamic loads, is in opposite direction of to the aerodynamic forces, therefore the wing supports itself without generating bending loads due to its own weight. The load *L* is averaged along the wing span proportionate to the wing chord. The distribution on the chord is assumed triangular with center of lift at 1/3 from the leading edge.

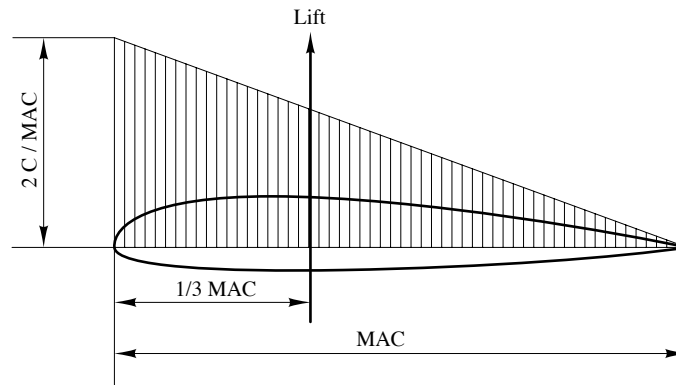


Figure 9-1

The wing including the wing fillet is considered a lifting surface only.

Maximum Speed. The coefficient of lift at maximum speed in gliders is one where:

$$C_L = 0.25 \cdot C_{L_{\max}}$$

at the same altitude.

In this condition the center of lift is always aft, thus there is a heavy load on the aft spar, its attachments and on the aft structure of the wing. The load factor is set at 0.75 of the one used for the calculation of the maximum lift condition. The load on the wing therefore will be:

$$L = 2 \cdot (0.75 \cdot N) \cdot (W_{\text{total}} - W_{\text{wing}})$$

This is divided among the ribs with the distribution shown in Figure 9-2 with a center of lift at 50% of the chord.

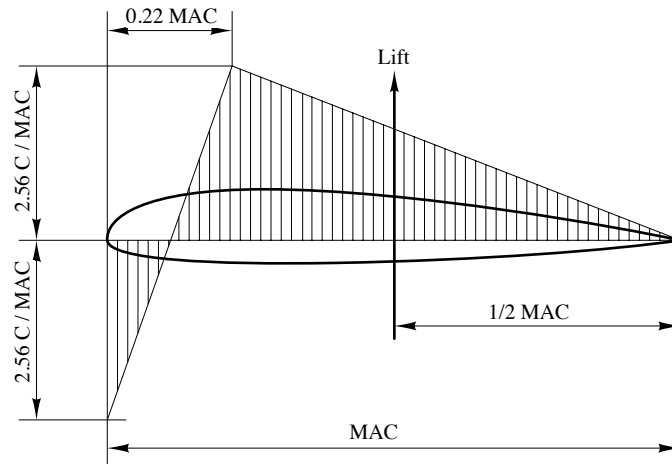


Figure 9-2

Zero Lift. The zero-lift condition is the equivalent of a straight-down nose dive at maximum velocity in acrobatic category aircraft and at a lesser velocity in normal and utility category aircraft. This produces the maximum torsion on the wing, therefore you must analyze the resistance of the wing and its attachment to the fuselage to this load. The minimum value of torsion is given by:

$$Torsion_{\min} = 0.20 \cdot N \cdot W_{\text{total}} \cdot MAC$$

where

N = load factor (3.5, 4.5, ...)

W_{total} = total weight

MAC = mean aerodynamic chord

The regulations also dictate that under a maximum load of 1.25 N the twist at the wing tips may not be over 4 degrees. In gliders, due to the length of the wings, this last condition is more critical than the resistance to twist itself, therefore special attention is given to the design in order to keep the elastic deformation within 4 degrees.

Hard Landing. In a hard landing the wing and its linkages are subjected to downwards forces of inertia when the aircraft touches ground. These forces are considered to be at 15 degrees forward of the perpendicular plane of the wing. The landing load in a glider is calculated by multiplying the combined weight of the all the wing elements complete with the accessories attached to the wing by a factor of 4, no matter what category of glider.

In this condition, as in the maximum lift condition, the wing is subjected to forces that are in a forward direction in the first case and a backward direction in the second case. Due

to scarcity of aerodynamic data, regulations dictates that in gliders, the maximum load in the wing plane in the forward direction be equal to:

$$\frac{1}{8} \cdot N \cdot W_{total}$$

where N and W_{total} are already established.

Following the civilian regulations we have briefly looked at the loads on the wing in various flight conditions. Later, we will study the load conditions for the fuselage, the empennage and other elements.

56. Wing Stress Analysis.

Let us again consider the wing and analyze what we have called the second phase of the design of the supporting structures, that is, the calculation of the structural stresses considering the architecture itself.

In this design phase, we enter a field of engineering that deals directly with construction. Since it is evident that we cannot discuss this topic in great length, or even assume that the reader will have complete knowledge of this discipline, we will discuss a simple and practical method of calculation.

1) Load distribution at maximum lift. The load on the half-wing

$$n = (Q - Q_a)$$

is distributed on the wing according to the area, and thus proportionally to the chord of the wing. In practice, the rounding of the wing tip is not considered, therefore the calculated area is slightly greater than the actual wing area. It is acceptable to do this, since we use worse-than-actual load conditions, because the center of the wing area will be located farther outboard.

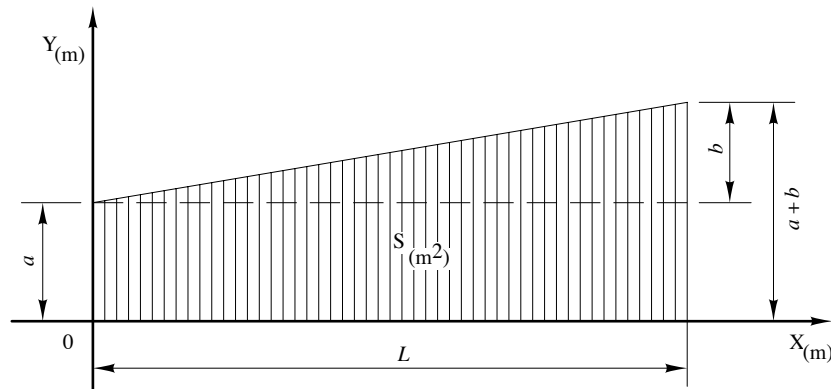


Figure 9-3

The drawing that shows the wing area also represents the load distribution on it. Since the stresses increase from the extremities to the center, the distances are counted starting from the wing tip where the origin of the x and y axis is placed.

If a is the minimum chord, $(a + b)$ is the maximum chord at the wing root, and L is the wing half-span, the intensity of the loads corresponding to these chords will be

$$\text{On the minimum chord: } C_1 = a * P/S \text{ (kg/m)}$$

$$\text{On the maximum chord: } C_2 = (a + b) * P/S \text{ (kg/m)}$$

Where P is the load on half-wing and S is the half-wing area.

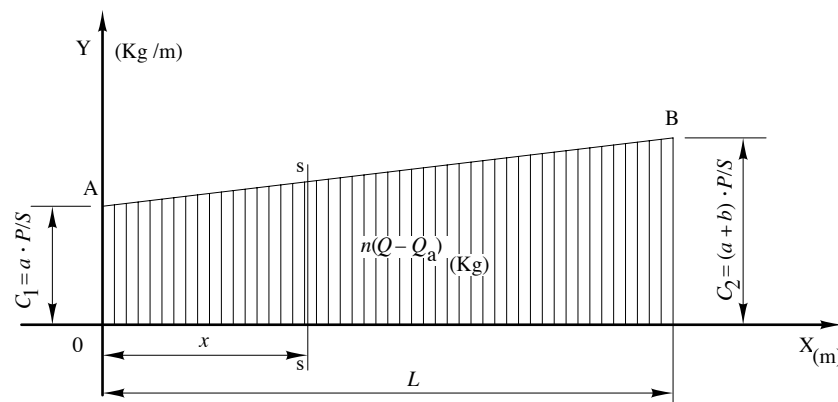


Figure 9-4

Example. Let us suppose that the wing of a glider has a minimum chord of $a = 0.5 \text{ m.}$; half-span $L = 8 \text{ m.}$; maximum chord $(a + b) = 1.5 \text{ m.}$; total weight $Q = 300 \text{ Kg.}$; wing weight $Q_a = 100 \text{ Kg.}$; $n = 3.5$; half-wing area $S = 8 \text{ m}^2$.

The load for the half-wing will be

$$n * (Q - Q_a) = 3.5 (300 - 100) = 700 \text{ kg.}$$

The load for the minimum and maximum chord will be

$$C_1 = a * P/S = 0.5 * 700/8 = 43.75 \text{ kg/m}$$

$$C_2 = (a + b) * P/S = 1.5 * 700/8 = 131.25 \text{ kg/m}$$

In the wing schematic, the chords in an appropriate scale represent the ordinates y of the load diagram.

Cantilever Wing. Shear stress. Bending moment. Let us consider first a tapered wing without external means of support. In a generic section S of the wing, the shear stress is none other than the sum of all the loads outside this section, while the bending moment is given by the product of this outside load and the distance d of the center of gravity of the section.

To determine these shear stresses and bending moments in the various sections of the wing, we may use two methods: analytic and graphic.

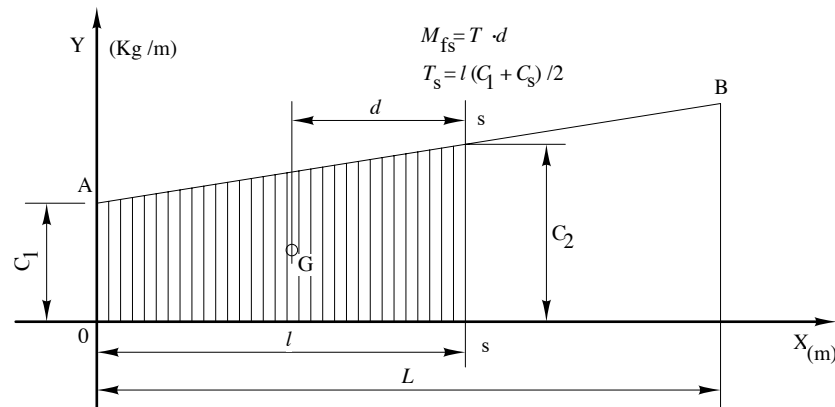


Figure 9-5

Analytic method for a tapered cantilever wing. The shear and bending loads are calculated by integrating the load once and then a second time. This gives us the relation that ties the load distribution to the wing span.

From Figure 9-4, we get the equation of the line AB that represents the load distribution

$$y = \left(\frac{C_2 - C_1}{L} \right) x + C_1 \quad [28]$$

for every value of x distance of the section to the tip, we get the value of load y .

Integrating this function will give us the one for shear stress

$$T_x = \frac{C_2 - C_1}{L} \cdot \frac{x^2}{2} + C_1 x \quad [29]$$

and integrated one more time will give us the function of the bending moment

$$M_{fx} = \frac{C_2 - C_1}{L} \cdot \frac{x^3}{6} + C_1 \frac{x^2}{2} \quad [30]$$

In these equations C_1 , C_2 , and L are known values, and for every value of x we get the values for T and M_f .

Example. Let us consider the wing from the previous example and obtain C_1 and C_2 , let's round off the values to

$$\begin{aligned} C_1 &= 44 \text{ kg/m} \\ C_2 &= 131 \text{ kg/m} \\ L &= 8 \text{ m} \end{aligned}$$

Let's suppose we want to obtain the values of T and M_f at a distance from the tip of $x = 4$ m.

$$T_x = \frac{C_2 - C_1}{L} \cdot \frac{x^2}{2} + C_1 x = \left(\frac{131 - 44}{8} \right) \cdot \frac{16}{2} + 44 \cdot 4 = \frac{87}{8} \cdot 8 + 176 = 263 \text{ kg}$$

$$M_f = \frac{C_2 - C_1}{L} \cdot \frac{x^3}{6} + C_1 \frac{x^2}{2} = \left(\frac{131 - 44}{8} \right) \cdot \frac{64}{6} + 44 \cdot \frac{16}{2} = \frac{87}{8} \cdot 10.7 + 352 = 468 \text{ kgm}$$

By repeating the calculation for the other values of x we obtain the shear loads and bending moments of the various sections of the wing.

In practice T and M_f are calculated for the location of wing ribs.

Rectangular cantilever wing. In the case of a rectangular wing, we will have a load diagram with a line parallel to the x axis as shown in Figure 9-6, so $C_1 = C_2 = C$.

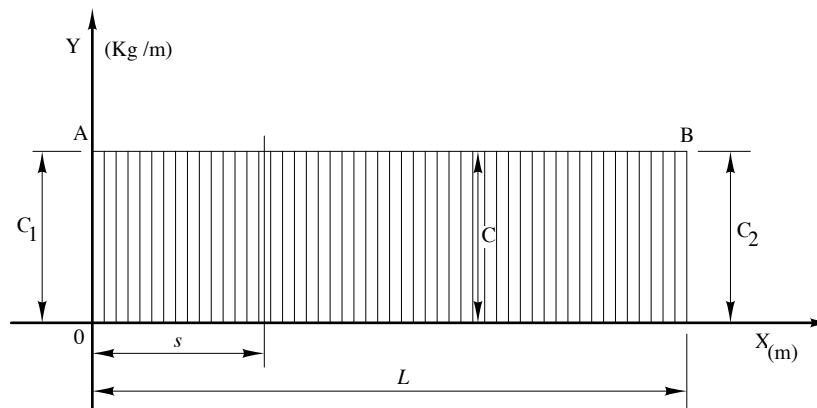


Figure 9-6

Therefore the load equation is $y = C$, thus the load is constant.

And with $C_2 - C_1 = 0$ the shear equation will be

$$T_x = C \cdot x \quad [31]$$

And for the bending moment

$$M_f = C \cdot \frac{x^2}{2} \quad [32]$$

Thus, the calculations for T and M_f are rather simple for a rectangular wing.

Rectangular-tapered cantilever wing. Finally, let us consider a wing with a rectangular center section and an outboard section tapered to the wing tip. See loading diagram in Figure 9-7.

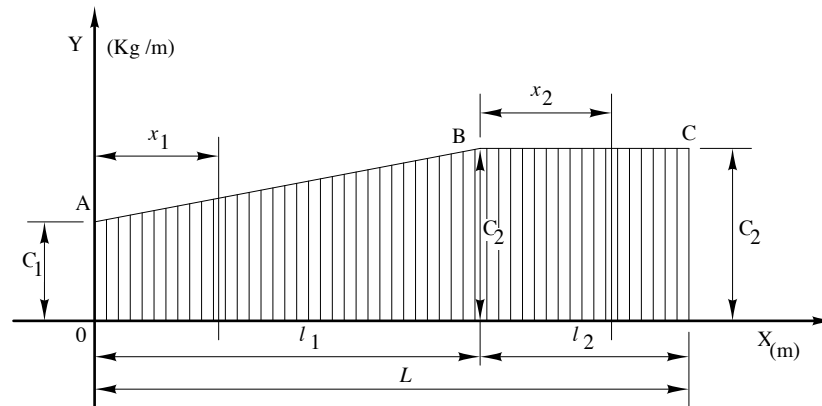


Figure 9-7

The shear equation for the tapered portion from the wing tip to Section B, as we have seen in equation 29 is

$$T_{x_1} = \frac{C_2 - C_1}{l_1} \cdot \frac{x_1^2}{2} + C_1 x_1$$

Where x_1 may vary from zero to l_1

$$0 < x_1 < l_1$$

For the rectangular portion from B to C, the shear is given by the summation of the maximum in B that is equivalent to

$$T_B = \left(\frac{C_2 - C_1}{l_1} \right) \cdot \frac{l_1^2}{2} + C_1 l_1$$

or

$$T_B = (C_2 - C_1) \cdot \frac{l_1}{2} + C_1 l_1$$

with the resultant of the rectangular portion starting from B that is equal to equation 31

$$T_{x_2} = C_2 \cdot x_2$$

Where x_2 is taken starting from B and may vary from zero to l_2

$$0 < x_2 < l_2$$

Therefore in a generic section between B and C shear is equivalent to

$$T_{x_2} = T_B + C_2 \cdot x_2$$

To represent a wing of this type, we use a diagram as shown in Figure 9-8 where the line is parabolic from 0 to the B section and linear from the B section to the fuselage.

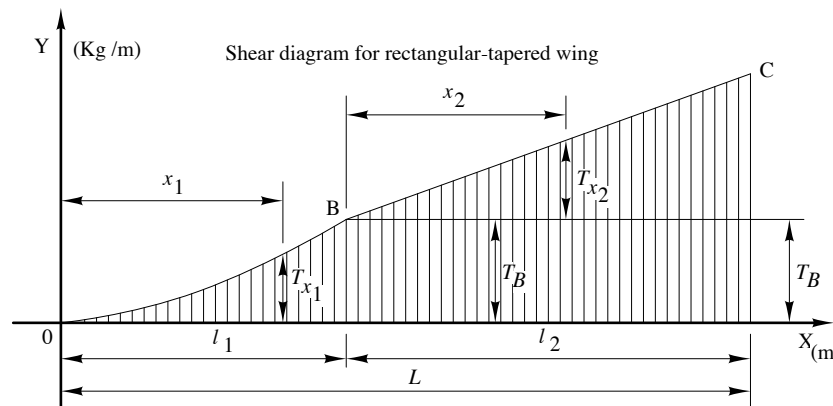


Figure 9-8

For the bending moment also, the two sections are considered separately. For the tapered portion from the tip to section B it is the same as we have previously seen in equation 30

$$M_{fx1} = \frac{C_2 - C_1}{l_1} \cdot \frac{x_1^3}{6} + C_1 \cdot \frac{x_1^2}{2}$$

For the rectangular section from B to C the moment is equal to the product of the load in the tapered section and the distance d from the center of gravity G for the generic section s under consideration as shown in Figure 9-9 and adding the moment of the rectangular section originating at B that is

$$M_{fx2} = \left(\frac{C_2 - C_1}{l_1} \right) \cdot \frac{x_1^3}{6} + C_1 \cdot \frac{x_1^2}{2}$$

The distance of the center of gravity G from the B section may be found either with a simple graphic method, or with the ratio between the bending moment and the shear in B .

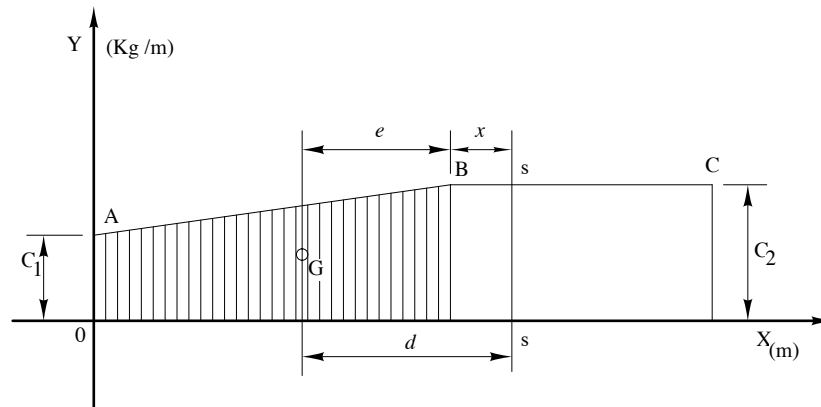


Figure 9-9

Calling this distance e , we have

$$e = \frac{M_{fB}}{T_B}$$

Finally, it follows that the bending moment equation in the rectangular section is

$$M_{fx} = T_B(e + x_2) + C_2 \cdot \frac{x_2^2}{2}$$

Where T_B is the shear stress at B , and $(e + x_2)$ is the distance of the center of gravity of the load on the tapered section we are considering.

Here also, the diagram of the total moment may be considered as the summation of the one given by the load in the tapered section (R), with the one given by the rectangular section (S) in Figure 9-10.

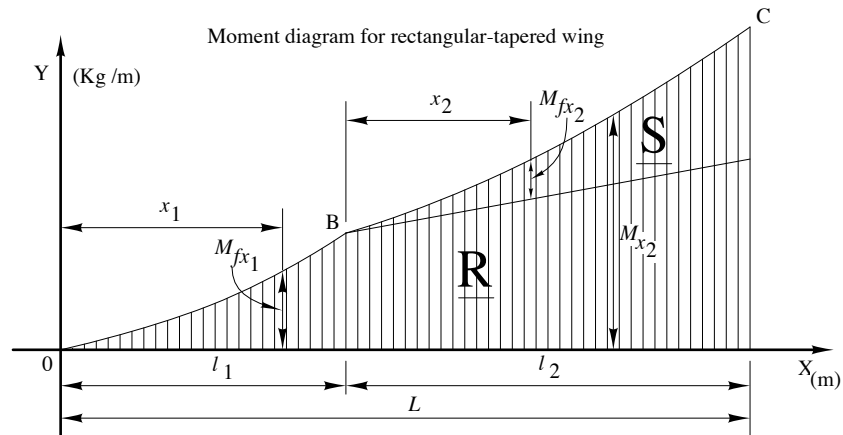


Figure 9-10

The resulting line is parabolic (cubic parabola) from 0 to B, linear from B to D, and again parabolic from D to C.

Example. Let us consider a wing of this type, a rectangular section followed by a linearly tapered section.

Let it be:

$$\begin{aligned}
 C_1 &= 40 \text{ kg/m.} \\
 C_2 &= 130 \text{ Kg/m} \\
 l_1 &= 4\text{m} \\
 l_2 &= 5\text{m}
 \end{aligned}$$

We want to determine T and M in a section s at 7m from the tip.

We will have therefore $x_2 = 3\text{m}$.

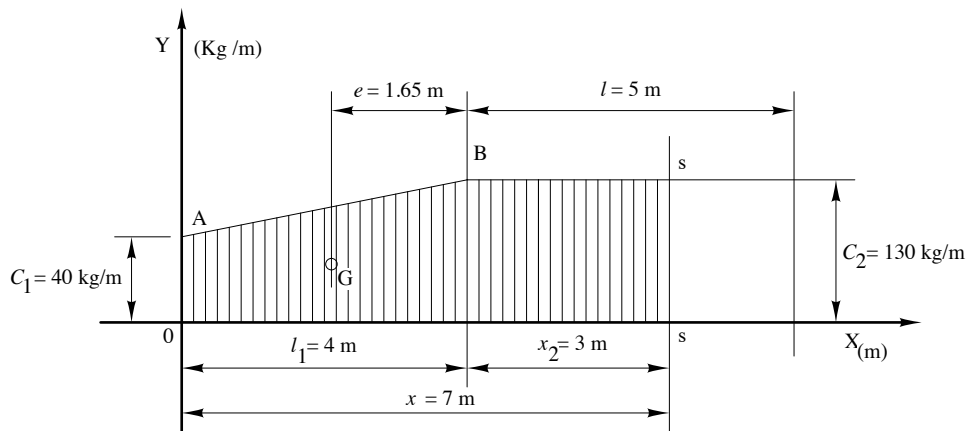


Figure 9-11

For shear at section B , the maximum value for the tapered section will be

$$T_B = \left(\frac{C_2 - C_1}{l_1} \right) \cdot \frac{l_1^2}{2} + C_1 l_1 = \frac{130 - 40}{4} \cdot \frac{4^2}{2} + 40 \cdot 4 = 340 \text{ kg}$$

The shear in this section s will be

$$T_s = T_B + C_2 x_2 = 340 + 130.3 = 730 \text{ kg}$$

Let us determine now M_f . In Section B it is equal to

$$M_{fB} = \left(\frac{C_2 - C_1}{l_1} \right) \cdot \frac{l_1^3}{6} + \frac{C_1 l_1^2}{2} = \frac{130 - 40}{4} \cdot \frac{4^3}{6} + \frac{40 \cdot 4^2}{2} = 560 \text{ kgm}$$

The distance e of the center of gravity of the load on the tapered section is

$$e = \frac{M_{fB}}{T_B} = \frac{560}{340} = 1.65 \text{ m}$$

The bending moment in the section s is therefore

$$M_{fs} = T_B (e + x_2) + C_2 \frac{x_2^2}{2} = 340(1.65 + 3) + 130 \frac{3^2}{2} = 2165 \text{ kgm}$$

We have seen how the shear stresses and moment in a tapered wing are calculated analytically. Let us now continue with a graphic procedure.

Graphic method. The stress determination of T and M_f are based on a graphic integration. In this method, the function of load is expressed graphically by a curve that when integrated one or two times will give us the diagrams of shear and bending moment.

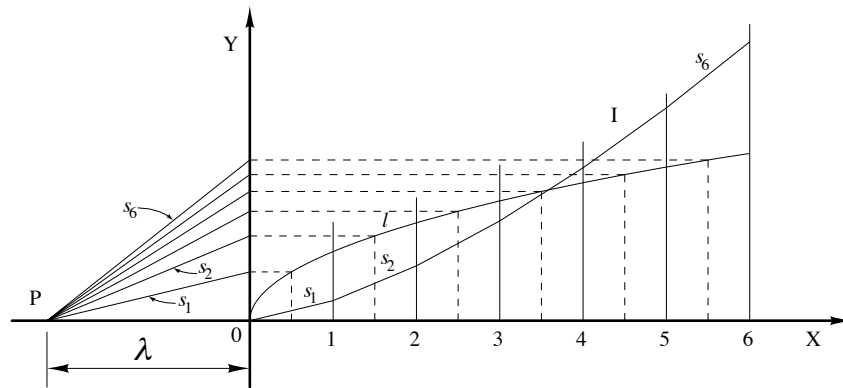


Figure 9-12

Generally to complete a diagram where l as an example is the line that determines it, we divide this in many parallel strips that are perpendicular to the x axis. We trace the middle of these strips, their intersection with the line l are projected horizontally to the y axis. We then take a point P at will on the x axis, and we connect this point with each of the projections on the y axis.

We will have a number of lines with various angles all originating from P . The distance of P from the vertical axis where the projected points of l were traced is called the polar distance, and it is indicated with the letter λ .

Starting from the axis origin O , we trace segments parallel to the lines $s_1, s_2 \dots s_n$ that will intersect the vertical lines in points $I, 2 \dots n$. The resulting segmented line I is the integral line we were looking for.

To read the diagram we need to establish the scale for the y axis. This is obtained by the product of the value of the x axis by the ordinate values of line I and the distance of polar λ .

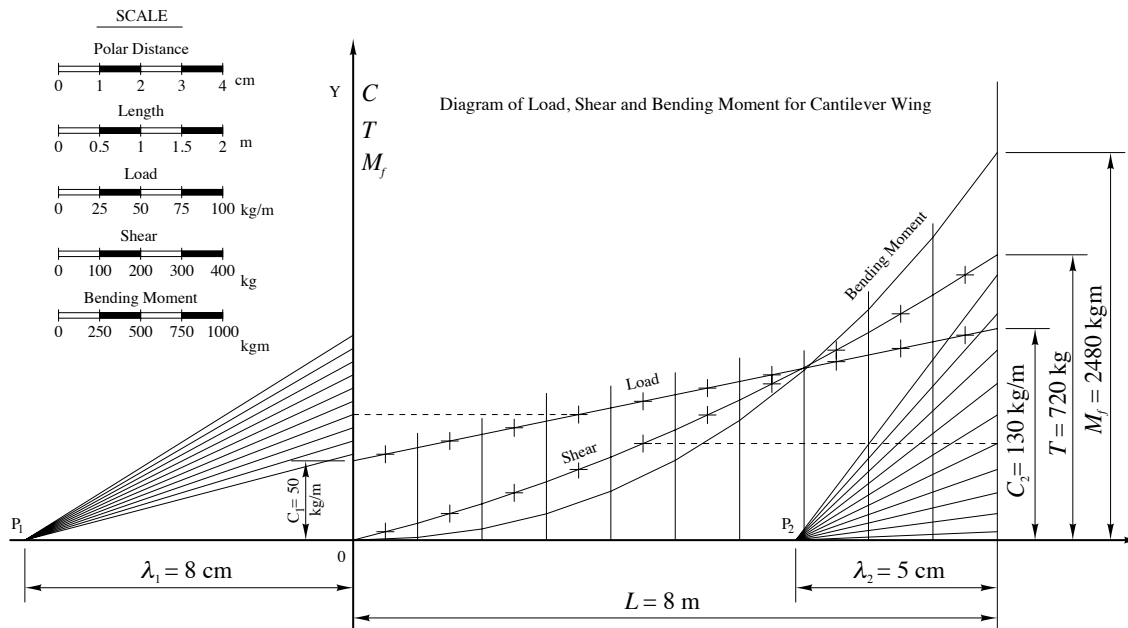


Figure 9-13

Example. Let's construct a graphic diagram of shear and moment. Let's use a convenient scale for the shear loads of a cantilever wing as shown in Figure 9-13

$$1 \text{ cm} = 0.5 \text{ m} \text{ for the dimensions on the } x \text{ axis}$$

$$1 \text{ cm} = 25 \text{ kg/m} \text{ for the loads on the } y \text{ axis.}$$

In relation to the wing's ribs, from the smallest one to the largest one, and with a linear variation in between them, the load is

$$C_1 = 50 \text{ kg/m}$$

$$C_2 = 130 \text{ kg/m}$$

The half-wing span is $L = 8\text{m}$. Taking P_1 at a distance from y axis

$$\lambda_1 = 8 \text{ cm}$$

we divide the loading diagram into ten strips, and as we have seen, we obtain the shear diagram.

We need now to establish the scale in order to read the diagram. This is given by the product of the loading scale, the length scale and the polar distance λ_1 . Thus the shear scale is

$$1 \text{ cm} = 25 * 0.5 * 8 = 100 \text{ kg}$$

In the diagram the maximum value of T is given as 7.2 cm , therefore

$$T = 7.2 * 100 = 720 \text{ kg}$$

To verify this, let's determine the total load on the half-wing, that is, the maximum shear. The average load intensity is

$$\frac{C_1 + C_2}{2} = \frac{50 + 130}{2} = 90 \text{ kg/m}$$

This multiplied by the span L gives us the total load of

$$P = 90 * 8 = 720 \text{ kg}$$

Exactly coinciding with the value found graphically.

Using the same procedure, we now integrate the shear diagram plotting a polar distance $\lambda_2 = 5 \text{ cm}$ to the right of the diagram, so not to interfere with the previous lines. The resulting new diagram will be the one for the bending moment.

The scale is given by the product of the shear with the length and the polar distance λ_2 . Thus, the moment scale is

$$1 \text{ cm} = 100 * 0.5 * 5 = 250 \text{ kgm}$$

From the diagram we obtain the maximum value of the bending moment as

$$M_f = 9.85 * 250 = 2460 \text{ kgm}$$

The advantages of the graphic method over the analytic one are several.

First of all, with the graphic integration method we can derive to the diagrams of shear much faster than we can analytically and also the procedure is not complicated by the various shapes of wing being considered, that is for the distribution of loads it is not always possible to analytically establish an equation that represents the distribution of the load itself.

The precision of the graphic method may be inferior to the analytic one, but with the graphic method is impossible to commit the gross errors are often easily made analytically. Also for greater safety, all analytically-found values should be reported graphically in order to check their validity.

In the graphic method, it is advisable to operate with a small scale in order to obtain maximum precision. In practice 1/10 used for the lengths, and the loads and shears diagrams are divided in many strips.

Strut-Braced Wing. We have studied wings in their various forms. Let's now see how we can calculate the values of T and M_f in the case of a strut-braced wing. Generally the wing is attached to the fuselage and a strut if the wing has one spar, and with two struts if there are two spars.

The angle that is formed by the strut and the wing should not be too small—not less than 30° . There are two important reasons for this: the first is so as not to stress the strut too much and the second is to keep the aerodynamic interference between the strut and the wing to a minimum.

It is very important that the attachment between the wing, fuselage and strut is hinged.

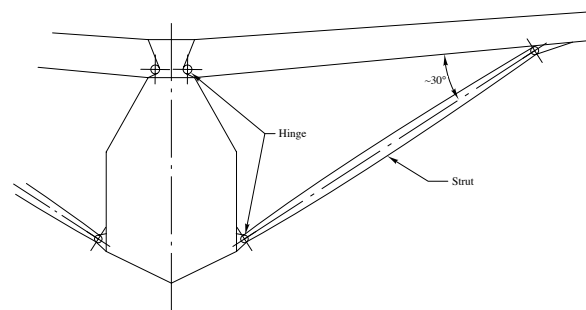


Figure 9-14

It is a mistake to think that attaching the wing to the fuselage with rigid attachments that will not allow movement along the longitudinal axis will give us a stronger structure. In this case we would get an overly rigid structure, with too many connections. We will not look further into this as it is not part of our exercise, but it is important to remember that in this case, although we would be reducing the stresses on the spar, we would also increase the stresses on the wing structure.

Furthermore, because of possible minor differences in assembly, there is the potential of very high secondary stresses. In the calculation method that we are going to use, we will assume a hinged attachment.

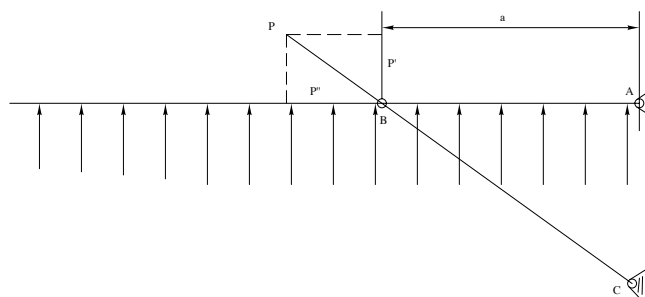


Figure 9-15

Let's show the strut-braced wing in this graph: it is stressed upwards because of the aerodynamic forces that are distributed based on the area and by a concentrated load P , applied at B , that acts from up to down in the direction of the strut. It represents the reaction of the strut (Figure 9-15). We can therefore proceed in a very simple manner to find T and M_f . We will assume first that the wing is attached at A without a strut, i.e. a cantilever wing. As we have already seen, we are finding both the shear stress and the bending moment, which will increase continuously from the wing tip to the midpoint A .

Let's consider the wing as it actually is. We know that the bending moment at A has to be zero because the hinge cannot transmit this moment. Therefore the diagram of the bending moment will have its maximum value at the strut B , and will decrease from B all the way to become zero at A . For this part of the diagram, from B to A , let's now consider the vertical component P' of the load. P is the reaction of the strut.

This makes for a bending moment of opposite sign from the earlier one which will vary from zero at B to its maximum value at A , which coincides with the absolute value in the strut-braced wing, because as we noted before, the moment at the hinge has to be zero. The diagram of the bending moment in P' is linear as it is only a function of the distance from B . We have now found its bending moment, even without knowing its value nor the value of P yet.

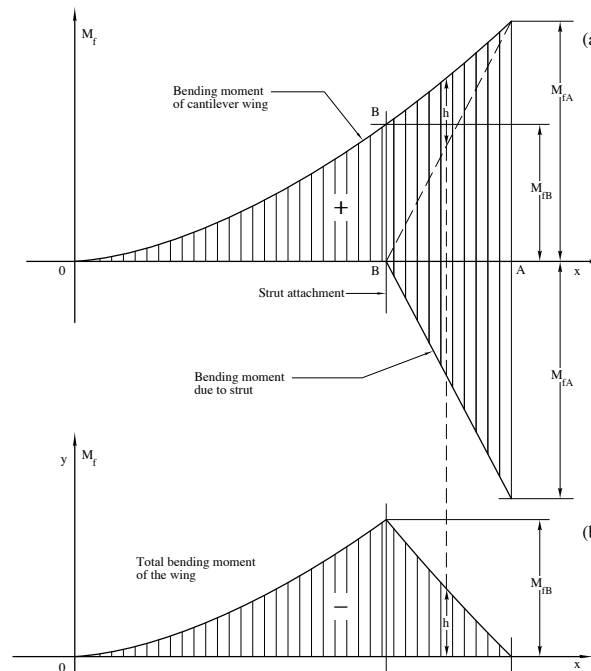


Figure 9-16

Therefore the diagram of the bending moment for the strut-braced wing is given by the diagrams of the two bending moments, one is relative to the cantilever wing and the other

to the load P' (Figure 9-16a). The resulting diagram is therefore the one shown in Figure 9-16b.

We can now determine the load P' and therefore also the bending moment of P , which is the tension on the strut. Thus, we have:

$$M_{fA} = P' \cdot a$$

where a is the distance of the attachment of the strut to the mid-section of the wing at A .

We therefore have:

$$P' = \frac{M_{fA}}{a}$$

Then, with the angle a formed from mounting with the wing, the value of P is calculated.

$$P = \frac{P'}{\sin a}$$

We can see how by decreasing the angle a we reduce sine a , and as a consequence the tension load on the strut increases.

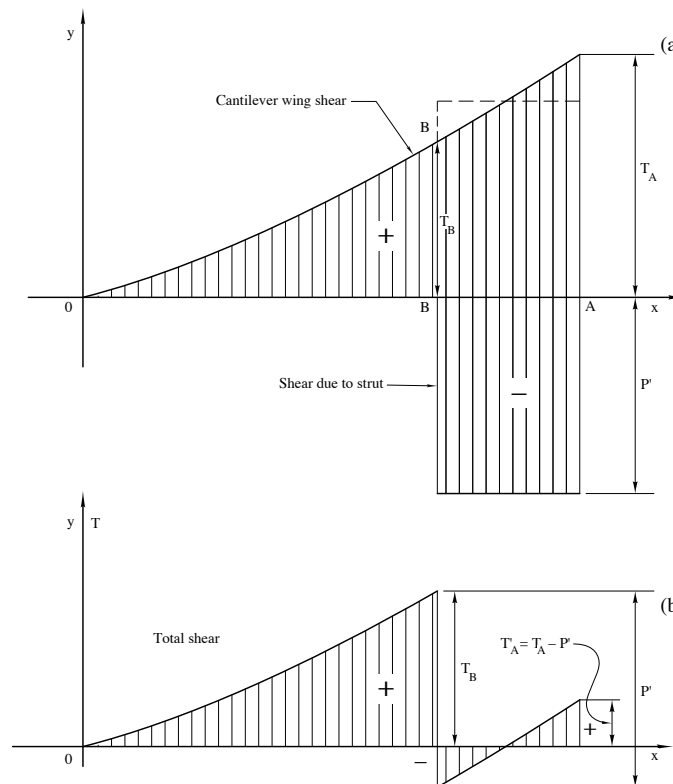


Figure 9-17

After we obtain the vertical component of P' of P , we can immediately determine the reduction in load from B to A . For this the diagram is the result of the difference between the two: one relative to the cantilevered portion of the wing, and the other is relative to the concentrated load at P' that is constant from B to A (Figure 9-17a). The resulting diagram is the one in Figure 9-17b.

The value of P' can be greater than the value of load at B for the cantilevered wing and therefore the diagram of the load changes sign, as can be seen in Figure 9-17b

Example. Let's anchor the wing in our last example (Figure 9-13) and let's assume that it is now braced with a strut attached at a distance of 2.4 meters from the mid-section. Since we already have the diagram of shear and bending moment for the cantilever wing, we now only have to determine these loads for the portion of wing between the strut and the attachment at the mid-section.

Because the maximum value of the bending moment at the mid-section is 2460 kg for the cantilever wing, this value is also the same (with exception of the sign) as the one for the vertical component P' of the load P on the strut. Thus we will have:

$$M_f = 2460 = P' \cdot 2.40$$

From which P' is found.

$$P' = \frac{2460}{2.40} = 1025 \text{kg}$$

By subtracting the value of $P' = 1025$ from the shear diagram of Figure 9-13 of the attachment of the strut to the mid-section, we have the diagram of the strut-braced wing (Figure 9-18). As you can see, the value of the shear changes sign at the attachment of the strut, and it has the maximum value at this location.

To obtain the bending moment we subtract the line given by P' (Figure 9-13) from the one for the cantilever wing. The result is shown in Figure 9-19. The maximum value is at the attachment of the strut and it is:

$$M_{fB} = 1142 \text{kgm}$$

If we assume that the angle between wing and strut is 30 degrees, the tension force is:

$$P = \frac{P'}{\sin 30^\circ} = \frac{1025}{0.5} = 2050 \text{kg}$$

We can also find the compression load on the spar, from the strut attachment to the mid-section. The P parallel component on the axis of the spar (P'' in Figure 9-15) is given by:

$$P'' = P \cos 30^\circ = 2050 \cdot 0.866 = 1775 \text{kg}$$

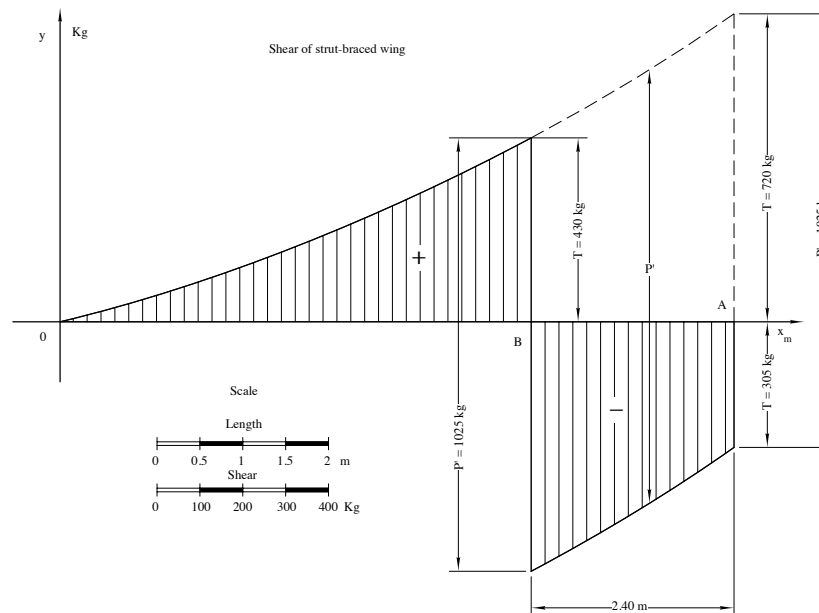


Figure 9-18

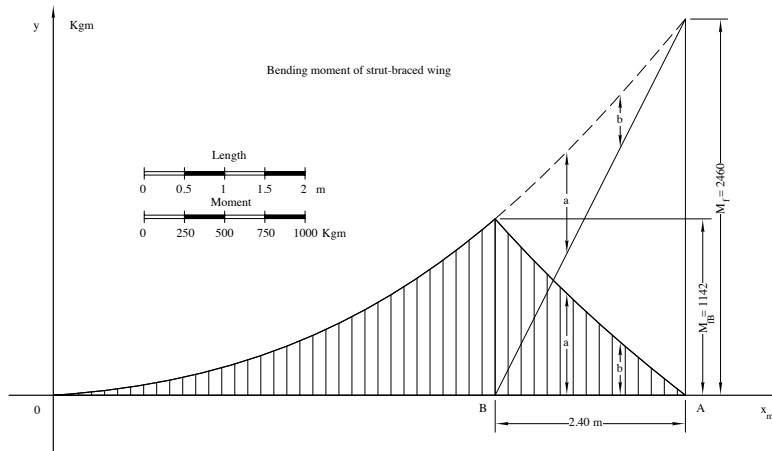


Figure 9-19

This compression load will be added to the normal stress of the wing attachments, derived from the bending when we dimension the spar.

We have therefore seen, with different examples, how to determine the highest shear stresses and the bending moment for the wing relative to the maximum lift. These loads are supported in the wing structure by the spar or spars.

We know that in gliders a monospar with a torsion box is very common design. In this type of design the bending loads are therefore carried by the only spar that is placed at the point of maximum thickness of the airfoil, normally between 30% and 35% of the chord.

However, if the structure is multispar, as in basic gliders of low aspect ratio, the shear loads on the wing will be shared by the two spars considering the load distribution along the wing chord. In the case of maximum lift as we have already seen, the load is distributed at 1/3 of the wing chord, or 35% (see Figure 3-7).

Example. Let us assume that the wing has a forward spar at 20% and an aft spar at 60% of the wing chord (Figure 9-20)

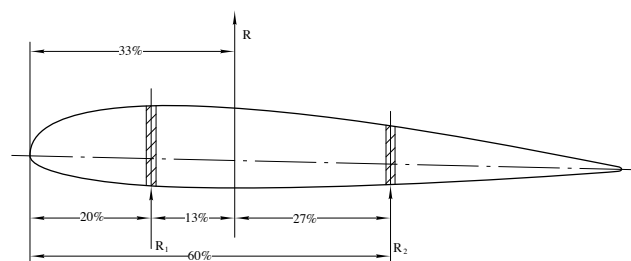


Figure 9-20

The distance, in percentage of the chord, of R (the load on the two spars) is therefore 13% from the forward spar and 27% from the back spar. The result of the equation for the bending moment is:

$$R_1 = R \cdot \frac{27}{13 + 27} = R \cdot 0.675$$

$$R_2 = R \cdot \frac{13}{13 + 27} = R \cdot 0.325$$

We therefore have stresses of shear and bending on the wing. Roughly 2/3 is on the forward spar and 1/3 are on the aft spar.

2. Maximum speed condition. In this flight condition we have a smaller load than in the previous calculation. In fact, for each half wing, it has a value of

$$0.75n(Q - Q_a)$$

For a single-spar wing, it would be pointless to calculate the shear and moment loads as these are less than the ones we have already calculated. But we should find the shear values, because in this condition we also have torsion, which induces a shear stress. The total stress in the spars could be even greater than in the maximum lift condition.

In normal gliders, however, the shear stress on the spars from torsion is always smaller than the bending loads, and we can safely skip this verification. Since torsion is smaller than for a zero-lift condition, this verification is pointless. In this last condition we will see how to determine its distribution along the wing span.

The maximum speed condition we are about to analyse, given the aft position of the aerodynamic force on the chord (see Figure 9-2), will particularly concern the strength of the elements behind the spar, wing ribs, and of the wing attachment to the fuselage. The wing rib can be considered as a restrained beam, (Figure 9-21) stressed by a triangular load.

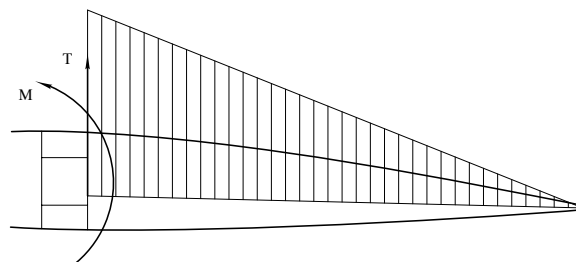


Figure 9-21

In practical terms, especially for normal gliders, it is not necessary to calculate stresses in the various parts of the wing rib. It is enough to obtain the maximum values of shear and

bending moment loads at the attachment to the spar. To obtain these loads T and M_f we have to find the load on the wing rib. Therefore, let's consider the sum of wing ribs lengths on a half wing and divide the load on it by this total length. This way, we will obtain the load per linear metre of wing rib. By multiplying this value, for the wing rib length, we will have the load on it.

This load is distributed on the chord as shown in Figure 9-2, in which the maximum value— $2.56 C/l$ —corresponds to 22% of the chord, and it decreases in a linear manner until it is zero at the trailing edge. Since the spar is always in an aft location, we will be interested in the aft triangular part of the load diagram. Of the load on the wing rib behind the spar, we will determine the resulting R' , which is, in fact, the value of the shear at the attachment to the spar. The bending moment will be the product of the resulting $R' = T$, *i.e.* of the shear, for the distance from the attachment to the spar (Figure 9-22).

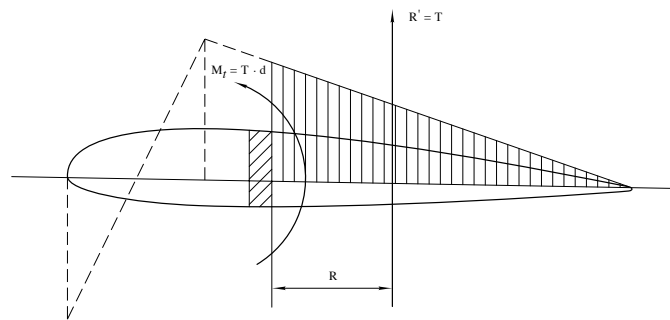


Figure 9-22

By dividing the bending moment found by the spar height H , we have the axial stress on the wing rib at the attachment to the fuselage. If we want a greater approximation, we can calculate the wing rib as a truss, thus also obtaining the stresses in the struts and the braces of the trellis.

3. Zero lift condition. This condition mainly concerns the torsion to which the wing is subject, (and it is the maximum that can be reached) and for which the structure is calculated. The value of the torsion moment M_t established by certification standards for the whole wing is:

$$M_t = 0.20 \cdot 2n \cdot Q \cdot l_m$$

and, therefore, for the half wing:

$$M_t = 0.20 \cdot n \cdot Q \cdot l_m$$

where:

n = limit load factor

Q = aircraft total weight

l_m = wing geometric mean chord

Since the torsion moment M_{tx} in a generic section X of the wing is a function of the area, once its maximum value M_t is established at the wing attachment, we now have to determine its distribution along the wing span. Let's consider a virtual wing, referred to a system of axes whose origin is at the end, as we have already done for bending.

The torsion moment M_{tx} is:

$$M_{tx} = \frac{S_x^2 \cdot L}{S^2 \cdot x} \cdot M_t$$

where:

S_x = area of the part contained between section X and the wing tip

L = half wing span

S = half wing area

M_t = half wing maximum torsion moment

x = distance of section X from the origin

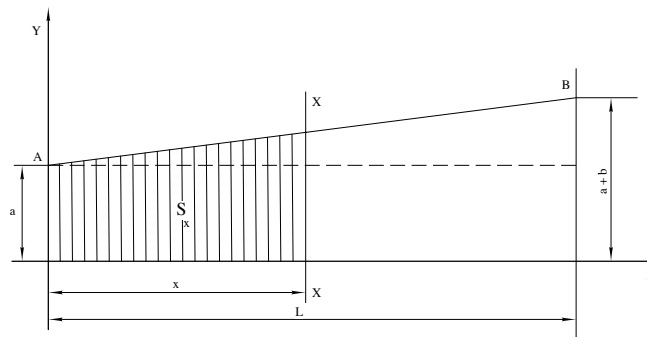


Figure 9-23

The relation seen can be undoubtedly used when introducing in it the value S_x , which is a function of distance x . Let's consider then the equation of the straight line AB of the wing area:

$$y = \frac{b}{L} \cdot x + a$$

that, once integrated, gives us the area equation:

$$S_x = \frac{b}{2L} \cdot x^2 + ax$$

By replacing this expression of S_x in the expression that gives us the moment, we have:

$$M_{tx} = \frac{\left(\frac{b}{2L}x^2 + ax\right)^2}{S^2 \cdot x} \cdot L \cdot M_t$$

an equation whose unknown quantity is only x ; therefore, for each value of it, we have the torsion moment M_{tx} in section X , at x distance from the origin.

Example. Given:

$$\begin{aligned} L &= 8 \text{ m} & S &= 9.20 \text{ m}^2 \\ Q &= 300 \text{ kg} & a &= 0.60 \text{ m} \\ n &= 3.5 & b &= 1.10 \text{ m} \\ & & (a + b) &= 1.70 \text{ m} \end{aligned}$$

The mean chord will be:

$$l_m = \frac{a + (a + b)}{2} = \frac{0.60 + 1.70}{2} = 1.15 \text{ m.}$$

The maximum torsion moment M_t per half wing is:

$$M_t = 0.20 \cdot 3.5 \cdot 300 \cdot 1.15 = 241.5 \text{ kgm}$$

By replacing the known values in the expression of the rudder torque M_{tx} , we have:

$$M_{tx} = \frac{\left(\frac{1.10}{16}x^2 + 0.60x\right)^2}{9.20^2 \cdot x} \cdot 8 \cdot 241.5$$

from which:

$$\frac{(0.0688x^2 + 0.60x)^2}{84.64 \cdot x} \cdot 1932$$

By simplifying:

$$M_{tx} = (0.00473x^3 + 0.36x + 0.0825x^2)22.82$$

and finally:

$$M_{tx} = 0.108x^3 + 1.885x^2 + 8.22x$$

which is the equation sought from the distribution of the moment on the wing span. As a verification of this, we find the moment at the attachment with the wing spar, which as we know is: $M_t = 241.5$ kgm. Let's introduce $x = 8$, as this is the half wing span, and we will have:

$$M_t = 0.108 + 512 + 1.885 \cdot 64 + 8.22 = 55.20 + 120.50 + 65.80 = 241.50$$

a value that, as we can see, perfectly coincides with the established standards.

With a similar procedure, we can obtain the values of the M_{tx} moment in any section of the wing by introducing in the relation found a given value for x .

Graphic determination of torsion moment. In a very similar manner to what we have done to find the shear and the bending moments, we can also get the diagram of the torsion moment with a graphic process.

From the formula of maximum moment:

$$M_t = 0.20nQl$$

we see that M_t is proportional to chord l and to load Q , which, as we know, is in turn proportional to chord l .

The torsion moment is, therefore, proportional to the *chord square value*.

Using an appropriate scale, we build the diagram of the chord squares, which we obtain by multiplying by themselves the values of the load diagram, or the area diagram, which is the same.

Then, by integrating this diagram as we already know, we obtain that of the torsion moment that we are looking for.

Now we have to determine the scale to read the ordinates. This is easily found, as we already know the value of the maximum ordinate at the wing attachment, since it is M_t , given by the standards.

By dividing this value by the maximum ordinate, in cm, we will have the moment scale:

$$1 \text{ cm} = x \text{ kgm.}$$

Example. Let's consider the wing of the previous example and obtain the torsion moment diagram.

Let's build, for this purpose, the diagram of the chord squares (which is a parabola) and divide it into ten parts (Figure 9-24).

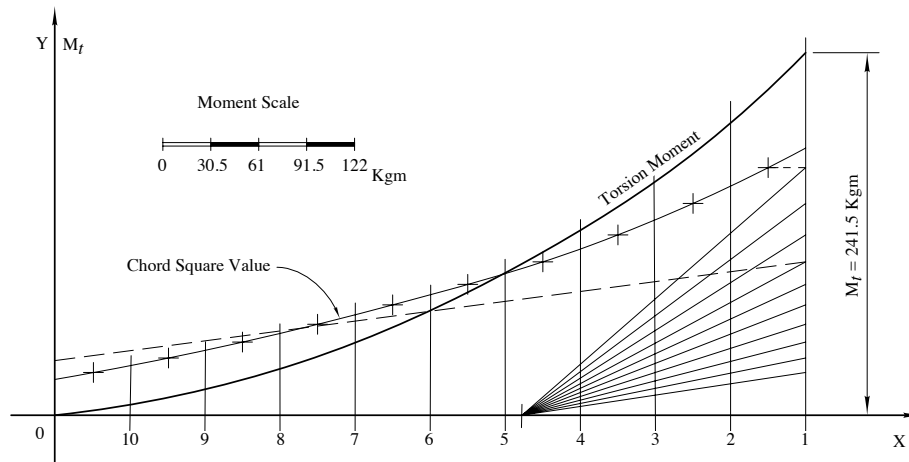


Figure 9-24

Using the procedure known, we integrate this diagram. The scale is immediately obtained from the drawing.

The maximum ordinate, in fact, is:

$$y = 7.9 \text{ cm}$$

therefore, since the moment must be:

$$M_t = 241.5 \text{ kgm}$$

we have:

$$1 \text{ cm} = \frac{241.5}{7.9} 30.5 \text{ kgm}$$

From the diagram, let's find, for example, the torsion moment in a section at 4 metres from the end. The ordinate in said section is:

$$y = 2.3 \text{ cm}$$

therefore:

$$M_{t_x} = 2.3 \cdot 30.5 = 70.15 \text{ kgm}$$

Sudden landing condition. Finally, let's see which stresses occur in the wing in this condition; stresses that have an opposite sign to those in the other conditions. The forces of inertia developing from the top towards the bottom are supposed to be applied with a

15° forward inclination compared to the wing reference plane. The limit load factor is fixed at $n = 4$ for all aircraft categories.

Assuming the load is evenly distributed on the wing according to the wing area, the bending load for the half-wing is:

$$n \cdot Q_a \cdot \cos 15^\circ$$

where

Q_a = wing total weight

n = limit load factor.

This load is generally a lot lower than that of the sudden pull-up in the first condition. Anyway, once the load is determined, the shear and bending moment stresses derived from it are found as we have seen in the first condition.

We still have to determine the stress from the load on the wing, where the maximum value is set by the rules at:

$$\frac{1}{8} \cdot n \cdot Q$$

for the half wing. Therefore, we can say that in the usual single spar wings of gliders these stresses have a small value and the verification of the structural strength for such stresses is not required.

We have now looked at the various load conditions for the wing, and we have also seen, through some examples, how to determine the various stresses to which the wing structure is subject. These stresses are supported by several elements of the structure.

The spar, or spars, support bending and, in particular, the spar caps support the tension and compression loads resulting from the bending moment, while the sides or webs of the spar support the shear loads.

As far as torsion is concerned, it is the wing skin that has the task of giving the wing strength to resist this stress.

Accounting for the actual stresses that occur in each and every element of the wing would greatly complicate the calculation without compensating for the slight lightening we might obtain the structure. Instead, it is always necessary, within limits, to simplify the structure so that calculation is made easier and so that it does not produce any uncertain results. The structures of today's aircraft are considerably simpler than those of the past and, therefore, calculation results are safer and more reliable.

In gliders, wooden structures are now universally adopted and for the wing the single spar with a wing skin on the leading edge that resists the torsion is the dominant structure. So, let's consider this type of structure and see, with some examples, how we proceed to calculate it, based on the loads on it.

We have thus come to the third phase of our work on dimensioning the structure, in other words, to the verification of strength, or as it is said using the terminology of construction science, *stability verification*. We talk about verification because in any construction first we proceed to an approximate dimensioning in an arbitrary manner of the structure, and then, based on the loads on it, we verify that the resulting *unitary stresses* do not exceed the maximum stresses allowed by the materials used.

57. Verification of the bending strength of the wing spar.

Let's start with the spar. This is a longitudinal beam in the wing that supports bending. It may have a hollow section or a solid one (Figure 9-25).

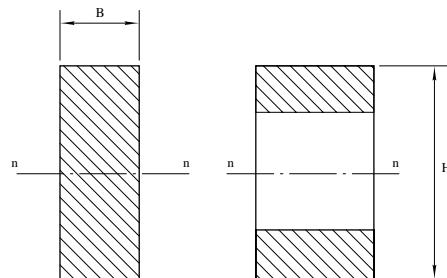


Figure 9-25

In case of a hollow spar, it is generally formed by two spar caps connected by sides, called webs. The caps carry axial loads; the upper cap for compression and the lower one for tension derived from the bending moment, while the webs carry the shear loads.

In case of inverted flight, axial stresses on the caps are inverted, but we are not interested in this flight condition, which is not even considered by certification standards, as gliders are not intended to fly inverted and the maximum inverted load is always much smaller than the up-right load.

To draw the sections of the spar, certain data must be established. The height H is already known, from the thickness of the airfoil we are using.

We have to fix the width B , which may also be constant along the entire wing span (for example with the spar in low aspect ratio wings, as we can find in gliders) or, as is more common, it may be tapered and decrease in thickness towards the wing tip.

Full spar. Let's first consider that the spar is a full beam. In this case, once B and H are fixed, we can obtain the normal unitary maximum stress, since the bending moment M_f is known in that section:

$$\sigma = \frac{M_f \cdot y}{J} = \frac{M_f}{W}$$

where:

σ = bending unitary stress

M_f = applied bending moment

y = distance of the most stressed fibre from the neutral axis

J = moment of inertia of the resisting section in relation to the neutral axis

W = resisting moment of the section = J/y

In our case of a rectangular section, the neutral axis is in the centreline, therefore:

$$y = \frac{1}{2}H$$

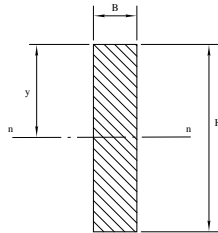


Figure 9-26

The *moment of inertia* J of a rectangular section in relation to the centroid is:

$$J = \frac{1}{12} \cdot BH^3$$

The *resisting moment* W will then be:

$$W = \frac{J}{y} = \frac{1}{12} \cdot B \cdot H^3 \cdot \frac{2}{H} = \frac{1}{6}BH^2$$

The expression of the unitary stress is:

$$\alpha = \frac{M_f}{W} = \frac{6M_f}{BH^2}$$

from which we can obtain, after assigning a value to σ , the unknown width B :

$$B = \frac{6M_f}{\alpha \cdot H^2}$$

Example. Let's determine the required length B of a spar with a full rectangular section, in whose section we have:

$$\begin{aligned} M_f &= 850 \text{ kgm} = 85000 \text{ kgcm} \\ H &= 15 \text{ cm} \\ \sigma &= 380 \text{ kg/cm}^3 \end{aligned}$$

By applying the last formula, we obtain:

$$B = \frac{6M_f}{\alpha \cdot H^2} = \frac{6 \cdot 85000}{380 \cdot 225} = 6 \text{ cm}$$

We have said that the full section spar is used only for low aspect ratio wings with low characteristics, such as in gliders, for the sake of construction simplicity.

In gliders, as also in all motor aircrafts, the spar is always hollow.

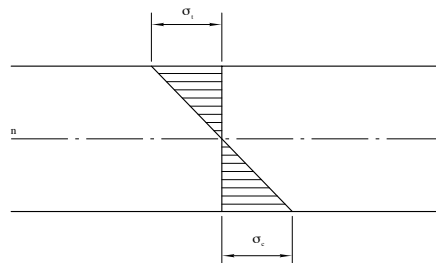


Figure 9-27

This is done because bending in a rectangular section causes a distribution of stresses as shown in Figure 9-27, where they vary from a maximum, at the ends of the section, to zero at the neutral axis, and by inverting the sign, we change from tension on one extreme to compression on the other. Stress is nil at the neutral axis, and near to it, it is always small.

It is therefore better to distribute the material as far as possible from the neutral axis, to make it work at the maximum allowed for it. In other words, the moment of inertia of the cross-sectional shape should be the greatest for the material used.

In practical terms though, this is limited by construction reasons, such as that of not excessively increasing the width B , which would lead to complications for the joints of metallic parts, etc.

Therefore, it is advisable that the spar width should never be greater than the corresponding height H and as a starting point we can keep $B = H/2$.

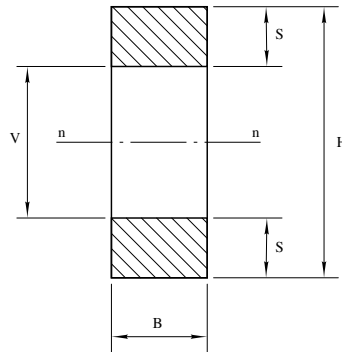


Figure 9-28

Symmetrical box spar. Let's now examine a spar, whose section is symmetrical in relation to the neutral axis, with equal caps (Figure 9-28) of a thickness S and where V is the internal height, which is:

$$V = H - 2S$$

as H is the height of the spar.

The moment of inertia J of the resisting section, in other words the moment of inertia of the area of the two spar caps in relation to the neutral axis $n - n$ is:

$$J = \frac{1}{12} B (H^3 - V^3)$$

and having here too:

$$y = \frac{1}{2} H$$

by replacing in the fundamental relation

$$\sigma = \frac{M_f \cdot y}{J}$$

having found the value of J and y , we have:

$$\sigma = \frac{6 \cdot M_f \cdot H}{B (H^3 - V^3)}$$

a relation that gives us the spar cap's maximum stress.

If instead we fix the maximum admissible value of stress σ for the material used, we can obtain the value of V and, therefore, the spar cap thickness:

$$V^3 = H^3 - \frac{6 \cdot M_f \cdot H}{\sigma \cdot B}$$

a commonly used formula for dimensioning caps when they are the same. The thickness is given by:

$$S = \frac{1}{2}(H - V)$$

Example. Let's keep considering the previous example, so that we can find which is the advantage obtained in weight with a hollow spar.

We had:

$$\begin{array}{ll} H = 15 \text{ cm} & M_f = 85000 \text{ kg/cm} \\ B = 8 \text{ cm} & \sigma = 380 \text{ kg/cm}^2 \end{array}$$

by applying the last formula:

$$\begin{aligned} V^3 &= H^3 - \frac{6M_f \cdot H}{\sigma \cdot B} = 15^3 - \frac{6 \cdot 85000 \cdot 15}{380 \cdot 8} \\ V^3 &= 3375 - \frac{7650000}{3040} = 3375 - 2520 = 855 \end{aligned}$$

and by extracting the cubic root:

$$V = \sqrt[3]{855} = 9.49 \text{ cm}$$

The spar cap thickness is, therefore:

$$S = \frac{1}{2}(H \pm V) = \frac{1}{2}(15 \pm 9.5) = 2.75 \text{ cm}$$

Let's analyse which is the material reduction obtained compared to the full spar.

The resisting section is, in this case:

$$2 \cdot S \cdot B = 5.5 \cdot 8 = 44\text{cm}^2$$

while in the previous case it was:

$$H \cdot B = 15 \cdot 6 = 90\text{cm}^2$$

As we found in the instance of a full spar, the resisting section, *i.e.* the material used, is more than double even though the stress σ is the same.

As a verification, it is a good rule to draw, even in a small scale, the resisting sections calculated, because the eye can give good advice. For example, it is a good rule that the relation between the cap thickness and its width B is not too small.

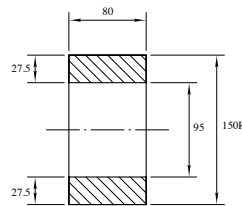


Figure 9-29

Let's draw in scale the calculated section and, as we can see, it is quite well proportioned (Figure 9-29).

In the examples we examined, we considered a rectangular section. In reality, this hardly ever occurs, because the spar follows the shape of the airfoil and, especially if it is quite wide, the top surface and the underside are sloping and not perpendicular to the sides.

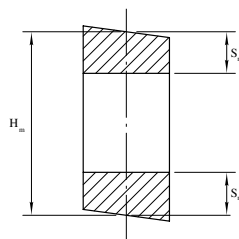


Figure 9-30

In these cases, we should keep into account the average height in correspondence with the centreline (Figure 9-30) for the height H and, similarly, S for the cap thickness.

Asymmetrical spar. In the previous calculations, we considered the bending stress value for fir wood:

$$\sigma = 380 \div 400 \text{kg/cm}^2$$

Almost all wood types do not have the same strength in tension and compression, but they have considerably less strength in compression than tension.

For example, fir has a compression strength of about 350-380 kg/cm², while the strength in tension is over 600 kg/cm².

For this reason, therefore, it is not convenient to build equal slabs, because if we do not exceed the admissible stress in the compressed one, we cannot exploit the material of the stretched one at its best.

The calculation of a beam with unequal caps though, is quite complex, and it must be carried out with extreme rigour.

We will follow an approximate method developed by the engineer E. Preti, whose precision is more than enough for the construction requirements of these aircraft.

Let's consider a section of unequal slabs of which the upper one is the biggest since it is the one that works by compression (Figure 9-31).

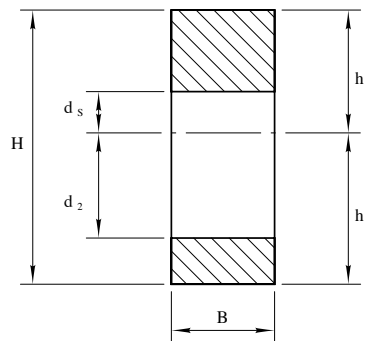


Figure 9-31

Then, let's indicate with h_s and h_i the distances from the neutral axis of the upper and lower ends of the caps respectively and with d_s and d_i the internal distances from the neutral axis.

The relation between the distances h_s and h_i is the same as between the maximum compression and tension loads σ_c and σ_t corresponding to the spar caps, so we can write:

$$\frac{\sigma_c}{\sigma_t} = \frac{h_s}{h_i}$$

Due to one of proportion properties, the previous equation is equal to:

$$\frac{\sigma_c}{\sigma_t + \sigma_c} = \frac{h_s}{h_s + h_i}$$

but since

$$h_s + h_i = H$$

we would have:

$$\frac{\sigma_c}{\sigma_t + \sigma_c} = \frac{h_s}{H}$$

from which we obtain the unknown value of h_s in function of H and of stresses σ_c and σ_t :

$$h_s = H \left(\frac{\sigma_c}{\sigma_t + \sigma_c} \right)$$

Similarly, we obtain h_i :

$$h_i = H \left(\frac{\sigma_t}{\sigma_t + \sigma_c} \right)$$

By indicating, for simplicity, with

$$a = \frac{\sigma_c}{\sigma_t + \sigma_c}$$

and with

$$b = \frac{\sigma_t}{\sigma_t + \sigma_c}$$

we finally have:

$$\begin{aligned} h_s &= a \cdot H \\ h_i &= b \cdot H \end{aligned}$$

By squaring, we have:

$$\begin{aligned} h_s^2 &= a^2 H^2 \\ h_i^2 &= b^2 H^2 \end{aligned}$$

from which

$$h_i^2 - h_s^2 = H^3(b^2 - a^2)$$

and since this must be true also for the equality of static moments of the caps in relation to the neutral axis:

$$h_i^2 - h_s^2 = d_i^2 - d_s^2$$

by replacing, we have:

$$d_i^2 - d_s^2 = H^2(b^2 - a^2)$$

therefore, by solving in relation to an unknown value, for example in relation to d_i , we have:

$$d_i = \sqrt{(b^2 - a^2)H^2 + d_s^2}$$

the first equation giving us the unknown value of d_i in function of the other d_s .

Now, we have to obtain a second expression of d_i so as to obtain a system of two equations with two unknown values.

The moment of inertia of the resisting section with width B in relation to the neutral axis, as we can obtain by simple calculation, is given by:

$$J = \frac{B}{3} \left[(h_s^3 + h_i^3) - (d_s^3 + d_i^3) \right]$$

and it is also given by the relation:

$$J = \frac{M_f \cdot h_s}{\sigma_c}$$

By equating, we have:

$$\frac{3M_f \cdot h_s}{B \cdot \sigma_c} = h_s^3 + h_i^3 - (d_s^3 + d_i^3)$$

By using A to indicate the second element:

$$A = h_s^3 + h_i^3 - (d_s^3 + d_i^3)$$

we have:

$$\frac{3M_f \cdot h_s}{B \cdot \sigma_c} = A$$

From this relation, we obtain A , because the terms of the first element are all known.

Since by definition:

$$A = h_s^3 + h_i^3 - (d_s^3 + d_i^3)$$

we obtain:

$$d_s^3 + d_i^3 = h_s^3 + h_i^3 - A$$

By using Z to indicate the second element, we have:

$$d_s^3 + d_i^3 = Z$$

where Z is the known value, as h_s , h_i , and A are known.

This last relation is the one we seek, which combined to the previous one seen gives us the following system:

$$d_i^3 = Z - d_s^3$$

$$d_i = \sqrt{(b^2 - a^2)H^2 + d_s^2}$$

which cannot be reduced, but which allows us to determine just as easily the unknown values of d_s and d_i , from which we obtain, by subtracting them from h_s and h_i , the upper and lower cap thicknesses S_s and S_i . By assigning an arbitrary value d_s from the first equation, we obtain d_i and we then verify in the second equation if the value of d_i coincides with the previous. By varying the assigned value of d_s we can get to the solution sought through a few attempts.

Example. Let's consider the previous example, where we had equal caps and let's see what advantage we can have now with the unequal caps calculation.

Our data are:

$$H = 15 \text{ cm}$$

$$B = 8 \text{ cm}$$

$$M_f = 85000 \text{ kgcm}$$

and let's suppose:

$$\begin{aligned}\sigma_c &= 380\text{kg/cm}^2 \\ \sigma_t &= 560\text{kg/cm}^2\end{aligned}$$

As we have seen:

$$a = \frac{\sigma_c}{\sigma_t + \sigma_c} = \frac{380}{940} \approx 0.40$$

$$b = \frac{\sigma_t}{\sigma_c + \sigma_t} = \frac{560}{940} \approx 0.60$$

therefore, the distances h_s and h_i of the caps external fibres from the neutral axis are:

$$h_s = a \cdot H = 0.40H = 0.40 \cdot 15 = 6.0\text{cm.}$$

$$h_i = b \cdot H = 0.60H = 0.60 \cdot 15 = 9.0\text{cm.}$$

and by squaring:

$$h_s^2 = 36$$

$$h_i^2 = 81$$

from which:

$$h_i^2 - h_s^2 = d_i^2 - d_s^2 = 81 - 36 = 45$$

and by obtaining d_i :

$$d_i = \sqrt{45 + d_s^2}$$

we have the first equation sought. Let's now get the value of A

$$A = \frac{3M_f \cdot h_s}{B \cdot \sigma_c} = \frac{3 \cdot 85000 \cdot 6}{8 \cdot 38} = 502$$

The value of Z is consequently:

$$Z = h_s^3 + h_i^3 - A = 216 + 729 - 502 = 443$$

The second relation is, therefore:

$$d_s^3 + d_i^3 = Z = 443$$

In the system sought:

$$\begin{aligned}d_i^3 &= 443 - d_s^3 \\d_i &= \sqrt{45 + d_s^2}\end{aligned}$$

Let's now suppose

$$d_s = 3\text{cm}$$

From the first equation we have:

$$d_i^3 = 443 - 27 = 416$$

from which

$$d_i = \sqrt[3]{416} = 7.46\text{cm}$$

and from the second equation:

$$d_i = \sqrt{45 + 9} = \sqrt{54} = 7.35\text{cm}$$

As we can see, the system is not satisfied for the value fixed as $d_s = 3$, because the result for d_i is not the same in the two equations.

Let's try by supposing:

$$d_s = 3.2\text{cm}$$

From the first we now have:

$$d_i^3 = 443 - d_s^3 = 443 - 32.76 = 410.24$$

$$d_i = \sqrt[3]{410.24} = 7.42\text{cm}$$

and from the second:

$$d_i = \sqrt{45 + d_s^2} = \sqrt{45 + 10.24} = 7.42\text{cm}$$

The result is now coinciding and the system is thus solved. So we have:

$$d_s = 3.2 \quad d_i = 7.42$$

from which we obtain the spar cap thickness:

$$S_s = h_s - d_s = 6 - 3.2 = 2.8\text{cm}$$

$$S_i = h_i - d_i = 9 - 7.42 = 1.58\text{cm}$$

The resisting section area is, therefore:

$$(2.8 + 1.58) \cdot 8 = 35.2\text{cm}^2$$

while in the instance of a symmetrical spar we had:

$$(2 \cdot 2.75) \cdot 8 = 44\text{cm}^2$$

The reduction of the resisting section, and therefore of the weight, is:

$$\left(\frac{44 - 35.2}{44} \right) = \frac{8.8}{44} = 0.20$$

that is by 20%, and as we can see, quite considerable.

For the dimensioning of the asymmetrical spar that we have just seen, *i.e.* with unequal caps, we must make some considerations. As we know, material near the neutral axis has little work to do, therefore, is not used efficiently.

Now, in the asymmetrical spar instance, where the upper cap is the biggest, the neutral axis is shifted up from the section and the cap material is little exploited, as we see in the section bending stress diagram (Figure 9-32).

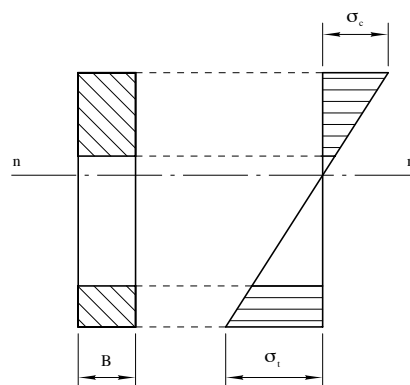


Figure 9-32

The width B of the spar should then be increased, so that the thickness of the upper cap is smaller and, therefore, its lower cap is not too close to the neutral axis (Figure 9-33).

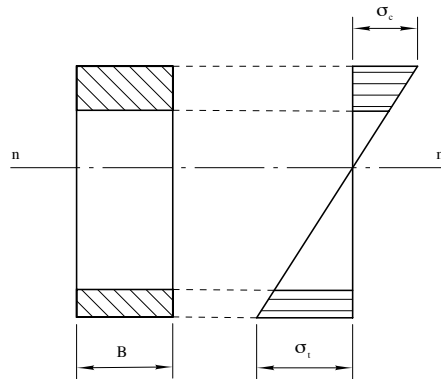


Figure 9-33

But for practical construction reasons we cannot exceed with the spar width and consequently, in very stressed sections, such as those near the attachment with the fuselage in cantilever wings, the upper cap is a lot thicker and the material is not used efficiently to carry the compression loads.

It is then appropriate to reduce the maximum tension stress, thus increasing the lower cap thickness with a subsequent lowering of the neutral axis and thus improving the compressed upper cap's working conditions. For these reasons it is not convenient to keep the tension load high to avoid strong section dissymmetry.

Based on practical experience, it has been found that for a good dimensioning of an asymmetrical spar, the compressed cap thickness should not be more than 1.5 times that of the one loaded in tension, and we can keep 1.3 as the optimal average value.

The practical values for maximum admissible stresses for fir are:

$$\begin{aligned}\sigma_c &= 380\text{kg/cm}^2 \\ \sigma_t &= 480\text{kg/cm}^2\end{aligned}$$

Later we will take the practical data of the mechanical characteristics of the various woods used in aeronautical construction.

58. Verification of the shear strength of the wing spar.

Having verified the bending strength of the spar, we now have to calculate the shear loads, which are supported by the plywood webs that connect the spar caps. We remember that if there is a shear load τ in a certain direction, there always is an equal τ in the perpendicular direction to the first, thus in the spar webs, we will have both a vertical and a horizontal stress as a result of the caps trying to slide relative to each other.

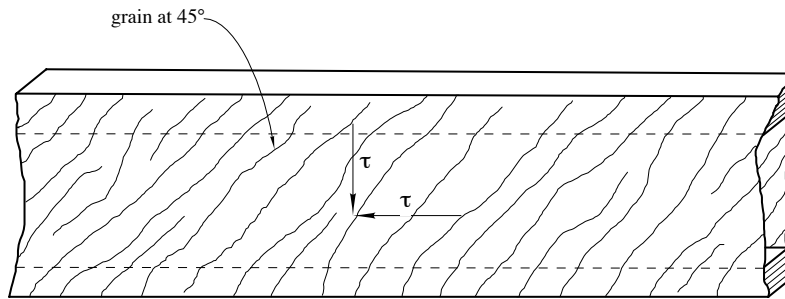


Figure 9-34

The plywood, therefore, should be installed with the grain direction at 45° to the spar axis so that it can support both the vertical and horizontal τ loads, and *it shall never be installed* with the grain running lengthwise, as it would do little to resist the shear loads.

The maximum shear load τ is given by:

$$\tau = \frac{1.5 \cdot T}{\delta \cdot h}$$

where:

T = shear load in the section (kg);

δ = web total thickness (cm);

h = web height (cm).

From the formula, having fixed the maximum admissible shear stress τ value, we obtain the required δ thickness:

$$\delta = \frac{1.5 \cdot T}{\tau \cdot h}$$

For birch plywood, we can use a shear load τ of 120 kg/cm² as an average value.

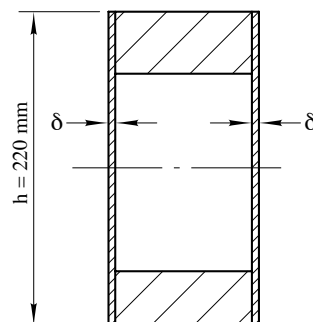


Figure 9-35

Example. Let's determine the thickness of the two plywood webs for a wing where we would have:

$$T = 700 \text{ kg.}$$

$$\tau = 120 \text{ kg/cm}^2 \text{ (plywood at } 45^\circ)$$

$$h = 0.398 \text{ cm.}$$

the total thickness is:

$$\delta = \frac{1.5 \cdot 700}{120 \cdot 22} = \frac{1050}{2640} = 0.398 \text{ cm}$$

thus the thickness of each of the two plywood webs is 2 mm.

The permitted loads of the plywood used for the spar webs increases if there are stiffening blocks that prevent buckling: in such case, the stress may vary from:

$$\tau = 120 \text{ kg/cm}^2 \text{ up to } \tau = 180 \text{ kg/cm}^2$$

with fibers at 45° angle and for a distance d between the stiffeners from:

$$d = 3 V \text{ up to } d = 1.5 V$$

where V is the free distance between the spar caps.

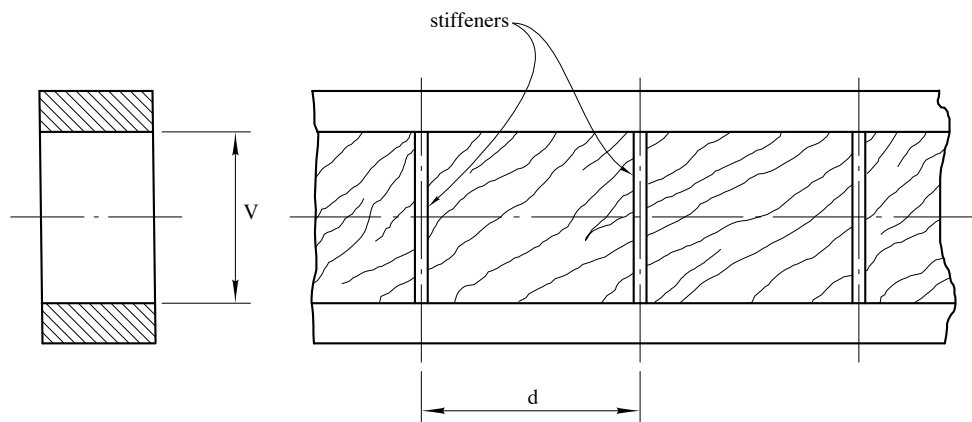


Figure 9-36

59. Verification of the torsional strength of the wing structure

In gliders, the wing structure that resists torsion is made up by the section formed by the leading edge skin and closed at the back by the spar web.

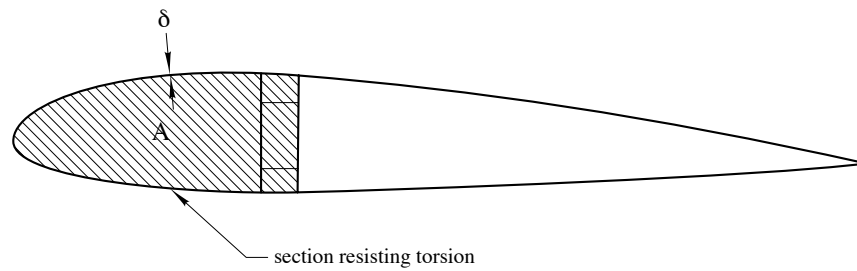


Figure 9-37

This structure is calculated with the Bredt formula regarding torsion stress of solids with a thin wall hollow section. It is given as:

$$\tau = \frac{M_t}{2 \cdot A \cdot \delta}$$

where:

M_t = applied torque

A = area enclosed in the section

δ = section walls thickness

For birch plywood, the shear strength may be used as

$$\tau = 120 \text{ kg/cm}^2$$

Since the torsion in a wing tends to twist it negatively, it would be appropriate to always place the plywood at a 45° angle, in the direction shown, and this is what is done in many cases. However, installing plywood at a 45° angle on curved surfaces involves greater construction difficulties; therefore, one often prefers to place it with the grain in the wing span direction.

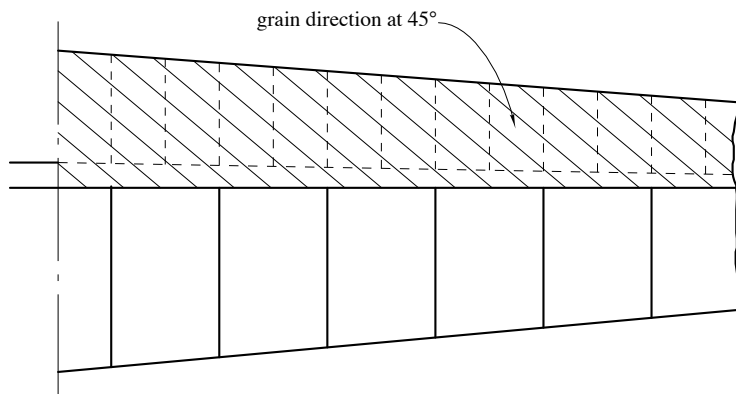


Figure 9-38

In this case, though, we must use a shear load of about 85% of that with fibers at 45°, that is:

$$\tau = 100 \text{ kg/cm}^2$$

We must remember that these values for plywood shear loads are influenced by the stiffening for preventing buckling. It is for this reason that on the leading edge, the wing ribs are closer together than those aft of the spar. Their purpose is, in fact, to prevent an elastic yielding of the plywood, which would consequently no longer resist the torsion loads.

Example. Let us determine the thickness of the plywood skin in a given wing section where:

$$M_t = 220 \text{ kgm} = 22000 \text{ kgcm}$$

$$A = 6 \text{ dm}^2 = 600 \text{ cm}^2$$

and the permitted shear loads, by placing the plywood at a 45° angle, is:

$$\tau = 120 \text{ kg/cm}^2.$$

With the Brendt formula, we obtain the thickness

$$\delta = \frac{M_t}{2A\tau} = \frac{22000}{2 \cdot 600 \cdot 120} = \frac{22000}{14400} = 0.153 \text{ cm} = 1.53 \text{ mm}$$

Because plywood sheets on the market are generally available in thickness increments of 0.5mm, we could adopt a thickness of 1.5mm (though that is a little short) or 2mm. Instead, if the plywood is not at a 45° angle, we would have use the permitted stress of:

$$\tau = 100 \text{ kg/cm}^2$$

and the thickness will be:

$$\delta = \frac{22000}{2 \cdot 600 \cdot 100} = \frac{22000}{120000} = 0.183 \text{ cm} = 1.83 \text{ mm}$$

and we would use 2mm thick plywood.

Torsional stiffness. With regard to torsion, in addition to the verification of the plywood thicknesses that resist such stresses, we must also verify the torsional stiffness of the structure. Certification regulations, in fact, require that the maximum torsional distortion—or twisting—at the wing tip, stressed by the elastic torsion coefficient (1.25 *n*), must not exceed 4°. In very long wings, such as those of gliders, this condition is

often more limiting than that for the actual torsional strength. The $d\phi$ torsional angle of a wing element that is $d x$ long, is given (in radians) by the relation:

$$\delta\phi = \frac{M_t \cdot P}{4A^2 \cdot \delta \cdot G} \cdot dx$$

where:

M_t = applied torsion

A = area enclosed in the section

G = tangential elasticity modulus of the covering material

δ = covering thickness

P = section perimeter

The total torsion ϕ angle at the wing tip is equal to the sum of the elementary angles $d\phi$, in other words, it is the integral of the expression of $d\phi$, extended to the entire half wing span. Therefore, we shall obtain the values of elementary $d\phi$ angles in radians, for various wing sections (those already being considered for determining the various shear stresses, torsion and bending), and we shall report them in a diagram. We then calculate the area of this diagram by means of graphic integration, or simply by measuring it with a planimeter or graph paper.

Once the diagram area is known, we obtain the value of angle ϕ , which represents the actual area, by multiplying said area by the scale of abscissas and by that of ordinates of the diagram itself. The angle will be obtained in radians; its value, multiplied by 57.3 (angle of a radian in sexagesimal degrees) will give us the ϕ angle sought in degrees.

Example. Let's calculate the maximum torsion angle of a wing being stressed by the elastic limit torsion (1.25 n), supposing that the distribution of the moment is that of the example in Figure 9-24 because the diagram values are those for strength (2 n), it will suffice to multiply them by the ratio 1.25/2, that is 0.625, to obtain those with the elastic coefficient.

Let us suppose then that we have obtained the area enclosed by the section and the perimeter of the latter, including the rear side of the spar, from the wing rib drawing, in the sections being considered for the moment. Assuming that we have already performed the torsion strength calculation and determined the δ thicknesses of the covering plywood, we can calculate the elementary angles $d\phi$, as we have all the required elements. The tangential elasticity modulus G for plywood is:

$$G = 40,000 \text{ kg/cm}^2.$$

Let us carry out the calculation for section 1, whose values are:

$$M_t = 151 \text{ kgm} = 15100 \text{ kgcm}$$

$A = 925 \text{ cm}^2 = \text{area enclosed in the section}$
 $A^2 = 855000 \text{ cm}^2$
 $P = 130 \text{ cm} = \text{section perimeter}$
 $\delta = 0.20 \text{ cm} = \text{plywood thickness}$

which, replaced by the formula

$$d\phi = \frac{M_t \cdot P}{4A^2 \cdot \delta \cdot G}$$

gives us:

$$d\phi = \frac{15100 \cdot 130}{4 \cdot 855000 \cdot 0.2 \cdot 40000} = \frac{1970000}{27300000000} = 0.0000725$$

By repeating the operation for the other sections, we shall have the values contained in the table.

Wing rib	M_t (kgcm)	A (cm ²)	P (cm)	δ (cm)	$d\phi$ (radians)
1	15100	925	130	0.20	0.0000725
2	12400	870	128	0.20	0.0000658
3	9900	765	121	0.20	0.0000640
4	7650	670	114	0.20	0.0000602
5	6000	580	107	0.20	0.0000600 0.0000800
5	6000	580	107	0.15	0.0000780
6	4600	495	100	0.15	0.0000755
7	3150	400	92	0.15	0.0000654
8	1820	315	81	0.15	0.0000590
9	1150	240	71	0.15	0.0000450
10	550	175	60	0.15	

Note that in wing station 5, where we have a change in plywood thickness, there are two values corresponding to $d\phi$ which are then shown as a sharp change in the diagram. This diagram is built by entering the wing span, in a 1:50 scale, on the horizontal axis, that is

$$1 \text{ cm} = 50 \text{ cm}$$

and the elementary angle $d\phi$ on the vertical axis, still in scale

$$1 \text{ cm} = 10^{-5} d\phi = 0.00001 d\phi$$

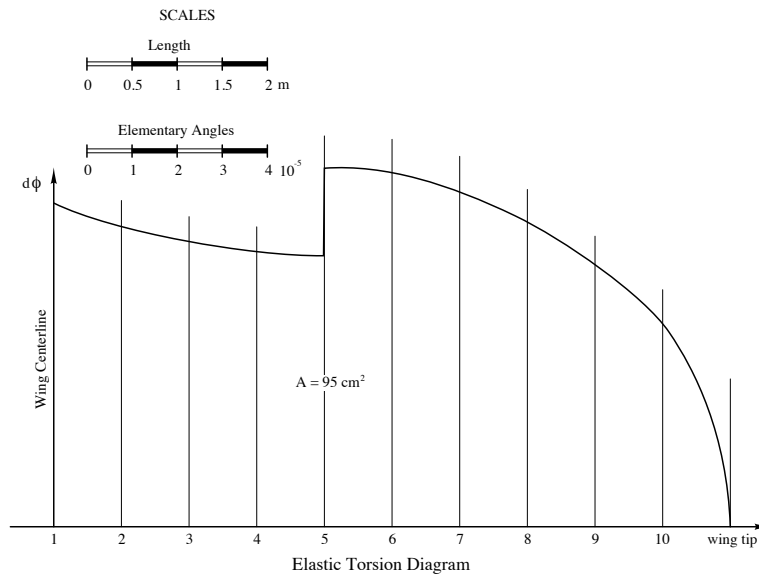


Figure 9-39

The diagram area is, therefore 95 cm^2 , which multiplied by the horizontal and vertical axis scales, gives us the total torsion angle ϕ in radians:

$$\phi = 95 \cdot 0.00001 \cdot 50 = 0.0475$$

and, finally, in sexagesimal degrees, we have:

$$\phi^\circ = 0.0475 \cdot 57.3 = 2.7^\circ = 2^\circ 42'$$

which is lower than the limit required by certification standards, and therefore the plywood thickness of the leading edge skin, established for torsion strength with the Brendt formula, is final.

60. Determination of the fuselage structural loads

The fuselage of common gliders, and generally all aircraft, is a tapered shaped body with the double purpose of containing the crew and the load, and to rigidly connect the wing, or wings with the tail surfaces required for longitudinal and directional stability.

The wing aerodynamic torsion—or pitching moment—must be balanced by an opposite moment by the horizontal tail surface. These moments that are relative to a fixed point, for example the wing leading edge or the aircraft center of gravity.

On the horizontal tail surface, therefore, the negative lift P_c is multiplied by the distance of its center of pressure from the wing leading edge, or from the center of gravity, produces the tail stabilizing moment. Therefore, the fuselage is subject to a bending load in the vertical plane.

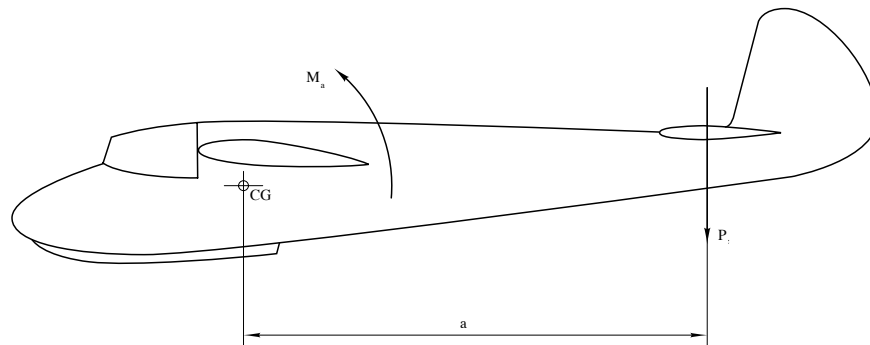


Figure 9-40

It may be thought of as a beam fixed with its wing attachments and stressed by a bending moment that varies in a linear manner from a zero value corresponding to the pressure centre of the horizontal plane to a maximum value corresponding to the fixed length being considered.

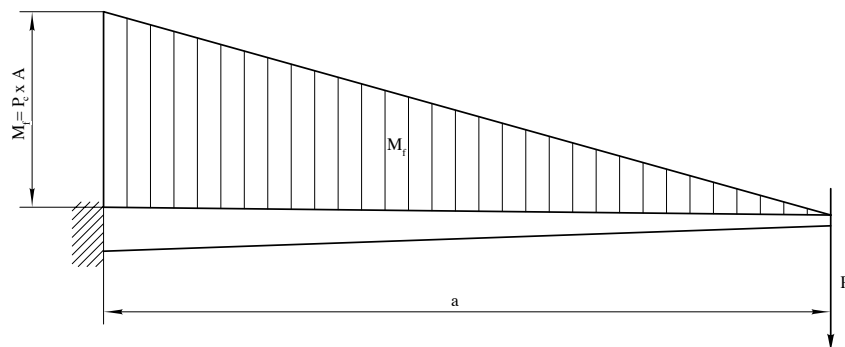


Figure 9-41

Because of the loads in the vertical plane, we also have a bending load on the fuselage in the horizontal plane. Furthermore, because the load on the vertical tail plane is almost never on the fuselage axis, but it is on top of it, a moment is produced that tends to twist the fuselage.

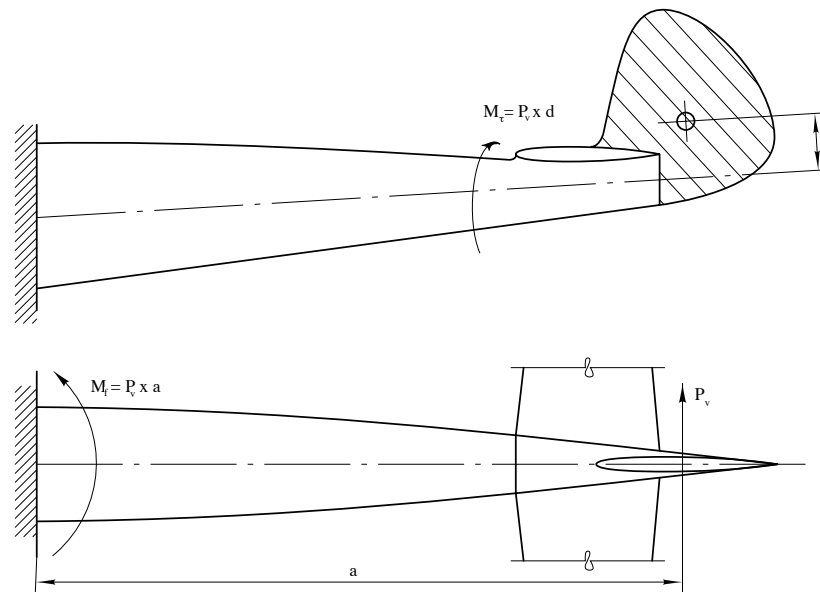


Figure 9-42

This bending moment, produced by the P_v force by the distance of its application point from the fuselage axis, is constant for all the fuselage sections, from the vertical plane to the wing attachment points on the fuselage.

These bending stresses, in the vertical and horizontal planes, and the torsion on the tail planes, are generated from the inertia of the aircraft mass and the air flowing over it, which oppose the rotation of the aircraft from the aerodynamic forces on the tail surfaces. Therefore, we must also consider the stresses that come from the inertial forces.

For example, in the forward part of a normal glider's fuselage, we will have that the loads of the pilot, equipment installations, instruments, etc., as well as the weight of the airframe itself. This part of the fuselage may be considered as a bracket that is fixed in relation to the wing attachment to the fuselage and stressed by vertical loads pushing downward.

In a steady horizontal flight condition, the loads are the actual weights; while in a sudden pull-up at maximum speed, the loads are represented by the centrifugal reactions of the weight of the fuselage and the weights of the pilot and equipment. A similar thing occurs in the aft section of the fuselage with mass reactions, in addition to the aerodynamic loads on the tail surfaces.

Hypothesis of load on the fuselage. By following, as we did for the wing, the certification standards, let's examine the various load conditions for the fuselage. The flight conditions established are: a) a sudden pull-up after a nose dive, to which the bending stress in the vertical plane corresponds and b) a load on the vertical tail, determined by the rudder maneuvering during flight. This condition results in bending stresses in the horizontal plane and in torsion.

Condition a).

The loads we need to determine are: 1) the initial limit load that is acting on the horizontal tail surfaces (stabilizer-elevator assembly), and 2) the centrifugal reactions from the mass of the fuselage and the loads contained in it.

The aerodynamic load P_c on the horizontal surface balances the wing maximum pitching moment, which we have seen as being:

$$M_\tau = 0.20 \cdot 2n \cdot Q l_m$$

therefore, since a is the distance from the elevator hinge to the aircraft center of gravity, the load P_c will be:

$$P_c = \frac{0.20 \cdot 2n \cdot Q \cdot l_m}{a}$$

In any case, the load P_c on the horizontal plane shall not be less than:

- Kg. 80 per m² for gliders
- Kg. 120 per m² for normal sailplanes
- Kg. 150 per m² for acrobatic planes.

The centrifugal loads in the fuselage are determined by multiplying the weight of the fuselage and that of the individual loads that are contained in it by the safety factor $2n$ that we previously defined.

In this load condition for the fuselage, the bending stresses in the vertical plane, from the aerodynamic load and centrifugal forces, are not contemporaneous. In fact, at the beginning of pull-up, we have the maximum load on the horizontal tail surface, which is the one determining the pull-up. Once the maneuver has begun, centrifugal reactions are generated, but the aerodynamic load on the actual tail surfaces diminishes until, when maximum acceleration is reached and therefore the centrifugal reaction maximum value, the aerodynamic load on the horizontal tail plane is reduced.

So, with regard to the bending in the vertical plane, the fuselage is designed for the greater of the loads created by bending moments from the aerodynamic load on the horizontal tail plane and the centrifugal reactions of masses. This applies, of course, for the aft section of the fuselage. For the part in front of the wing, the stresses result only from the centrifugal forces.

In this condition *a)* that we have just examined for the fuselage, both the loads on the horizontal plane and the mass reactions are directed from the top to the bottom.

Example. Stresses on the vertical plane from the load on the horizontal tail plane.

Let's consider the aircraft of the example in Figure 7-3 where we have partial loads in the fuselage, and let's calculate the maximum bending moment in the fuselage vertical plane. We start by calculating the shear loads and the moment due to the aerodynamic load P_c on the horizontal tail plane. Supposing that the wing average chord is:

$$l_m = 1.10 \text{ m}$$

and the aircraft total weight is

$$Q = 250 \text{ kg}$$

the wing bending moment is:

$$M_t = 0.20 \cdot 2n \cdot Q \cdot l_m = 0.20 \cdot 7 \cdot 250 \cdot 1.1 = 385 \text{ kgm}$$

that must be balanced by the tail moment

$$P_c \cdot a = M_t$$

in which the distance of the aircraft center of gravity from the elevator hinge is:

$$a = 3 \text{ m}$$

from which the load on the plane is:

$$P_c = \frac{M_t}{a} = \frac{385}{3} = 128 \text{ kg}$$

Now we need to verify if this load is greater or smaller than the minimum load resulting from the load required by certification standards. Supposing that the plane surface is

$$S_c = 2.10 \text{ m}^2$$

because the minimum load required by the standards is 120 kg/m^2 (for normal category), the minimum load must therefore be:

$$P_c = 120 \cdot S_c = 120 \cdot 2.10 = 252 \text{ kg}$$

which is definitely greater than that strength required to balance the wing pitching moment and, therefore, it is this that we must consider.

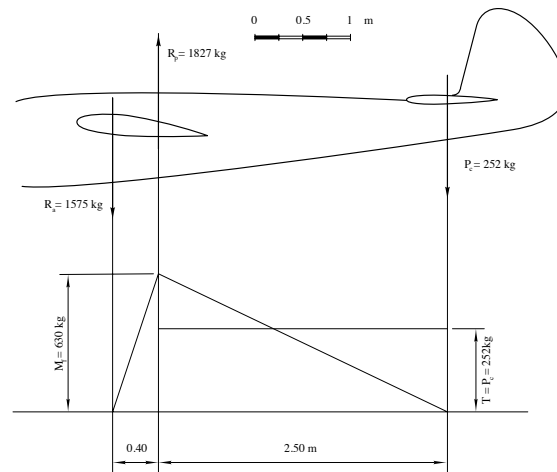


Figure 9-43

Such load P_c generates a bending moment on the fuselage with a triangular trend in which the maximum value corresponds with the aft wing attachment point. The distance from the horizontal tail hinge to the aft wing attachment section is 2.50m and the bending maximum moment is, therefore:

$$M_t = P_c \cdot 2.50 = 252 \cdot 2.50 = 630 \text{ kgm}$$

The torsion, however, is constant and its value is, in fact, that of the load on the plane:

$$T = P_c = 252 \text{ kg}$$

The bending moment decreases to 0 at the forward attachment of the wing with the fuselage, which is 0.40m from the aft one, as we can see in the figure. Therefore, we can calculate also the stresses on these attachment points. In fact, the relation R_a on the forward attachment point must be such that its moment, in relation to the center of the rear connection coincides with that given by the load on the plane, which is:

$$R_a \cdot 0.40 = 630$$

from which we have

$$R_a = \frac{630}{0.40} = 1575 \text{ kg}$$

and it is directed to the bottom, which is to say in the same direction as load P_c .

The reaction on the aft wing attachment R_p , therefore, will be the result of P_c and R_a :

$$R_p = 252 + 1575 = 1827 \text{ kg}$$

because for the balance of forces, the result of P_c , R_a and R_p must be null, which means that R_p must be equal and opposite of $P_c + R_a$. Furthermore, their moment must also be null, compared to any point.

If, for simplicity, we choose a point in the center of the aft wing attachment, the tail moment must be equal to that of R_a (because that of R_p is null, as its arm is null), which means:

$$P_c \cdot 2.50 = R_a \cdot 0.40$$

that is the relation from which we obtained R_a .

Stresses in the vertical plane due to the centrifugal reactions of masses. Let's now calculate which are the shear stresses and the moment in the fuselage vertical plane, due to the masses reactions by the effect of a pull-up.

The maximum moment for the fuselage rear part in the section, already considered, of the aft wing attachment will be given by the addition of the partial moments of the various loads and the partial weights of the fuselage actual structure. In a similar way, we find the maximum moment, relative to the section corresponding to the forward wing attachment, for the forward part of the fuselage.

So, we transcribe a table the values of the individual weights, the distances from the aft attachment sections for the weights of the aft end, and from the forward attachment for the forward end of the fuselage. The products of these weights for the corresponding distances give us the partial moments with a coefficient 1 (see Figure 7-3).

N	Name	Weights (kg)	Distances (m)	Moments (kgm)
12	Vertical plane	4.0	2.86	11.40
11	Horizontal plane	7.0	2.35	16.45
10	Fuselage ends	4.0	2.40	9.60
9	Fuselage rear part	5.0	1.54	7.70
8	Fuselage rear part	7.0	0.62	4.34
	<i>Fuselage rear part:</i>	Total shear 27.0	Total moment	49.49
	Fuselage bow	6.0	1.24	7.45
1	Dash board	5.0	1.00	5.00
2	Pilot cabin	19.0	0.64	12.20
3	Skid	5.0	0.61	3.05
4	Pilot	80.0	0.58	46.50
5	<i>Fuselage bow part:</i>	Total shear 115.0	Total moment	74.30

Therefore, the maximum bending moment in the aft part:

$$M_f = 49.49 \cdot 7 = 346 \text{kgm}$$

and in the shear:

$$T = 27 \cdot 7 = 189 \text{kg}$$

which, as we can see, is quite smaller than for the corresponding values deriving from load P_c .

For the front part we have:

$$M_f = 74.30 \cdot 7 = 520 \text{kgm}$$

$$T = 115 \cdot 7 = 805 \text{kg}$$

Based on these calculation results, we will verify the fuselage structure, in particular, for the aft part, we will keep into account the stresses deriving from the aerodynamic load P_c on the horizontal plane, while for the forward part, the loads are only those resulting from the centrifugal mass reactions.

Condition b)

In this load condition for the fuselage, we have bending in the horizontal plane and torsion due to the aerodynamic load on the vertical tail surfaces. This load for strength is, for gliders:

$$P_v = 2n \frac{Q}{S} \text{ kg/m}^2$$

where:

Q/S is the wing load.

Such load shall not be lower than the value of:

Kg. 80 per m^2 for gliders

Kg. 120 per m^2 for normal sailplanes

Kg. 150 per m^2 for acrobatic planes.

Example. Let us determine the bending stresses in the horizontal plane and torsion for the aft part of the wing of the fuselage, supposing that:

Q/S = wing load = 18 kg/m^2 ;

S_v = vertical plane area = 1.2 m^2

d = distance of tail plane centroid from the fuselage axis = 0.35 cm ;

D = distance from the attachment of the fuselage to the vertical plane CG = 3 m .

The aerodynamic unitary load P_v on the vertical tail plane is:

$$P_v = 2n \cdot \frac{Q}{S} = 7 \cdot 18 = 126 \text{ kg}$$

which is greater than the minimum required for normal category aircraft (120 kg/cm^2).

The total load on the tail plane is, therefore:

$$P_v = 126 \cdot 1.2 = 150 \text{ kg}$$

which is then the shear value, constant for the entire part of fuselage being considered.

The bending moment in the fuselage attachment section is:

$$M_f = P_v \cdot D = 150 \cdot 3 = 450 \text{ kgm}$$

which has a triangular trend.

The rudder torque is:

$$M_t = P_v \cdot d = 150 \cdot 0.35 = 45 \text{kgm}$$

and it is constant for the entire length of the fuselage up to the wing attachments.

61. Verification of fuselage stability

With a procedure similar to that used for the wing, we first examined the various load conditions of the fuselage, and then we determined the stresses generated in this hypotheses. This how we arrived to the step regarding dimensioning and the stability verification of the fuselage structure. Of the various hypotheses we did not consider that concerning landing, which for gliders is generally less serious.

To summarize, we have said that the fuselage is stressed: by bending in the vertical plane, deriving from the aerodynamic load on the horizontal tail plane and from the centrifugal reactions of mass; by bending in the horizontal plane and by torsion deriving from the aerodynamic load on the vertical tail plane. The fuselage forward section containing the pilot's cockpit is stressed in bending in the vertical plane by mass reactions and it must be dimensioned for this load.

Simple polygonal fuselage. As our first instance, let us suppose that the fuselage is formed simply by four longitudinal stringers, connected by braces and covered with plywood on the four sides.

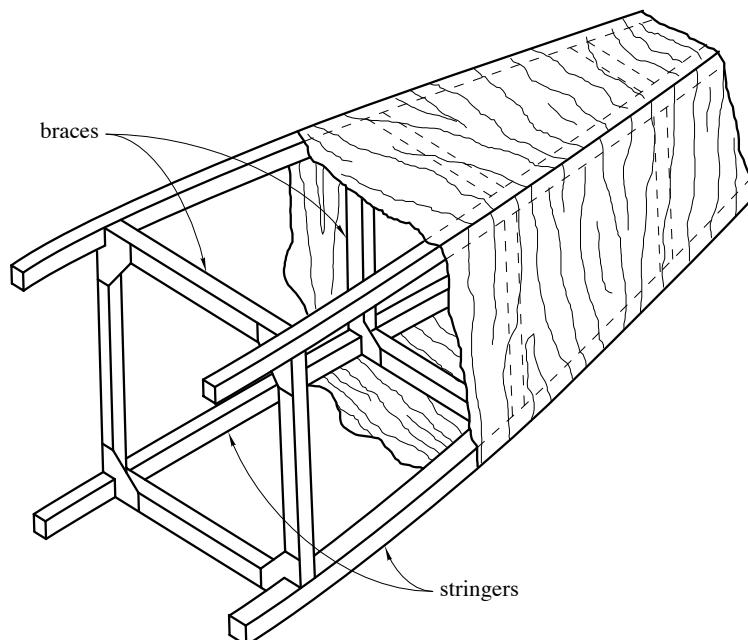


Figure 9-44

For stresses in the vertical plane, we can consider the two vertical sides, each made up by the upper and lower stringer: (Figure 9-45-a), while for stresses on the horizontal plane,

we will consider the horizontal sides, made up by the two upper stringers in one case, and the two lower ones in the other (Figure 9-45-b).

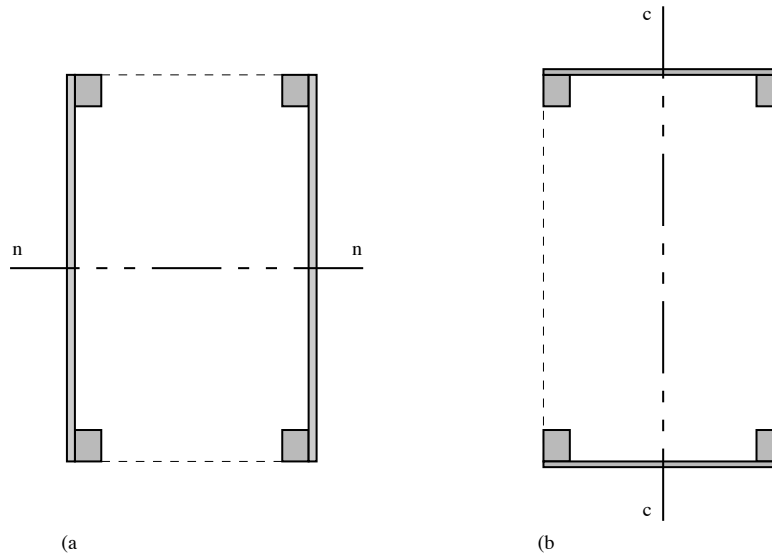


Figure 9-45

The calculation, therefore, is reduced to that of one beam formed by the two caps connected by a web, as we saw for the wing spar. Thus, the stresses due to the bending moment will be supported by the two stringers, while the shear stress will be supported by the plywood webs.

Example. In the wing connecting section of a fuselage having a rectangular section, we have a bending moment of:

$$M_f = 750 \text{ kgm}$$

and shear load of:

$$T = 270 \text{ kg}$$

in the vertical plane, and:

$$M_f = 480 \text{ kgm}$$

$$T = 160 \text{ kg}$$

in the horizontal plane, and a torsion load of:

$$M_t = 65 \text{ kgm.}$$

The section dimensions are:

$H = \text{height} = 80 \text{ cm}$

$L = \text{width} = 48 \text{ cm}$

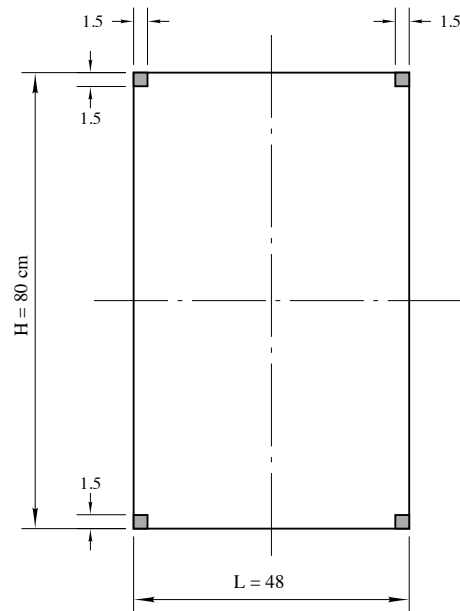


Figure 9-46

Let us suppose that the stringers are made of spruce and having a 15 x 15mm square section, and that the side skins are made of birch plywood, 1.5 mm thick. Let's verify now the section for shear loads and bending moment in the vertical plane. As we said earlier, we are considering the two vertical sides, which shall, therefore, support half the moment and shear, in other words:

$$\frac{1}{2} M_f = 375 \text{ kgm}$$

$$\frac{1}{2} T = 135 \text{ kg}$$

From the already known relation:

$$\sigma = \frac{6 \cdot M_f \cdot H}{B(H^3 - V^3)}$$

where in our case we have:

$H = 80 \text{ cm}$

$B = 1.5 \text{ cm}$

$$M_f = 375 \text{ kgm} = 37500 \text{ kgcm}$$

$$V = 80 - 3 = 77 \text{ cm}$$

we obtain the bending load on the stringers:

$$\sigma = \frac{6 \cdot 37500 \cdot 80}{1.5(80^3 - 77^3)} = \frac{18000000}{1.5(512000 - 456533)}$$

$$\sigma = \frac{18000000}{1.5 \cdot 55467} = \frac{18000}{87} = 207 \text{ kg/cm}^2$$

Given the relatively low value of the load, we could reduce the stringers size taking it, for example, to 12 x 12 mm.

The new values would be:

$$V = 80 - 2.4 = 77.6 \text{ cm}$$

$$B = 1.2 \text{ cm}$$

and the load would be:

$$\sigma = \frac{18000000}{1.2(512000 - 467288)} = \frac{18000}{1.2 \cdot 44712} = \frac{1800}{53.6} = 335 \text{ kg/cm}^2$$

The σ stress could be increased more, but it is not convenient to further reduce the stringer size for several construction-related reasons, and also in consideration of any accidental local loads.

The torsion load τ is given by the relation:

$$\tau = \frac{1.5T}{H \cdot \delta}$$

where:

$$T = \text{shearing stress} = 135 \text{ kg}$$

$$H = \text{web height} = 80 \text{ cm}$$

$$\delta = \text{web thickness} = 1.5 \text{ mm}$$

By replacing the values, we have:

$$\tau = \frac{1.5 \cdot 135}{80 \cdot 0.15} = 16.90 \text{ kg/cm}^2$$

thus the shear load is quite low.

We can reduce the plywood thickness to 1 mm, so that the torsion load will be:

$$\tau = \frac{1.5 \cdot 135}{80 \cdot 0.10} = 25.4 \text{ kg/cm}^2$$

which is still a very low value. We must keep into account that plywood buckling would be very likely with thin plywood and would result in a considerable reduction of the structure stiffness. Therefore, it is a good practice not to adopt a plywood thickness that is too low and less than 1mm (also as they are not easily found on the market) and covering distances not exceeding 30-35 cm, so as to avoid such buckling, which occurs more easily if the panel is flat, rather than curved.

Let us now verify the structure for loads in the horizontal plane, having for each horizontal beam:

$$M_f = 240 \text{ kgm}$$

$$H = L = 48 \text{ cm}$$

$$B = 1.2 \text{ cm}$$

First, we calculated the sides as beams made up by two caps connected by a web in a manner similar to that used for the wing spar.

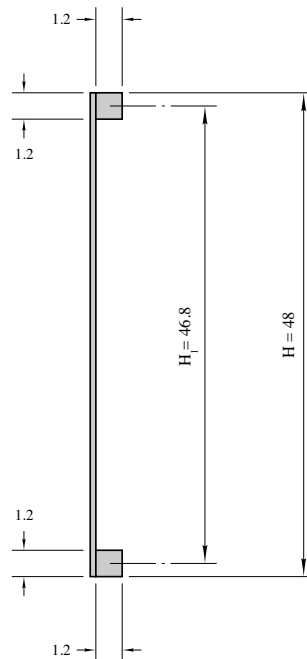


Figure 9-47

In such cases, though, where the caps—stringers—have very small dimensions compared to the H height of the beam, we can proceed with calculation in a much simpler, but not

less exact manner, by considering the area of the stringer section as concentrated in its centroid, or center of mass. By dividing the bending moment by the height H , we will obtain the tension or compression loads on the stringers between the stringer centroid, and then, by dividing this value by the area A of the section, we will have the load.

In our case, the height between the section centroids is:

$$H_1 = 46.8 \text{ cm}$$

therefore, the axial stress on the stringers will be

$$S = \frac{M_f}{H_1} = \frac{24000}{46.8} = 513 \text{ kg}$$

The stress in the stringers is, therefore:

$$\sigma = \frac{S}{A} = \frac{513}{1.44} = 356 \text{ kg/cm}^2$$

where:

$$A = \text{stringer section area} = 1.2 \times 1.2 = 1.44 \text{ cm}^2$$

For the shear loads, we have:

$$\tau = \frac{1.5T}{H \cdot \delta} = \frac{1.5 \cdot 135}{48 \cdot 0.1} = 42.2 \text{ kg/cm}^2$$

This value is still low for birch plywood. Finally, we must verify the structure stability for torsional stress. This is done by simply applying the Brendt formula:

$$\tau = \frac{M_t}{2A \cdot \delta}$$

where:

$$M_t = \text{rudder torque} = 65 \text{ kgm} = 6500 \text{ kgcm}$$

$$A = \text{section area} = 80 \times 48 = 3840 \text{ cm}^2$$

$$\delta = \text{plywood thickness} = 1 \text{ mm} = 0.1 \text{ cm}$$

and the skin shear load will be:

$$\tau = \frac{6500}{2 \cdot 3840 \cdot 0.1} = \frac{6500}{768} = 8.5 \text{ kg/cm}^2$$

Here we see how the tangential stress, deriving from torsion, is particularly small, as were the shear loads, both in the vertical and in the horizontal plane.

Nevertheless, we must note that since the shear and the torsion values are constant for the entire aft part of the fuselage, we will have the maximum loads where their traverse dimensions are minimal, that is at the aft end.

Let us suppose that the dimensions in the minimum section are:

$$H = 25 \text{ cm}$$

$$L = 18 \text{ cm}$$

so that area A is

$$A = 25 \cdot 18 = 450 \text{ cm}^2$$

In this case, torsion load is:

$$\tau = \frac{M_t}{2A \cdot \delta} = \frac{6500}{2 \cdot 450 \cdot 0.1} = 72 \text{ kg/cm}^2$$

a value that is not excessive, but neither excessively low as in the connecting section.

From what we have seen in the example, we can deduce that we should reduce the thickness of plywood from the end to the connection of the fuselage with the wing. But as the thickness required at the end is generally no greater than 1.5 mm, for these aircraft, the thickness is kept constant.

On the other hand, with regards to the longitudinal stringer dimensions, it might seem convenient to reduce the section as we go toward the rear end of the fuselage, since, as we have seen, the bending moment decreases (Figure 9-43).

But if we consider the dimensions that these stringers will have, we see that the weight savings is meaningless, while the tapering work becomes complicated. The section is, thus kept constant for stringers as well.

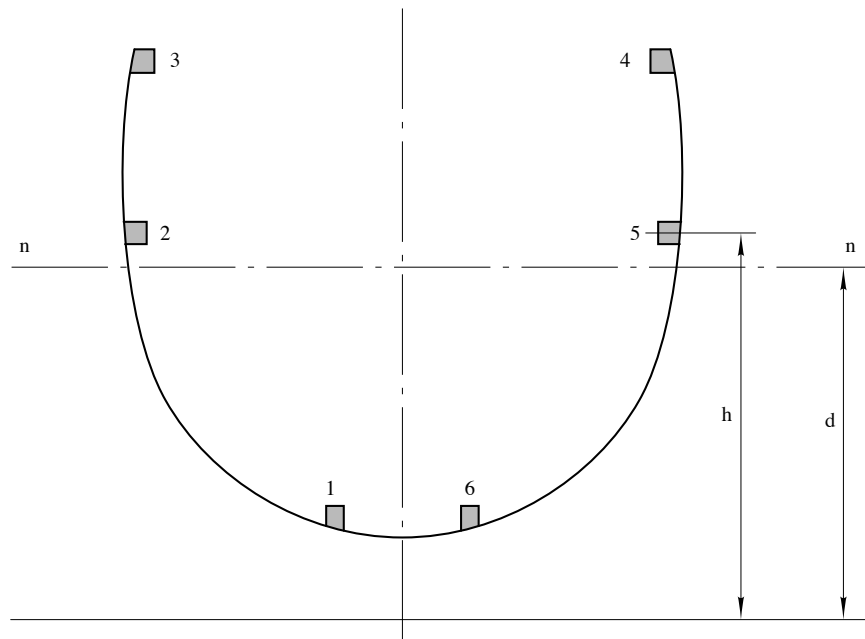


Figure 9-48

Shell fuselage. What we have seen in the example applies to a fuselage of a very simple shape, such as a square one. Nevertheless, even in the instance of more complex polygonal sections, we can still end up considering a simple shape structure, while ignoring other elements during the calculation, as if their task was only that of contributing to the shape. The actual contribution that they will add to the total strength of the structure will be an advantage to safety. Instead, if we want to consider the example of the real contribution of all the stringers, we can proceed as follows.

Example. Let us verify bending in the section of the fuselage front part, in correspondence with the pilot cockpit, with six stringers having the same section of 12 x 12mm. The bending moment is $M_f = 280$ kgm.

To make things easy, let's enter in the table the stringers distances h from any chosen reference plane, the stringers sections S , and the products $S \times h$ of the areas by the distances, which are the *static moments* in relation to the reference. Then, by dividing the sum $\sum S \times h$ of the areas static moments by the sum of the areas, we can obtain the distance d of the neutral axis from the reference plane. Knowing thus the neutral axis position, we have the distances H of its stringers. We then enter in the table all the H , H^2 and the products $S \times H^2$.

String.	S (cm ²)	h (cm)	$S \times h$	H (cm)	H^2	$S \times H^2$
1	1.5	0.45	0.68	32.15	1030	1545
2	1.5	42.8	64.50	10.20	104	156
3	1.5	55	82.50	22.40	500	750

4	1.5	55	82.50	22.40	500	750
5	1.5	42.8	64.50	10.20	104	156
6	1.5	0.45	0.68	32.15	1030	1545
$\Sigma S = 9.0$		$\Sigma S \times h = 294.16$		$\Sigma S \times H^2 = 4902 \text{ cm}^4$		

$$d = \frac{\Sigma S \cdot h}{\Sigma S} = \frac{294.16}{9} = 32.6 \text{ cm}$$

From the table, we have obtained d and then the products SH^2 , which are the *inertia moments* of the stringers sections in relation to the neutral axis. Their sum is, therefore the inertia moment J of the fuselage section in relation to the neutral axis:

$$J = \Sigma SH^2 = 4902 \text{ cm}^4$$

because the bending load is

$$\sigma = \frac{M_f \cdot y}{J}$$

its maximum value will be in the farthest stringers, which are the 1st and the 6th, and it will be:

$$\sigma = \frac{28000 \cdot 32,15}{4902} = 184 \text{ kg/cm}^2$$

We could reduce the fillet section, also in consideration of the contribution added by the covering plywood. In fact, in addition to the area that is directly glued to the fillet, and thus working with it, there is also an area around the fillet that collaborates for bending, because it does not suffer from the buckling given by the stiffening caused by the fillet itself. Said collaborating area is considered about 2-3 times the width of the fillet. By repeating the calculations, we could get down to a stringers section of about 10 x 10, still remaining within low stress values.

62. Determination of the Tail Plane Loads

For the tail plane dimensioning, we follow a process similar to that used for the wing. The loads, as we saw for the fuselage, are calculated according certification standards.

Horizontal Tail Plane. The minimum load P_c on the stabilizer-elevator assembly must be such to balance the wing pitching moment. Its minimum value is therefore:

$$P_c = \frac{0.20 \cdot 2_n \cdot Q \cdot l_m}{a}$$

with their known meaning. For the required strength this value P_c shall not be lower than:

- 80 kg/m² for gliders
- 120 kg/m² for normal sailplanes
- 150 kg/m² for acrobatic planes.

As we could see earlier, in normal gliders, the load P_c required to balance the wing moment is lower than that resulting from the required minimum unitary load.

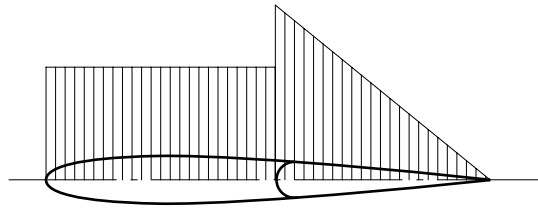


Figure 9-49

The load P_c must be shared between the stabilizer and the elevator in proportions according to their areas and with a rectangular distribution for the stabilizer and a triangular one for the elevator.

In actual practice though, the spar, or spars, of the stabilizer are dimensioned for the total load P_c on the entire tail plane, considering of the greater bending elasticity of the elevator, which thus transmits its load, by means of the hinges, to the stabilizer.

The elevator, on the other hand, is dimensioned for the load bearing on it, proportional to its area.

We do not think it is necessary to give a calculation example, since the method is exactly the same that we used for the wing. We only need to add that, since the loads on the tail plane are the same both up and down, the spars will be made with equal sized spar caps, and not different, as we did for the wing.

Vertical tail plane. Also for the vertical plane a minimum point load is fixed, where the required strength is:

$$P_v = 2_n \cdot \frac{Q}{S} \text{ kg/m}^2$$

and that shall be no less than the value of:

- 80 kg/m² for gliders
- 120 kg/m² for normal sailplanes
- 150 kg/m² for acrobatic planes.

Example. For a normal sailplane $2n = 7$ with a wing load $Q/S = 16.5 \text{ kg/m}^2$ and a point load on the vertical tail plane shall have a required strength of:

$$P_v = 7 \cdot 16.5 = 115.5 \text{ kg/m}^2$$

This is lower than the required minimum of 120 kg/m^2 , which we shall use.

Although, if the wing load was, for example, 22 kg/m^2 , the load on the tail plane would be, for the required strength:

$$P_v = 7 \cdot 22 = 154 \text{ kg/m}^2$$

and this would be the load to consider for dimensioning the vertical plane.

For the distribution of this load P_v on the fin and rudder, what we said for the horizontal tail plane applies and structures are calculated in a similar manner.

63. Calculation of Wing Attachments

The structural components of an aircraft are joined together by means of metal connections.

Among the most important ones for gliders, we have the wing attachments. Generally, in aircraft with cantilevered wings the half wings are joined together with steel plates bolted to the wing spars and connected together by means of pins, which may be cylindrical or conical. The wing is then connected to the fuselage, by means of small pins, with slotted fittings on the lower plates.

In a similar connection diagram, the maximum bending stress is maintained by the plates and the main pins, while the weight of the fuselage, hanging from the wing, is born by the slotted fittings with secondary pins.

Let's say for now—and later we will see through calculation—that the stresses on the union pins of the half wings are considerably higher than those connecting the fuselage.

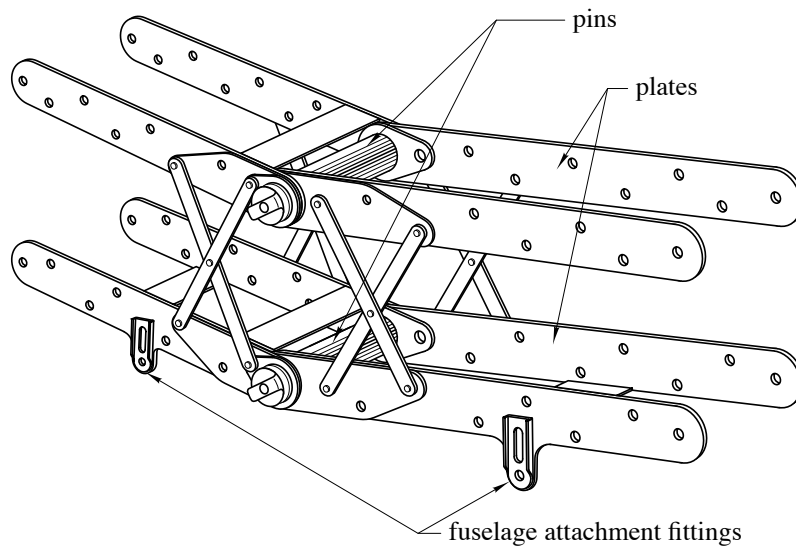


Figure 9-50

Example. Let's proceed with calculating the wing attachments.

Let's suppose they are made up by four plates per half wing, two on the upper spar caps and two on the lower one. The distance between pin holes is 20cm and the associated wing bending moment is a load of 2500 kgm.

Pin-Plate eyelet. The load on each pin comes from the stress along the axis of the spar cap calculated from the center of gravity in line with the pin. This stress is:

$$S = \frac{M_f}{h} = \frac{2500}{0.20} = 12,500 \text{ kg}$$

where:

M_f = bending moment acting on the pins;
 h = distance between the pin centers.

Assuming the pins are cylindrical, we calculate the required diameter.

The shear load, considering that there are two resisting sections, one per plate, is:

$$\tau = \frac{S}{2A} = \frac{S}{2 \cdot \frac{\pi}{4} \cdot d^2}$$

where:

S = total shear load on the pin;

$A =$ area of the pin with a diameter $d = \frac{\pi d^2}{4}$.

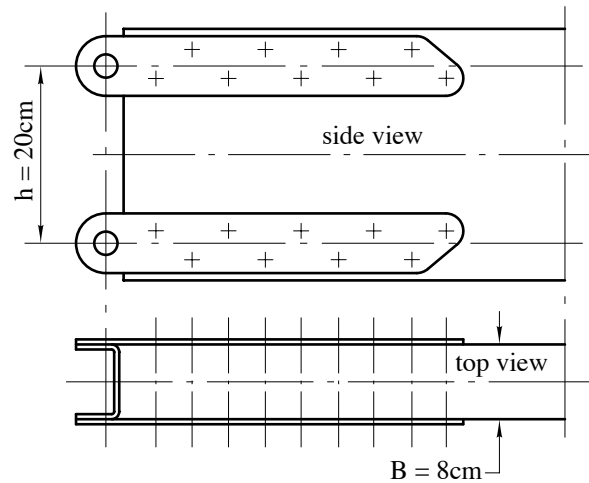


Figure 9-51

Given an admissible breaking stress of the material used:

$$R = 50 \text{ kg/mm}^2$$

by solving the relation seen with regards to d , we have:

$$d = \sqrt{\frac{S}{\pi \cdot \tau / 2}} = \sqrt{\frac{12500}{3.14 \cdot 50 / 2}} = \sqrt{\frac{12500}{79}} = \sqrt{158} = 12.6 \text{ mm}$$

Admitting, for the time being, this value as the actual one for the pin, let's now determine the thickness of the connection plates.

The section most stressed is that in correspondence with the hole, *i.e.* the *eyelet*. Given a plate height of 50 mm, and the unknown thickness s , the tension load σ in section A-A is given by:

$$\sigma = \frac{S}{A} = \frac{12500}{2(50 - 12.6) \cdot s}$$

and given for the plate material

$$\sigma = 40 \text{ kg/mm}^2$$

we have the thickness:

$$\tau = \frac{6250}{250} = 25 \text{ kg/mm}^2$$

By increasing the plate thickness to 7 mm, the supporting surface is

$$A = 24 \cdot 7 = 170 \text{ mm}^2$$

and the specific pressure

$$p = \frac{6250}{170} = 36.5 \text{ kg/mm}^2$$

still has a high value.

To increase the supporting surface without further increasing the thickness of the entire plate, let's weld a washer with a thickness of 5 mm on the eye. We now have:

$$A = (7 + 5) \cdot 24 = 288 \text{ mm}^2$$

and the specific pressure

$$p = \frac{6250}{288} = 21.6 \text{ kg/mm}^2$$

now has an acceptable value.

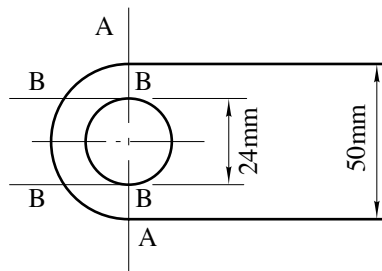


Figure 9-53

Let's verify again, based on the 7mm thickness of the plate, the tensile eye in section A-A without considering the washer contribution. The verification in section B-B is superfluous, since in this case the shear resisting area is greater than the tension resisting area.

The resisting area of section A-A is:

$$A = (50 - 24) \cdot 7 = 182 \text{ mm}^2$$

and the tension stress σ becomes, being 6250 kg, the load weighing on each plate:

$$\sigma = \frac{6250}{A182} = 34.4 \text{ kg/mm}^2$$

an acceptable value.

Spar connecting bolts. The pairs of plates are connected to the wing spar with through bolts that strongly press it against the wood. These are, therefore, stressed simultaneously in tension along their axis and in shear for the axial stress on the plates. In practice, though, the axial load on bolts is ignored, as it is always small, and also no consideration is given to the contribution of friction between the plates and the wood that helps to decrease the total cut stress that the bolts must bear.

Thus, let's suppose to put eight bolts for each plate for connection and calculate the required diameter.

Each one must therefore bear a load of:

$$Q = \frac{12500}{8} = 1560 \text{ kg}$$

and since there are two shear sections for each, by using a point shear stress of 40 kg/mm², their diameter shall be:

$$d = \sqrt{\frac{Q}{\pi\tau/2}} = \sqrt{\frac{1560}{3.14 \cdot 40/2}} = \sqrt{\frac{1560}{62.8}} = \sqrt{24.8} \sim 5\text{mm}.$$

The bolt works into the wood for 80 mm, so the supporting surface is:

$$A = 80 \cdot 5 = 400\text{mm}^2 = 4\text{cm}^2$$

and the specific pressure on wood is, therefore:

$$p = \frac{1560}{4} = 390\text{kg/cm}^2$$

that is not an admissible value for fir or spruce, which the material normally used to make spar caps. The maximum value for these materials that must not be exceeded is about 200 kg/cm².

Let's then obtain from the previous relation the required supporting surface, by fixing the specific pressure to 200 kg/cm²:

$$A = \frac{1560}{200} = 7.8\text{cm}^2 = 780\text{mm}^2$$

thus the bolts diameter shall be:

$$d = \frac{780}{80} = 9.7\text{mm}$$

For his we shall adopt eight bolts having a 10 mm diameter.

Plate dimensions. Finally, let's define the dimensions and thickness for the plates. The distance between the bolts in the connections with wooden parts is usually kept at 4 - 6 times their diameter and they are alternated by height.

Let's keep a horizontal distance of 40 mm between the bolts and a distance of 50 mm of the first from the pin axis in order to have a sufficient margin of spar material, since this ends before the pin hole. The total length of the plate is of 370 mm, given a radius of 15 mm at the end.

We have earlier determined its thickness in correspondence with the eye, where the stress is greatest. Let's now consider the stress in three other sections: *C-C*, *D-D* and *E-E*.

The load of said sections for each plate is half that weighing on the bolts outside the plates (assuming that the load on the bolts is the same for all, which in actual fact is not completely true).

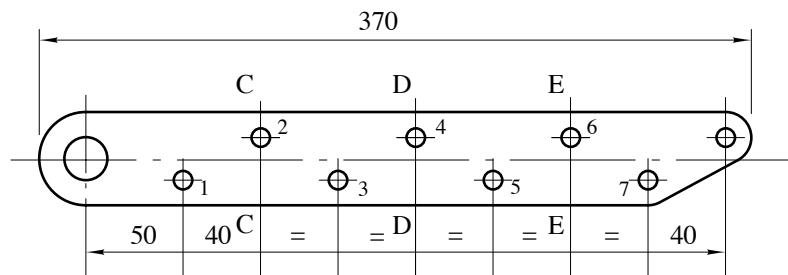


Figure 9-54

In section *E-E*, this load is therefore:

$$Q = \frac{3 \cdot 1560}{2} = 2340 \text{ kg}$$

in section *D-D* is

$$Q = \frac{5 \cdot 1560}{2} = 3900 \text{ kg}$$

and in section *E-E* is:

$$Q = \frac{7 \cdot 1560}{2} = 5460 \text{ kg}$$

Considering that the plate height is 50 mm constant along the entire length, let's obtain the thickness of the sections considered (having first fixed a stress of 40 kg/mm² for the material used)

Section *E-E*:

$$s = \frac{2340}{(50 - 10) \cdot 40} = \frac{2340}{1600} = 1.45 \text{ mm}$$

Section *D-D*:

$$s = \frac{3900}{(50 - 10) \cdot 40} = \frac{3900}{1600} = 2.45 \text{ mm}$$

Section *C-C*:

$$s = \frac{5460}{(50 - 10) \cdot 40} = \frac{5460}{1600} = 3.40 \text{ mm}$$

In glider construction for simplicity and low cost these metal elements are almost always made of welded steel sheet, thus eliminating as much as possible the need for machine tools (especially for milling).

In our case, we could build plates with several elements, overlaid and welded together: the first set with a thickness of 2 mm, the second to bolt 5 also 2 mm thick, and the third to bolt 2 with a thickness of 3 mm, as we can see in the figure below.

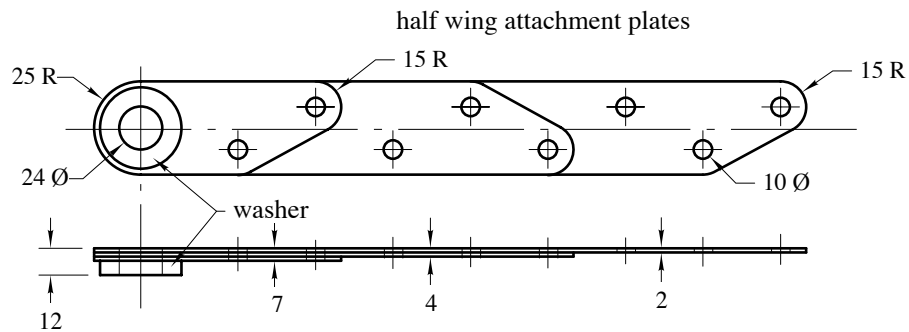


Figure 9-55

With regards to the specific pressure on bolts, we shall verify it where thickness is smaller, *i.e.* 2 mm.

The bolt supporting surface on each plate is:

$$A = 10 \cdot 2 = 20\text{mm}^2$$

and since the load is

$$Q = \frac{1560}{2} = 780\text{kg}$$

the specific pressure shall be:

$$P = \frac{780}{20} = 39\text{ kg/mm}^2$$

an admissible value for fixed elements such as the connection bolts in this case, considering also the contribution given by the friction between plates and wood, which actually reduces the load on them.

Wing-fuselage connection ears. As we said, the wing is connected to the fuselage through ears on the lower plates.

The load weighing on them, for each half wing, is given by the maximum cut of the half wing in the first hypothesis (maximum lift). Let's suppose that the maximum cut for robustness per half wing is:

$$T = 825\text{ kg}$$

and that the geometrical center of the half wing is 3.05 m from the centerline. Let's then say that the two pairs of ears of the two half wings are 46 cm from each other.

For a symmetrical load on the wings, we will obviously have a load on each of the two pairs of ears equal to that of the half wing of 825 kg, that is

$$q = \frac{825}{2} = 412.5 \text{ kg}$$

per ear.

But a much greater load occurs when we have an asymmetrical stress. Certification standards, for the heaviest condition, require a load dissymmetry of 70% of one half wing compared to the other.

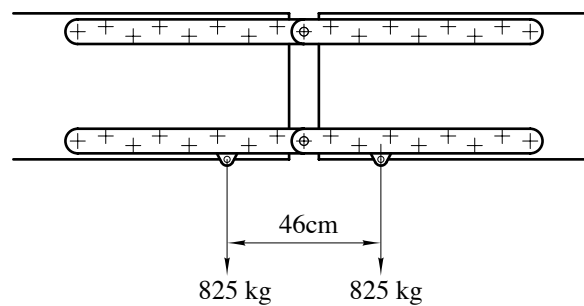


Figure 9-56

To illustrate, we can consider the wing as an only beam resting on two points, the unions in question, and loaded at the ends (corresponding to the half wing geometrical centers) with two different loads: one of 825 kg, and the other of:

$$825 \cdot 0.7 = 578 \text{ kg.}$$

From the Figure 9-57 diagram, we obtain through simple calculation that the maximum traction rises up to 2344 kg and for this load we shall dimension our unions with the fuselage.

Let's set a pin diameter

$$d = 10 \text{ mm}$$

to which corresponds an area of the section:

$$A = \frac{\pi d^2}{4} = \frac{3.14 \cdot 100}{4} = 78.5 \text{ mm}^2$$

and since there are two cutting sections, the unitary stress is, therefore:

$$\tau = \frac{2344}{2 \cdot 78.5} = 15 \text{ kg/mm}^2$$

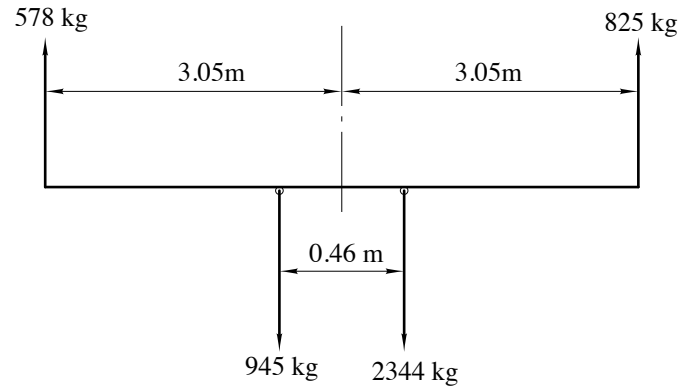


Figure 9-57

Let's set a width for the ear of 35 mm, and a thickness of 3 mm.

Section A-A resisting to traction is, for each ear:

$$A = (25 - 10) \cdot 3 = 45 \text{ mm}^2$$

and the stress becomes:

$$\sigma = \frac{2344}{2 \cdot 45} = 26 \text{ kg/mm}^2$$

Let's calculate the specific pressure on the pin. The supporting surface is:

$$10 \cdot 3 = 30 \text{ mm}^2$$

so the specific pressure

$$p = \frac{2344}{2 \cdot 30} = 39 \text{ kg/mm}^2$$

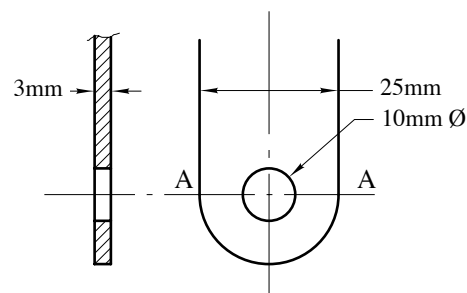


Figure 9-58

To reduce this value, also in this case we shall have to use a washer with a 3 mm thickness. The supporting area is now 60 mm² and the specific pressure decreases to:

$$p = \frac{2344}{2 \cdot 60} = 18 \text{ kg/mm}^2$$

With this example, we have seen in a simple manner how to proceed to the dimensioning of a metallic connection.

Summarizing, let's remember that we must verify:

- the tension effort σ in the various most critical sections of the connection;
- the shear stress τ for the eye, pins and bolts;
- the compression loads on pins, bolts, with plates;
- the compression loads of bolts on wood.

64. Calculation of controls and related transmissions.

Control stick. According to standards, the loads that stress a control stick are: on the longitudinal plane (elevator control): 100 kg for the required strength in both directions; on the cross plane (aileron control): 50 kg for the required strength in both directions.

These efforts are limited to the members that precede the appropriate limit stops, while the rest of transmission is calculated based on the efforts generated by loads on the maneuvering surfaces (ailerons, elevator).

Example. Let's suppose that the control stick has the dimensions shown in the Figure 9-59.

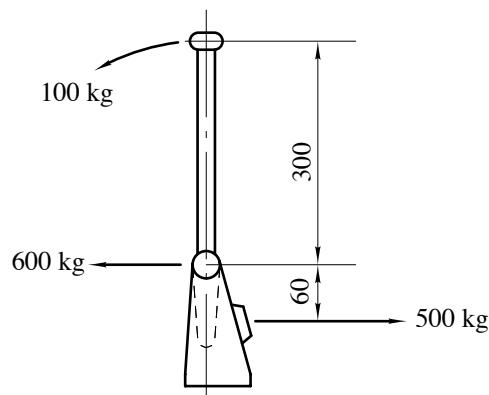


Figure 9-59

With a simple calculation, we obtain the effort on the stick pin of 600 kg and on the limit stops of 500 kg. A bolt with a 6 mm diameter is enough for the stick pin. The resisting surface is, in fact:

$$A = \frac{\pi d^2}{4} = \frac{3.14 \cdot 36}{4} = 28.4 \text{ mm}^2$$

and since the surfaces resisting to cut are two, the unitary stress shall be:

$$\tau = \frac{600}{2 \cdot 28.4} = 10.5 \text{ kg/mm}^2$$

For a stick support of 1.5 mm thick, the pin supporting area is, therefore:

$$A = 6 \cdot 2 \cdot 1.5 = 18 \text{ mm}^2$$

and the specific pressure will be:

$$p = \frac{600}{18} = 33.2 \text{ kg/mm}^2$$

that is too high a value. Let's take the pin diameter to 8 mm and the support thickness to 2 mm.

We now have:

$$A = 8 \cdot 2 \cdot 2 = 32 \text{ mm}^2$$

and the specific pressure

$$p = \frac{600}{32} = 18.8 \text{ kg/mm}^2$$

has an acceptable value.

The reaction on the limit stops is of 500 kg. Assuming that plates are 1 mm thick and 20 mm wide, the section resisting to traction is

$$1 \cdot 20 \cdot 2 = 40 \text{ mm}^2$$

and the stress

$$\sigma = \frac{500}{40} = 12.5 \text{ kg/mm}^2$$

Aileron transmission. The unitary load on ailerons is, for robustness according to standards

$$0.6 \cdot 2n \cdot \frac{Q}{S} \text{ kg/mm}^2$$

and never below the required strength of:

- 60 kg/m² for gliders
- 80 kg/m² for normal sailplanes
- 100 kg/m² for acrobatic airplanes.

Example. Let's assume that we are dealing with a normal sailplane, with a wing load of 18 kg/m², the unitary load for robustness on the aileron is:

$$0.6 \cdot 7 \cdot 18 = 76 \text{ kg/mm}^2$$

This is lower than the required minimum of 90 kg/m², a value that we will consider for calculation.

Let's suppose that the aileron has these dimensions:

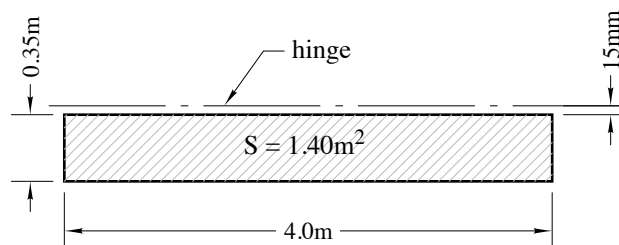


Figure 9-60

so the resulting surface will be 1.40 m². The load weighing on it is, therefore

$$80 \cdot 1.40 = 112 \text{ kg.}$$

Since the distribution along its chord is triangular, the load center of gravity is at one third of the chord, that is at a distance

$$\frac{35}{3} = 11.6 \text{ cm}$$

with a distance from the hinge of 11.6 cm + 1.5 = 13.1 cm.

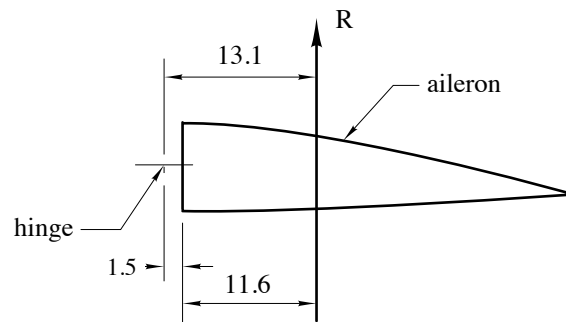


Figure 9-61

The hinge moment is, therefore

$$M = 112 \cdot 13.1 = 1450 \text{ kg/cm}$$

By setting the aileron lever radius at 12 cm, the effort on control cables (or on the control stick, if rigid) is:

$$S = \frac{1450}{12} = 121 \text{ kg.}$$

The 3 mm cables that are generally used for the controls on these aircraft are amply sufficient to support such loads.

Rigid transmissions, Buckling load. If the transmission is rigid, with aluminum tubing, they also work by compression, they must be verified for the *buckling load*, i.e. for the compression *critical load* P_{critic} that a solid with a rectilinear axis with a constant section may support without yielding and bending.

This verification of the buckling load is necessary when the solid, loaded by compression, has a very high *slenderness coefficient*. Said coefficient is the ratio between the solid free bending length L and the *inertia radius* ϱ of the normal section:

$$\frac{L}{\varrho} = \text{slenderness coefficient}$$

where the inertia radius ϱ is given by:

$$\varrho = \sqrt{\frac{J}{A}}$$

where:

J = moment of inertia of the resisting section
 A = area of the resisting section.

To calculate tubular rods loaded on their tip, where the slenderness coefficient is greater than 80 - 100 (long struts) Euler's formula applies:

$$P_{crit} = \frac{K \cdot \pi^2 E \cdot J}{L^2}$$

while for rods with a slender coefficient smaller than 80 (short struts) the formula by Johnson shall apply

$$P_{crit} = C - \frac{C^2 A^2}{L \cdot K \cdot \pi^2 \cdot E \cdot J}$$

where:

E = modulus of elasticity of the material
 J = moment of inertia of the section
 L = length of free bending
 C = yield strength of the material
 K = coefficient according to the end constraints.
 For hinged ends $K = 1$
 For restrained ends $K = 2$.

Example. Let's consider that the transmission rod of the aileron in the previous calculation is a pipe made of aluminum with an external diameter of 20 mm and a thickness of 1 mm, and has a free bending length of 3 meters.

The moment of inertia of the resisting section is (being diameter $D = 20$ mm and the internal one $d = 18$ mm):

$$J = \frac{\pi}{64}(D^4 - d^4) = 0.05(20^4 - 18^4)$$

$$J = 0.05(16000 - 105000) = 2750mm^4$$

and being the resisting section A :

$$A = \frac{\pi}{4}(D^2 - d^2) = \frac{\pi}{4}(20^2 - 18^2) = 0.785 \cdot (400 - 324) = 59.5mm^2$$

the radius of inertia shall be:

$$\varrho = \sqrt{\frac{J}{A}} = \sqrt{\frac{2750}{59.5}} = \sim 6.8 \text{ mm.}$$

The slenderness coefficient will be:

$$\frac{L}{\varrho} = \frac{3000}{6.8} = 440$$

therefore, we are no doubt in the field of applicability of Euler's formula. In our case, let's set:

$$\begin{aligned} E &= 6800 \text{ kg/cm}^2 \\ K &= 1 \\ L &= 3000 \text{ mm} \\ J &= 2750 \text{ mm}^4 \end{aligned}$$

We shall have:

$$\begin{aligned} P_{crit} &= \frac{K\pi^2 EJ}{L^2} = \frac{\pi^2 \cdot 6800 \cdot 2750}{3000^2} \\ P_{crit} &= \frac{9.85 \cdot 6800 \cdot 2750}{9,000,000} = \frac{184,000,000}{9,000,000} = \sim 20.5 \text{ kg.} \end{aligned}$$

The load bearable by the rod is, therefore, considerably smaller than the load weighing on it, which is 121 kg.

To increase resistance without increasing the rod dimensions, we shall reduce the free bending length L by placing two supporting bars, equally distant from each other. This way, the free bending length is now $L = 1 \text{ m} = 1000 \text{ mm}$.

The slenderness coefficient is:

$$\frac{L}{\varrho} = \frac{1000}{6.8} = 147$$

and we shall apply again Euler's formula:

$$P_{crit} = \frac{9.85 \cdot 6800 \cdot 2750}{1,000,000} = \frac{184,000,000}{1,000,000} = \sim 184 \text{ kg.}$$

A value that is now definitely higher than the stressing one.

In a similar way to the buckling load, we can calculate the wing stanchions stressed by compression in the sudden landing condition.

L'ALIANTE

Stelio Frati

